Universidade de Aveiro
Departamento de Electrónica, Telecomunicações e Informática,
2012

Luis Filipe Dias

Sistemas de Recolha de Energia sem Fios de Alta Eficiência

(High-Efficiency Electromagnetic Energy-Harvesting)

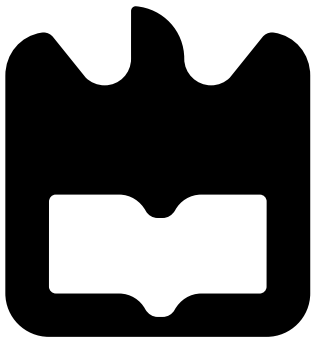

Universidade de Aveiro
Departamento de Electrónica, Telecomunicações e Informática,
2012

Luis Filipe Dias

Sistemas de Recolha de Energia sem Fios de Alta Eficiência

(High-Efficiency Electromagnetic Energy-Harvesting)

Dissertação apresentada à Universidade de Aveiro para cumprimento dos requisitos necessários à obtenção do grau de Mestre em Engenharia Electrónica e Telecomunicações, realizada sob a orientação científica do Dr. Nuno Borges de Carvalho, Professor associado com agregação do Departamento de Electrónica, Telecomunicações e Informática da Universidade de Aveiro.

o júri / the jury

presidente / president

Professor Doutor Rui Manuel Escadas Ramos Martins
Professor Auxiliar do Departamento de Electrónica, Telecomunicações e Informática da Universidade de Aveiro)

vogais / examiners committee

Professor Doutor Pedro Renato Tavares Pinho
Professor Adjunto do Departamento de Engenharia de Electrónica e Telecomunicações e de Computadores do Instituto Superior de Engenharia de Lisboa

Professor Doutor Nuno Borges de Carvalho
Professor Associado com Agregação do Departamento de Electrónica, Telecomunicações e Informática da Universidade de Aveiro

agradecimentos / acknowledgements

Embora apenas de um nome conste a autoria deste trabalho, este não foi, nem poderia ter sido feito sem o apoio de inúmeras pessoas.

Começo por agradecer aos meus colegas de curso, aos quais devo em muito o sucesso obtido ao longo destes 5 anos, assim como aos colegas do Instituto de Telecomunicações, em especial ao Ricardo Fernandes, Alírio Boaventura, Miguel Lacerda, Paulo Gonçalves e Hugo Mostardinha, pela ajuda e conselhos prestados.

Deixo ainda um enorme agradecimento ao meu orientador prof. Nuno Borges de Carvalho pela motivação contagiante e inúmeras ideias, assim como disponibilidade para a qualquer momento aconselhar soluções para os problemas.

A nível pessoal um agradecimento muito especial aos meus pais por sempre terem provisionado todas as condições que necessitei, sem nunca olhar a meios, assim como pelos valores e ideais que me transmitiram ao longo dos anos.

Finalmente o maior obrigado vai para a minha eterna companheira de aventuras,e principal inspiração, Tânia, que em todos os momentos importantes esteve ao meu lado, e sem a qual sei, não teria chegado tão longe, tão cedo, tão bem!

Resumo

Numa época em que os avanços tecnológicos se concretizam a um ritmo frenético, verifica-se uma desporporcional evolução das capacidades das baterias, essencialmente nos equipamentos móveis de uso comum. Por outro lado aumentam os dispositivos cuja localização remota torna a manutenção de baterias algo expensiosa e por vezes insustentável, tais como as Wireless Sensor Networks (WSN)

O intuito deste trabalho prende-se não só com o aumento da eficiência de sistemas de recolha de energia de radiação electromagnética da banda dos $100MHz$, como também com a introdução de novos métodos úteis à a sua análise. Paralelamente é ainda proposto um sistema de iluminação alimentado por circuitos de rectificação com um enfoque mais específico e menos relacionado com as suas eficiências.

Ao nível dos melhores resultados obtidos para os circuitos de alta eficiencia, estes foram alcançados por um circuito rectificador série simples, com valores de eficiência experimental de $\approx 45\%$ para uma potência de entrada de $5dBm$, gerando uma tensão de saída de $\approx 1.6V$. Relativamente aos circuitos desenvolvidos para o sistema de iluminação foi possível, através de um multiplicador de tensão, gerar tensões DC ligeiramente acima de $8V$ para uma potência de entrada de $10dBm$, desta forma conseguindo alimentar uma célula de três LEDs de baixo consumo.

Os resultados obtidos destinam-se não apenas a apresentar conclusões inovadoras, mas também a fornecer ferramentas adequadas a posteriores desenvolvimentos de sistemas similares, servindo desta forma como um contributo de utilidade para a comunidade científica.

Abstract

At a time when technological advances happen every day, a disproportional evolution of batteries capabilities has been verified, specially for mobile devices. On the other hand the number of devices whose remote location makes battery maintenance very expensive, Wireless Sensor Networks (WSN), is increasing.

The objective of this work is not only to increase the efficiency of energy harvesting systems on the frequency of $100MHz$, as it is introducing new methods for it's analysis. At the same time a no-cost illumination system, fed with more specific rectification systems, with less consideration for the efficiency is proposed here.

As of the best results obtained for the high efficiency circuits, these were achieved for a simple series rectifier, with efficiencies around 45% for an input power of $5dBm$, thus generating output voltages of $\approx 1.6V$. The circuits developed for the lighting system, consisting in voltage multipliers, generated output voltage values around $8V$ for $P_{in} = 10dBm$, that is, enough to power up a low consuming 3 Light-Emitting Diode (LED)s cell.

These obtained results are destined not only to present innovative conclusions, but also to provide adequate tools for subsequent developments of similar circuits, thus serving as a contribute for the scientific community.

Contents

Contents i

List of Figures iii

List of Tables v

List of Acronyms vii

1 Introduction 1
- 1.1 Motivation . . . 2
- 1.2 Objectives . . . 2
- 1.3 Overview of Involved Concepts . . . 3
  - 1.3.1 Wireless Power Transmission WPT . . . 4
  - 1.3.2 Schottky Diode . . . 8
  - 1.3.3 Charge-Pump Mechanism . . . 10
- 1.4 Lighting System . . . 12
- 1.5 Conclusion . . . 13

2 State of the Art 15
- 2.1 Non-Linear Element (NLE) . . . 15
  - 2.1.1 Schottky Diode as NLE . . . 15
  - 2.1.2 MOSFET as NLE . . . 17
- 2.2 Rectifying Topology . . . 18
- 2.3 Bandwidth of the Energy Harvested . . . 19
- 2.4 Other Techniques . . . 20
- 2.5 Conclusion . . . 23

3 Study of the Non-Linearities 24
- 3.1 Description of Non-Linear System(s) (NLS) . . . 24
- 3.2 Methods for the study of NLS . . . 25
  - 3.2.1 Linearisation and Series Expansion Methods . . . 26
  - 3.2.2 Describing Functions (DF) . . . 28
- 3.3 Conclusion . . . 33

4 Rectifier Design 35
- 4.1 Simulation Tools . . . 35
  - 4.1.1 Advanced Design System (ADS) . . . 35

4.1.2 Harmonic Balance (HB) . . . 36
4.2 Lighting System . . . 37
4.3 Rectifier with Polarization Source . . . 39
4.3.1 Problems and Limitations . . . 40
4.4 Rectifier with Matching Network . . . 41
4.4.1 Source-Pull Mechanism . . . 43
4.5 3-Port Network Analysis . . . 44
4.6 Voltage Multipliers . . . 48
4.7 Conclusion . . . 49

5 Simulations and Experimental Results **51**
5.1 Rectifier with Polarization Source . . . 51
5.1.1 Current Polarization . . . 52
5.1.2 Voltage Polarization . . . 54
5.1.3 Parasitic Resistance equal to Zero . . . 56
5.1.4 Circuit Efficiency . . . 57
5.2 Rectifier with Matching Network . . . 58
5.2.1 Source-Pull Mechanism . . . 58
5.2.2 Fixed Matching Network . . . 61
5.3 3-Port Network Analysis . . . 62
5.4 Simple Rectifier Implementation . . . 63
5.4.1 Diode in Series . . . 64
5.4.2 Diode in Parallel . . . 68
5.5 Voltage Multipliers Implementation . . . 70
5.5.1 Villard Voltage Multiplier . . . 70
5.5.2 Dickson Voltage Multiplier . . . 71
5.6 Lighting System . . . 72
5.6.1 Outdoor Measurements . . . 74
5.7 Conclusion . . . 77

6 Conclusions and Future Work **79**
6.1 Conclusions . . . 79
6.2 Further Work . . . 80

Bibliography **81**

List of Figures

1.1 Generic Inductive Charging Platform (source [8]) . . . 5
1.2 Resonant Induction Recharging System (source: [9]) . . . 6
1.3 Typical WPT Electromagnetic Radiation System . . . 7
1.4 Structure of the Wireless Power Transmission (WPT) System (source [11]) . . . 7
1.5 HSMS-2850 IV curve (source: [14]) . . . 9
1.6 HSMS-2850 Equivalent Linear Circuit Model (source: [14]) . . . 10
1.7 Cookcroft-Walton/Villard Voltage Multiplier (source: [15]) . . . 11
1.8 Dickson Voltage Multiplier (source: [15]) . . . 12
1.9 Green Illumination Neighbourhood . . . 12

2.1 Rectifier with Transmission Lines (source: [19] and [1]) . . . 16
2.2 Top View of Fabricated Schottky Diode (source: [21]) . . . 17
2.3 Ultra Low Power DC Sensing Circuit (Source: [23]) . . . 17
2.4 Schematic Diagram of Optimized Diode-connected CMOS (source [24]) . . . 18
2.5 Measured RF Power Density (source: [34]) . . . 20
2.6 RF/DC Converter with Complementary Configuration (source: [35]) . . . 21
2.7 Simple Resonant Tank (source: [15]) . . . 22
2.8 Crystal Equivalent Circuit and Frequency Response (source: [37]) . . . 22

3.1 Typical Control System Block Diagram . . . 28
3.2 General Linear Approximator for a Non-linear Operator (source: [46]) . . . 29
3.3 Gain-Changing Element Characteristic (source: [46]) . . . 31
3.4 Saturation Function (source: [46]) . . . 32
3.5 General Piecewise-linear Non-linearity (source: [46]) . . . 33

4.1 1-LED IV Curve . . . 38
4.2 3-LED IV Curve . . . 38
4.3 1-Stage Simple Rectifier with Polarization Source . . . 39
4.4 Application of KCL to the Circuit . . . 41
4.5 Parallel Diode Rectifier with Matching Network . . . 42
4.6 Series Diode Rectifier with Matching Network . . . 42
4.7 Equations and Smith Charts on DDS . . . 44
4.8 Generic 3-Port System . . . 45
4.9 HSMS-2850 Model with Parasitic Elements . . . 46
4.10 3-Port Network for Diode in Parallel . . . 46
4.11 Complete 3-Port System . . . 48
4.12 Villard Voltage Multiplier with 2-Stages . . . 48

4.13 Dickson Voltage Multiplier with 2-Stages 49
4.14 Dickson Voltage Multiplier with 2-Stages 49

5.1 Diode IV Curve for Discrete Input Power 52
5.2 2nd Harmonic Output vs Polarizing Current for Discrete Input Power 53
5.3 Voltage Output vs Input Power for Discrete Polarization Current 53
5.4 2nd Harmonic Output vs Input Power for Discrete Polarization Current 54
5.5 2nd Harmonic Output vs Polarizing Voltage for Discrete Input Power 55
5.6 2nd Harmonic Output vs Input Power for Discrete Polarization Voltage 55
5.7 Figures 5.1 & 5.3 with and without R_s 56
5.8 Figures 5.2 & 5.4 with and without R_s 57
5.9 Output Signal Forms with and without R_s 57
5.10 Efficiency for DC without Polarization 58
5.11 Efficiency for the 2nd Harmonic 58
5.12 Voltage and Efficiency for the Diode in Parallel with $P_{IN} = -10dBm$ 59
5.13 Voltage and Efficiency for the Diode in Parallel with $P_{IN} = 0dBm$ 59
5.14 Voltage and Efficiency for the Diode in Parallel with $P_{IN} = 10dBm$ 59
5.15 Voltage and Efficiency for the Diode in Series with $P_{IN} = -10dBm$ 60
5.16 Voltage and Efficiency for the Diode in Series with $P_{IN} = 0dBm$ 60
5.17 Voltage and Efficiency for the Diode in Series with $P_{IN} = 10dBm$ 60
5.18 Diode in Parallel with Different Matching Networks 61
5.19 Diode in Series with Different Matching Networks 61
5.20 ADS Simulated Circuit 62
5.21 Voltage Values for 3-Port Network Simulation 63
5.22 Output Voltage Values vs Input Power for 3-Port Network Simulation 64
5.23 HSMS-2850 IV Curve 65
5.24 Efficiency and Output Voltage with 5% Tolerance Components (Series Circuit) 66
5.25 Efficiency and Output Voltage with 2% Tolerance Components (Series Circuit) 67
5.26 Frequency Response with 2% Tolerance Components (Series Circuit) 68
5.27 Efficiency and Output Voltage with Longer Transmission Lines (Series Circuit) 68
5.28 Frequency Response with Longer Transmission Lines (Series Circuit) 69
5.29 Efficiency and Output Voltage (Parallel Circuit) 69
5.30 Frequency Response (Parallel Circuit) 69
5.31 Efficiency and Output Voltage (Villard Multiplier) 70
5.32 Frequency Response (Villard Multiplier) 71
5.33 Efficiency and Output Voltage (Dickson Multiplier) 71
5.34 Frequency Response (Dickson Multiplier) 72
5.35 Dickson Multiplier with 3-LEDs Cell (shorter lines) 72
5.36 Dickson Multiplier with 3-LEDs Cell (longer lines) 73
5.37 Yagi Antenna for $100MHz$ 74
5.38 Map Location with Antenna X 75
5.39 Map Location with both Antennas 76

List of Tables

1.1 HSMS-2850 Spice Parameters 10

4.1 S Parameters 43

5.1 FM Antennas Characteristics 75

List of Acronyms

AC Alternate Current

ADC Analogue-to-Digital Converter(s)

ADS Advanced Design System

AGC Automatic Gain Control

AM Amplitude Modulation

CMOS Complementary Metal Oxide Semiconductor

DC Direct Current

DDS Data Display Window

DF Describing Function(s)

DUT Device(s) Under Test

EEH Electromagnetic Energy Harvesting

EU European Union

FDTD Finite-Difference Time-Domain

FM Frequency Modulation

KCL Kirchoff's Current Law

GaAs Gallium Arsenide

GaN Gallium Nitride

SiC Silicon Carbide

GSM Global System for Mobile Communications

HB Harmonic Balance

LCD Liquid Crystal Display

LED Light-Emitting Diode

LSSP Large Signal S Parameters

MIT Massachusetts Institute of Technology

MOSFET Metal Oxide Semiconductor Field Effect Transistor(s)

MW Micro-Wave

NASA National Aeronautics and Space Administration

NLS Non-Linear System(s)

NLE Non-Linear Element(s)

NMOS N-Channel Metal Oxide Semiconductor

OOK On-Off Keying

PMOS P-Channel Metal Oxide Semiconductor

RFID Radio-Frequency Identification

RF Radio-Frequency

SDD Symbolically Defined Device

SIDF Sinusoidal Input Describing Function

SMIC Semiconductor Manufacturing International Corporation

SOT Small Outline Transistor

SPICE Simulated Program with Integrated Circuits Emphasis

TSMC Taiwan Semiconductor Manufacturing Company

TV Television

UHF Ultra-High Frequency

WF Weighting Function

WSN Wireless Sensor Network(s)

WPT Wireless Power Transmission

Chapter 1

Introduction

The general challenge addressed in this work was the development of optimized energy harvesting circuits, commonly known as rectifiers, with different topologies designed to maximize the efficiency of the converted RF energy into DC power for working at $100MHz$. Parallel to this, a couple of circuits were developed and implemented, whose objective was to power up a low consumption lighting system.

In this first chapter the main objectives of this work are presented, as well as the motivation for it's existence over the actual scientific situation. Besides, some of the involved concepts essential for the understanding of it's contents are introduced, divided as the process by which the energy is transferred from an emitter to a receptor: WPT, the non-linear components used, Schottky diodes, and the charge-pump mechanism responsible for generating higher output voltages. Another focused point is the objective of creating a no-cost lighting system, where some of the system possible applications and advantages are highlighted.

Secondly, on the state of the art chapter the current and most successfully solutions to the studied problematic of harvesting energy from electromagnetic waves are presented. The latest developments on the area are presented, covering a very wide angle of specific needs, being the scientific content organized in the non-linear element used, the rectifying topology, the bandwidth of the harvested energy and other techniques for efficiency increase. Here the main virtue of knowing what has been done so far, is getting to know the most common obstacles, the best and worse methods to address them, as well as having highlighted what still lacks adequate study and needs further investigation, thus helping directing this work. For instance, it can be pointed out that only a few papers study the power values in the circuits, and try to minimize the power wasted in reflections, [1] and [2], something that should be essential for every research.

Something else that is lacking in most of the literature is a careful study of the non-linear behaviours in the circuit. This is done in chapter 3, were a study of these properties is made, in order to recognize the processes that are the sources of the RF/DC conversion. In addition to it's characterization, tools are provided for it's study, being the linearisation and series expansion together with the describing functions the most focused on.

Chapter 4 presents the studied and implemented rectifier topologies, as well as the techniques used for achieving the best results, and starts by characterizing the lighting system and it's electrical needs, which have to be covered by some of the developed circuits. Here the progress of the work can be clearly seen, since not obtaining desirable results for the first proposed circuit triggers the study of new solutions. In this chapter distinct research from most

of the literature is presented, first with the polarization of the rectifying device, and then by providing an innovative graphical source-pull analysis for achieving best efficiencies and output voltages. Additionally more complex circuits with voltage multipliers were studied for the more practical objective of powering up the lighting system, together with a mathematical approach on one of the simpler rectifier circuits.

The results from both simulation and experimental measurements are presented in chapter 5 and follow the same structure as the previous chapter being the results organized accordingly to it. Since the first circuit achieved poor simulation results, as said before, this circuit was not built, however the better simulation output obtained for the following cases allowed experimental results.

Finally, on the last chapter an analysis of the obtained results, confronting them with the objectives purposed is made together with the signalization of possible directions for further investigation.

1.1 Motivation

Technology is advancing at a frenetic pace, as everyday breakthroughs are made in different areas, and innovative products are released to the market, due to the experienced bigger proximity between the investigation and the public needs.

Energy-aware RF circuits have been following this trend, and although they have been used for some time in Wireless Sensor Network(s) (WSN) applications both for military and civil purposed, as well as in Radio-Frequency Identification (RFID) for tracking, automation, access control or public transportation ticketing, an increased interest has rose over the last years in this field. The commodity and savings from not having to replace/charge batteries or plugging devices to the grid, is very well seen from consumers, essentially if these devices are of everyday use such as mobile devices.

Of course there is still much to do both about the improvement of the harvested power as well as in the reduction of the current consumption, however, at a medium/long term this type of solution will be most likely of general use. In fact, large electronics companies are already investing in this, which can be seen as a good indicator for the feasibility of the technology in a near future. Nokia for instance is currently developing a battery-free low-power consuming cellphone that harvests from many RF sources from $500MHz$ to $10GHz$, [3], while Intel created a wall-mounted weather station with an LCD screen using a TV antenna pointed at a local TV station $4km$ away [4].

Another two events that may act as catalysts for the success of energy harvesting systems are the use of these on biomedical applications were replacing batteries raises understandable problems and the dropping of polluting energy sources for reusable sources instead, guaranteeing an environmental friendly solution.

It's this world of possibilities that works as the main motivation for this work, the ability of being a part and contributing for something that will be of a vital importance in a near future.

1.2 Objectives

As said before the main objective of this work was to create a set of circuits to study the behaviour of different approaches and proposed solutions.

Nevertheless the more specific objectives that were purposed initially kept changing dynamically with the challenges and findings, being dependent on the results obtained. As an example the first circuit simulated, whose very low efficiencies led the work to change it's direction and drop the idea of external polarization.

Such an analysis permitted a better adjustment to the requirements and needs, and so the decisions were made better suitable to the final purposes. Furthermore, the objectives of implementing the proposed topologies would only be made if the obtained results were satisfactory.

So, the objectives which this work was made to address can be listed as:

- Understand the non-linear mechanisms behind the energy conversion;
- Simulate and analyse results for circuits with polarization;
- Optimize the energy harvesting circuits for the frequency of $100MHz$ and expected input power values;
- Implement circuits with good simulation results, so as to obtain experimental results in accordance;
- Harvest energy from local FM radio emitter with these circuits;
- Power up a low consumption lighting system with the harvested energy;
- Develop innovative solutions useful for subsequent researches;

Initial trials used a frequency synthesiser with a determinate input power, in order to make some measures over the circuit's efficiency and output voltage, however after this objective was accomplished a simple Yagi antenna was built to harvest the energy from a specific RF source, in this case an emitting Radio Station, and so proving the system operation.

1.3 Overview of Involved Concepts

For a better understanding of the processes and circuits studied in this work, a couple of concepts should be carefully presented before anything else. Although numerous concepts were involved in this study, only a few of the most important and general will be dealt with here, while the rest will be introduced on-the-fly.

Starting with the the mechanism that allows the transmission of the energy from an emitter to a receiver, WPT, a brief analysis over it's operation principles is made, together with the presentation of both the processes it compresses: the direct induction and electromagnetic radiation. Both are briefly characterized and exemplified with some practical applications currently on the market together with some ideas for the future.

Following, the non-linear element, responsible for the RF/DC conversion, where a quick presentation of the Schottky diode is made, both in general and for the specific component used. As of the phenomena by which this conversion is made, it will be seen in detail in the chapter of the non-linear systems.

Finally a quick look over the charge-pump mechanism is taken, which is essential for understanding some of the implemented circuits that rectify the input power with more than one stage, in order to generate higher output voltages.

1.3.1 Wireless Power Transmission WPT

Wireless power transmission is the process by which energy is transferred from one source to a load without conductive connections. Although this topic has been much in vogue recently, it's studies are not that recent, since they date back to 1888, when Hertz highlighted the existence of the electromagnetic waves imagined by James Maxwell a few years before, in 1873, by successfully engineering adequate instruments to transmit and receive radio pulses.

The investigation on power transmission by radio waves went further with Nikola Tesla, whom in 1899, with the support of the Colorado Springs Electricity Company, built a gigantic coil in a large square building, over which rose a mast of 70 meters with a copper sphere at the end [5]. This coil, which was resonated at $f = 150KHz$ and fed up with $P_{IN} = 300KW$, produced, accordingly to Tesla, a potential as high as $V = 100MV$ and created very long and visible discharges from the coil's sphere to the ground. Even though high amounts of power were clearly radiated, there is no clear record of it's quantities or if this power was ever collected.

More recent developments in this area are related with the RFID [6], which was first introduced in 1973, and whose range kept increasing over the years, and a couple of other developments in the last 5 years, namely:

- Wirelessly powering up a $60W$ light bulb with 40% efficiency from 2 meters distance, (MIT, 2007) [7]
- Development of a wireless high efficiency $3W$ LED lamp (Brunei University, 2008)
- Deployment of a cellphone chargeable with a wireless source (HP Palm, 2009)
- Creation of a wireless induction powered TV, with $60W$ powered at a distance of $50cm$ (Sony, 2009), followed by the first completely wireless LCD television (Haier Group, 2010)
- Development of a high efficiency system for power and data transmission in biomedical implants (University of Utah, 2012)

As of the type of energy transmission, a distinction can be made between two methods: direct induction and electromagnetic radiation. The first, generally having a more local characteristic, requires two inductive elements coupled together as an electrical transformer and causes energy transmission through a magnetic field, while the latter uses the far-field radiation, which contains both electric and magnetic fields, to harvest energy emitted from sources many kilometres away. Included in the last are the studied and implemented circuits in this work, since they rectify the far-field energy emitted by a remote source.

Direct Induction

When electrical current moves through a wire, a circular magnetic field is created around it, magnetic field which is greatly amplified if the wires are bent around a coil. By adequately placing a second coil with a similar structure very near, this magnetic field provokes an opposite effect to the previous, and induces a current in the secondary element.

This energy transmission method which is already deployed in the market nowadays, is used for instance to power up electrical tooth brushes, so as to reduce the hazard from having the wires in contact with water. Another application of this method is used by the Splashpower

Figure 1.1: Generic Inductive Charging Platform (source [8])

Recharging Mat or the Edison Electric's Powerdesk, which generate a magnetic field capable of charging various electronic devices at the same time, provided that they have corresponding plug-in receivers. This solution provides a very practical charging mechanism since no wires are involved, being only necessary to place the devices on top of a platform to charge, as depicted in figure 1.1.

This type of system however, produces very small magnetic fields, and so the emitter and receiver must be at all times close to each other. To achieve larger and stronger fields to induce current from farther distances, without performing changes to the emitter and receiver, enormous amounts of energy have to be radiated, since the magnetic field is spread in all directions what makes the process very low efficient and energy waster.

Nevertheless in November 2006, a team of researchers from MIT reported that a more efficient way to transfer energy between two coils separated from a few meters had been found, by adding resonant elements to the system, having named the process "WiTricity" as in Wireless Electricity, [7]. A possible application of this system is found on figure 1.2. More specifically it was proved that if the electromagnetic fields around the coils were to resonate at the same frequency, the mechanisms of induction would become somewhat altered, thus permitting an increase in the range of inductive WPT.

Using a curved coil as an inductor and capacitance plates at the end of it creates a controlled resonance, whose frequency can be tuned and matched between emitter and receiver. This way energy is exchanged strongly without having an effect on other surrounding objects, specifically the human bodies, as explained in [10].

The fact that the frequencies used are rather low (wavelength around $30m$) also reduces the human interference, because a couple of meters away from the emitter the waves are still in the near-field, where only the magnetic field exists. This non-existence of electric field makes the emitted radiation harmfulness since the human body only absorbs this type of energy, and not the magnetic. Moreover the energy not transferred to the receiver is re-absorbed by the emitter antenna if both are resonating at the same frequency, resulting that not much energy gets lost flowing away in the air.

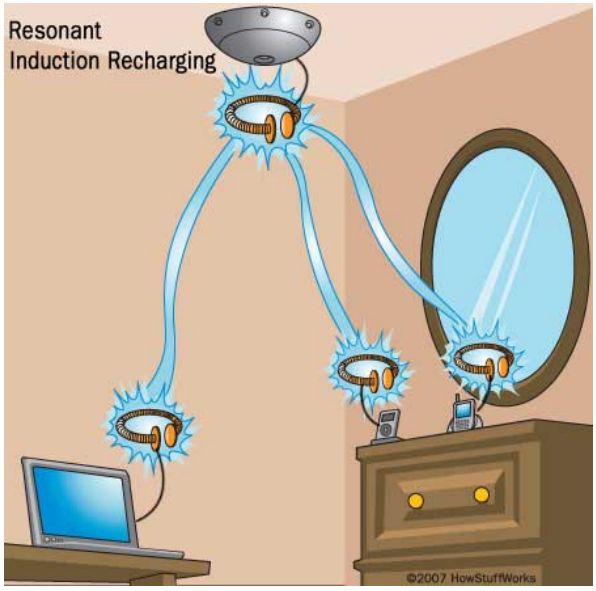

Figure 1.2: Resonant Induction Recharging System (source: [9])

Electromagnetic Radiation

The main step-back of the inductive method, specially without resonance, is the fact that the emitted radiation pattern is isotropic, and the energy just disperses all around the emitter, hardly reaching the far-field with significant amount of energy at a specific area.

On the other hand the far-field methods can reach longer distances, as far as multiple kilometres, mostly because the emitters employ directivity in the radiated waves, matching them with the shape of the receiver's area. This method is better suitable for higher frequencies, reason why typically this type of power transmission is made at radio or microwave frequencies, where the wavelength is much smaller than the inductive examples provided before.

As of the system's structure, a well-defined model for the receiver is generally used, consisting in a receiving antenna, a rectifying circuit to convert the RF to DC, and a regulator, capacitor or load at the output, being the whole commonly known as rectenna, pictured in figure 1.3. The emitter on the other hand has no typical configuration, since energy can be harvested from multiple distinct sources of RF energy, such as TV, FM and AM stations, GSM or even local WPT systems as employed in the RFID ticket systems, as will be shown in a following section.

As an example of electromagnetic radiation systems deployed in the market are some WSN, whose remote locations are ideal for this type of system since the replacement of batteries is a complicated task. Alternatively a different example of a complete electromagnetic radiation system can be found on [11], were a lunar wireless power transfer system is proposed, with multi-kilowatt power transmission. This project, sponsored by NASA, relates with the objective of establishing a permanent base in the moon, and studies a method to address the electrical needs of such a construction.

The provided solution comes as an alternative to the traditional line system, whose main step-backs for this purpose can be listed as:

- Estimated mass for five load stations vey large in comparison with the WPT (7500 Kg

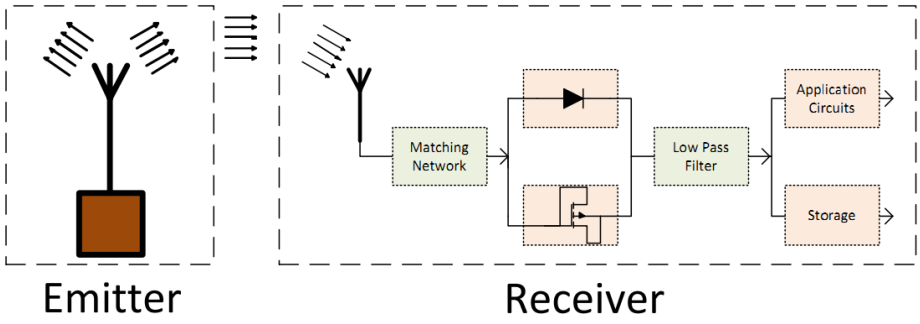

Figure 1.3: Typical WPT Electromagnetic Radiation System

vs 4200 Kg);

- Large distances the transmission lines would have to traverse;
- Transportation of the cables from earth to moon;
- Susceptibility to solar flare effects;
- Safety hazard it may cause to lunar operations;
- Difficult management.

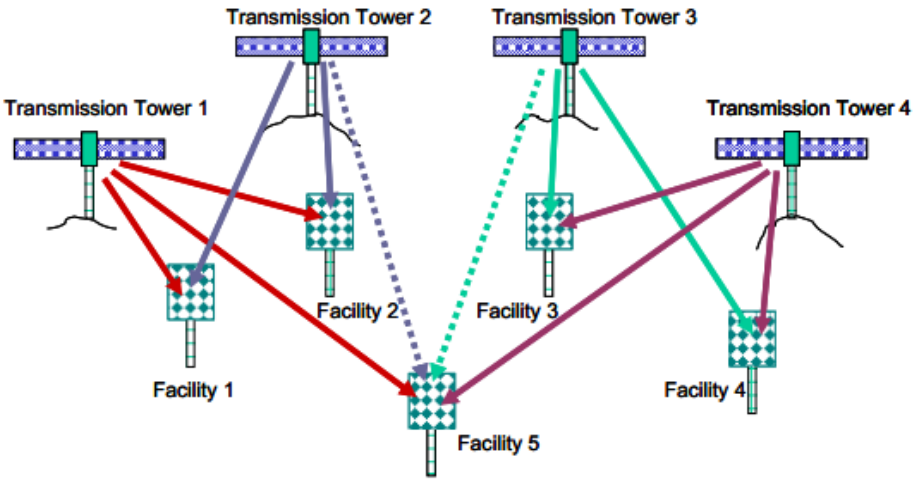

Figure 1.4: Structure of the WPT System (source [11])

The proposed structure is pictured in figure 1.4, were the moon facilities are each remotely powered by two or more transmission towers with solar power stations, ranging the distances between the emitter and receptor from 0.5 Km to 2 Km.

A final note for the fact that this system uses far-field high-frequency radio-wave powering systems, instead of inductor coupling since it would be impossible to achieve this kind of power

transmission for these distances with any other approach, even with resonance structures. Also, the system has incorporated highly-directional antennas for beaming, with high-efficiency transmitters and high-efficiency receiving rectifiers to get the best results possible.

1.3.2 Schottky Diode

A Schottky diode is a particular type of diode, invented by Walter H. Schottky, that consists on a metal-semiconductor junction, instead of a semiconductor-semiconductor junction as in conventional diodes, where one side contains negative charge carriers or electrons (n-type), and the other positive charge carriers or holes (p-type). In this diode the metal side acts as the anode and the semiconductor of n-type acts as the cathode, so only n-type carriers play an important role in it's operation, resulting in a *majority carrier* semiconductor device. These majority carriers are quickly injected into the conduction band of the metal contact, and so there is no slow recombination of n and p-type carriers what results in the Schottky barrier being lower than conventional (from $0.7V$ to $1.7V$ in p-n diodes versus $0.1V$ to $0.5V$ in the Schottky).

In addition to these structural differences, the recovery time of Schottky diodes, that is responsible for the switching of the diode from the non-conduction to the conducting state and vice versa, is very different in both cases. In typical diodes, this time varies between hundreds of nanoseconds for high-power components and dozens of nanoseconds for faster switching types, while for the Schottky this time is almost null and only depends on the capacitive loading. The justification is in the in-existence of a carrier depletion region at the junction, since there aren't holes/electrons-recombination when those enter the opposite type of region. These special features allow the production of devices with smaller areas, what reduces the time constants, allowing them to be used at frequencies an order of magnitude above, up to $50GHz$.

For p-n diodes switching, there is also the issue of reverse recovery current, that may result in electromagnetic interference noise for high-power semiconductors, while for Schottky diodes the almost instant switching makes this quite insignificant.

There are however some limitations, mostly related with the low reverse voltage rating and high reverse leakage current. The latter, for instance, being temperature dependent may lead to thermal instability, thus limiting the reverse voltage to well below the actual rating, and so must be controlled.

The differences from the conventional p-n diodes guarantee this type of diodes advantages for specific applications, specially if high frequencies are involved:

Prevent Reverse Current Stand-alone photovoltaic systems use this diodes to prevent batteries from discharging through the solar cells at night. Similarly it is used in grid-connected systems with multiple strings in parallel, to prevent reverse current flowing between adjacent strings;

High-Frequency Rectifiers and Diode Ring Mixers High switching speed, high frequency capability and low capacitance together with the low forward voltage are ideal for high frequency applications. This is the reason why these diodes were used in this work, since they fit the needs of the RF/DC rectifier;

High-Power Applications High current density and low voltage drop, mean that less power is wasted in comparison with p-n diodes. This is rather appealing for high-power recti-

fiers, where an increase in efficiency, means less dissipated power, and so smaller heat sinks can be incorporated;

Clamp diode The diode is inserted between the collector and base of a driver transistor to work as a clamp. To produce a logic *0* the transistor is driven hard on, so the presence of a Schottky diode helps draining most of the current, thus reducing the turn off time of the transistor and increasing the speed of circuit.

Additional information on the Schottky diode and it's operation principles can be found in [12] and [13].

Diode Agilent HSMS-2850

The most used diode during this work was the zero bias Schottky detector HSMS-2850 from Agilent Technologies, [14], which is a rather low-cost diode with good response up to 1.5 GHz, with a high detection sensitivity (up to $50mV/W$ at $915MHz$) and low flicker noise ($-162dBV/Hz$ at $100Hz$) that doesn't need DC bias. The device's IV curve is pictured in figure 1.5, where it can be noted that the forward voltage is $150mV$ at $0.1mA$ or $250mV$ at $1.0mA$, what is lower than the great majority of Schottky diodes, and can be useful when dimensioning high-sensitivity rectifiers since it requires less input power to for biasing.

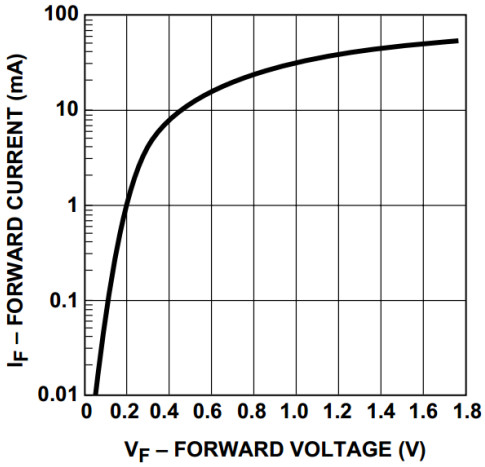

Figure 1.5: HSMS-2850 IV curve (source: [14])

The equivalent linear model, which is found in figure 1.6 consists of a variable resistance R_j that works as the voltage dependent current source:

$$R_j = \frac{8.33 \times 10^{-5} nT}{I_b + I_s} \tag{1.1}$$

, where I_s is the saturation current and I_b the applied current, but also of a series resistance, R_s and a capacitor, C_{j0}, whose values can be found on the SPICE parameters table 1.1, amongst others.

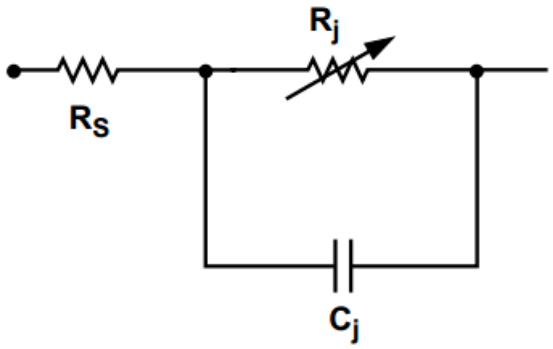

Figure 1.6: HSMS-2850 Equivalent Linear Circuit Model (source: [14])

Parameter	Units	HSMS-2850
B_v	V	3.8
C_{j0}	pF	0.18
E_G	A	3e-4
I_s	A	3e-6
N		1.06
R_s	Ω	25
$P_B(V_j)$	V	0.35
$P_T(XTI)$		2
M		0.5

Table 1.1: HSMS-2850 Spice Parameters

Although this diode had many virtues, a couple of disadvantages were found, namely about the series resistance and the real IV curve. The former proved to be larger than desirable, since it's Joule loss effect had some effect on the overall results obtained, reducing the efficiency, while the latter was an invalid model, since some trials with it resulted in very poor results, while a manual curve obtained experimentally lead to much more realistic results.

Finally, the package model was the SOT-32, which has rather small parasitic elements and is very well suitable for applications at $100MHz$.

1.3.3 Charge-Pump Mechanism

The quest for generating high voltage supplies from lower available sources has been a recurrent issue throughout the story. One can go back as far as 1831 to find the first reference of such a mechanism with Faraday's "induction ring", but it can be said that it was the need of particle accelerators that served as a catalyst for most of the important discoveries that are still used today. Amongst these, are the studies made by Cockcroft and Walton on the issue, who successfully created a charge pump consisting only of discrete diodes and capacitors, and the Dickson modifications over this circuit which made it suitable for modern integrated circuits.

Starting with Faraday's discovery it basically used a transformer to increase the voltage,

where the voltage relationship between the input and the output is given by the well-known equation:

$$\frac{V_o}{V_i} = \frac{N_i}{N_o} = N \tag{1.2}$$

In order to maintain the same power, this change of voltage is nevertheless accompanied with an equally inverse change in the current, assuming an ideal system.

Amongst the main disadvantages of this solution are the fact that it only works with AC-AC conversion, making necessary a rectifier on the output to generate a DC value, and that it requires very large transformers for high voltage generation, which are known to have substantial losses and to be are far from ideal unlike it's smaller counterparts.

The Cookcroft-Walton charge pump (also known as Villard rectifier), on the other hand can directly provide a DC output, and achieve voltages of many KV. In fact by the time of their experiments, Cookcroft and Walton were able to generate a potential as high as $800.00KV$ to feed a particle accelerator, and ended up winning a Nobel prize for it.

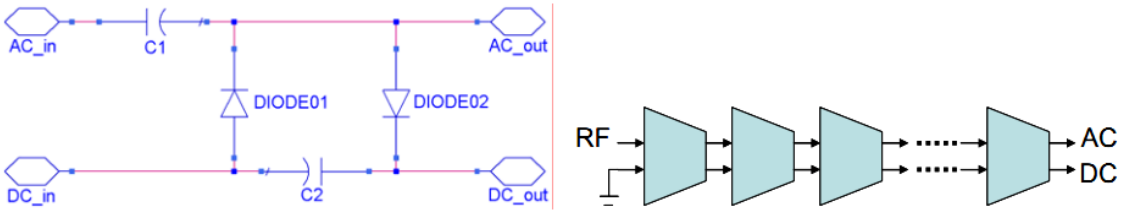

Figure 1.7: Cookcroft-Walton/Villard Voltage Multiplier (source: [15])

A great advantage of this system, whose topology can be found in figure 1.7, is that is made of diodes and capacitors, making it much cheaper and lighter than it's counterpart and also having with much smaller losses. The output of a such converter, assuming n the number of stages, $AC_{out} = 0V$ and ideal diodes, can be listed as:

$$V_{DC_{out}} = 2nV_{AC_{peak}} - V_{load} \tag{1.3}$$

, where the maximum output is obtained for an open load, that is $V_{load} = 0$. It is also important to realise that for larger n values the parasitic capacitances start to matter, and for a certain number of stages the output stops increasing, and starts decreasing. This problem is rather important for integration on chip, since the parasitic capacitances are closer to the discrete capacitors, and is why a different solution was proposed by Dickson.

Dickson's main innovation consisted in placing the nodes of the diode chain connected to the input via capacitors in parallel instead of in series, as can be seen in figure 1.8, so all the capacitors with-stain the voltages along the chain, thus making the current drive capability independent of the driving stages. Furthermore to completely integrate this charge-pump circuit on chip with CMOS fabrication processes the diodes in the scheme may be replaced by MOSFETs in diode configurations.

The circuit proposed by Dickson seemed very general and applicable to all situations for a long time, until a decrease in circuits supplies brought them to voltages under $2V$ and a problem related with the body effect started to gain importance, problem which is analysed in more detail on [16].

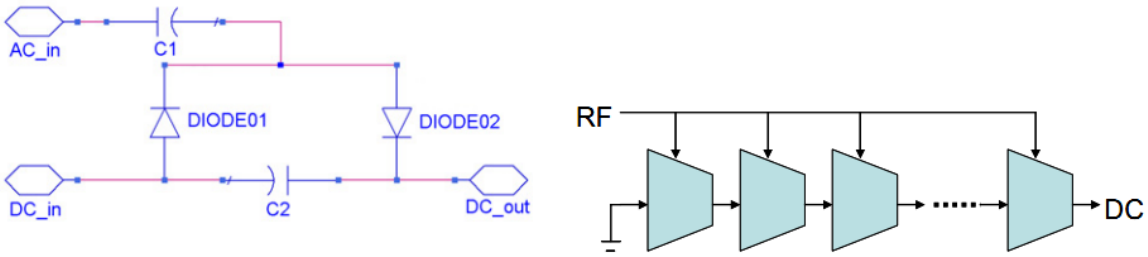

Figure 1.8: Dickson Voltage Multiplier (source: [15])

1.4 Lighting System

Besides the development of maximum efficiency circuits, without concern for no application specifications, a study was made to create a system to power up an illumination source, only using harvested energy. This system, which had different requirements, was also sized to harvest from the $100MHz$ band, more specifically from local radio emitter stations, and was appropriated to the lighting system electrical characteristics.

Both the system characteristics, as well as of the rectifier's are presented in a following chapter, since for now only the concept is to be introduced.

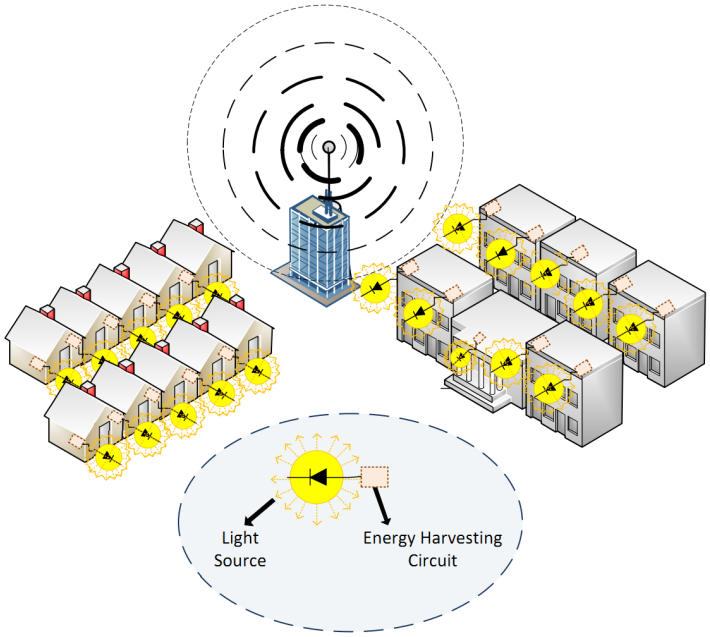

Figure 1.9: Green Illumination Neighbourhood

An example of this lighting system, is pictured in figure 1.9, in the form of a green illumination neighbourhood, where the green stands for the environmental compromise of re-utilizing ambient energy instead of simply consuming it. In a context of crisis, which is predicted to stay for some time, and when the price of electricity continues to increase (in Portugal the price is 18.8 Euro per $100KWh$ against the EU average of 18.4 Euro), this is the type of

solution that may help swimming against the tide.

Besides being a country that invests in reusable energies and is moving to a complete electricity autonomy, this is an additional help in doing so. The fact that the system is optimized for the frequency of $100MHz$ and is to be placed near radio station emitters, is also only a reference since similar circuits could be developed for different frequencies, thus taking advantage of the fact that the amount of energy amongst us is growing, as different technologies with different frequencies arise.

1.5 Conclusion

Having defined the major motivation factors behind the development of this work, together with the main objectives to be addressed a quick scope into the work was made in this introductory chapter.

Some of the involved concepts, important for contextualization were provided, such as the WPT method were the electromagnetic radiation process corresponds to the method of harvesting energy studied here, the Schottky diode (with particular distinction for the HSMS-2850 since it was used in all circuits) used as the rectifying element, and the charge pump mechanism, another important concept, specially in the point of view of the latest developed circuits, whose objective was to obtain higher output voltages.

Finally the illumination system to be powered up with harvested energy, and respective concept of no-cost illumination were analysed and it's practical implications in the current sensitive economical context revised.

Chapter 2

State of the Art

The latest developments on the subject of energy harvesting have taken different directions, trying to solve specific needs and presenting them to distinct solutions. In the following pages a closer look on the most state of the art techniques for electromagnetic energy harvesting will be presented, being divided in the following sections: the non-linear element, the rectifier topology, the bandwidth of the energy harvesting, and other techniques for increasing efficiency.

2.1 Non-Linear Element (NLE)

Generally the first thing to do in designing energy harvesting systems is to select the element that will generate the harmonics responsible for the conversion of the RF energy into DC, that is, the non-linear element. In theory, since any device has non-linear behaviour, as will be explained further ahead, any device could be selected, however the high non-linearities present in the diodes and the MOSFET turn them into desirable targets.

2.1.1 Schottky Diode as NLE

The most regular choice for the Non-Linear Element(s) (NLE) is the diode, more specifically the Schottky diode, due to it's low forward voltage, together with valid responses up to higher frequencies, as explained in the previous chapter. The main problem is the hard fabrication using conventional techniques for integration on chip, so off-the-shelf components are generally employed instead, with the inherent disadvantages of using generic components not specifically adapted to the purposes.

The group of papers [1],[17], [2], [18] and [19], for instance, study the *MA4E2054* Schottky diode under two similar topologies (figure 2.1), allowing many conclusions about the operation of energy harvesting circuits with such component. These are studied at $f_{IN} = 5.8GHz$ and employ transmission lines instead of discrete components for output filtering, being able to achieve efficiencies higher than 60%.

On [1], where a diode in series with the input port is used followed by a low pass filter, a theoretical study is made, providing an equation for the output voltage. This equation results which are proven to be in accordance with the simulation values, allow a bigger insight on the involved processes and a better understanding of the circuit operation, thus facilitating the process of increasing the efficiency.

A dual topology, with the diode in parallel with the load, is shown in [2], using the Finite-Difference Time-Domain (FDTD) method to calculate the efficiency and then successfully comparing with the experimental results. It uses transmission lines both in the output filter, and in series with the diode, that are carefully tuned to minimize reflections and thus maximize the power conversion. The series of figures that portray this dependence on the length of the lines, show that a maximum value of $\eta = 65\%$ can be achieved. Furthermore a table of the consumed/converted power presents the estimate of all the power values in the circuit: the converted power, the reflection of the fundamental mode of the input, the harmonics on the input, the consumption of the diode and the radiation loss.

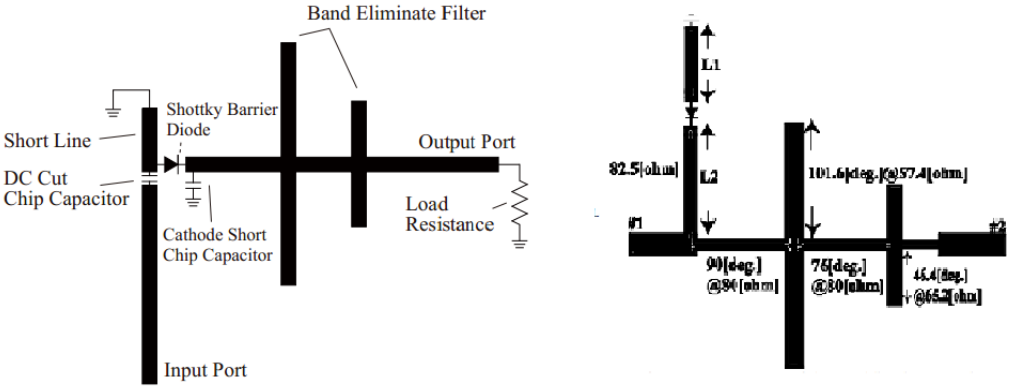

Figure 2.1: Rectifier with Transmission Lines (source: [19] and [1])

The influences of the diode parameters on the efficiency is studied on [17], which employs a diode in series with a low pass filter. The circuit is simulated with both SPICE, and FDTD method, but only the second one shows consistent data, since SPICE results are very distinct from the experimental data. This article highlights the dependence of these results with the NLE capacitance and resistance, whose non-existence catapults simulation efficiencies to values higher than 85%.

The last paper of the group introduced, [20] uses full wave rectification instead of half wave. However this option does not significantly improve the efficiency and only reduces it's dependency with the load, also allowing higher resistances to be used. The maximum efficiency is again close to 70%, and is obtained for $P_{IN} = 45mW$ and $R_L = 925\Omega$.

A very different approach is taken on [21], where a decision was made to fabricate the diode using an ALGaAs/GaAs Heterostructure, in order to obtain a more customized component (figure 2.2). This allowed a direct on chip integration of the Schottky diode into a planar dipole antenna without insertion of any matching circuit, resulting in a reduced barrier height. This ought be beneficial for improved RF response and rectification as it requires a lower turn-on voltage, and a smaller contact area which means less resistance. Reducing the resistance also meant less power dissipated/wasted on the diode as well as good responses at higher frequencies (up to $20GHz$). A too small resistance however may limit the detection before the device burns up, so there must be a careful design compromise. Due to it's particular characteristics this type of device can be regarded as a very good option for low input power and low DC voltage applications.

A bigger insight on Schottky diode's creation can be found on [22], where high-performance

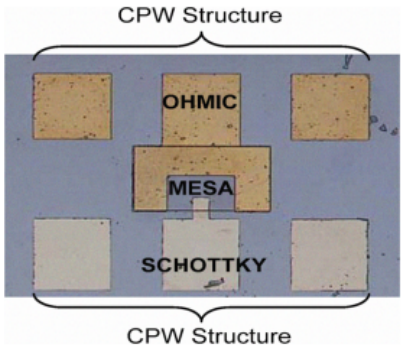

Figure 2.2: Top View of Fabricated Schottky Diode (source: [21])

low-loss Schottky varactor diodes have been fabricated in a silicon-on-glass substrate transfer technology. These show high quality factors from 100 to 300, at $f_{IN} = 2GHz$, that are obtained due to a successful reduction of the ohmic contact of the device.

2.1.2 MOSFET as NLE

The use of MOSFET in diode connected configurations is also rather common, so some information can also be found in the literature. This choice is generally made when integration on chip is required, so the circuit can be fabricated as a whole, what is not so easily done for the diodes as explained earlier.

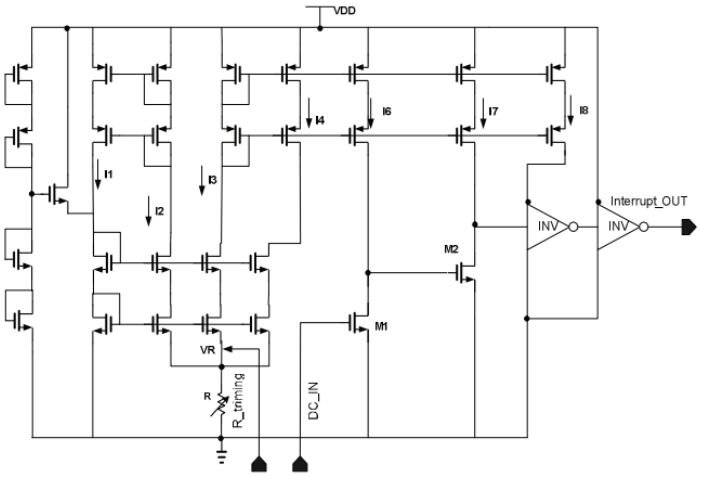

Figure 2.3: Ultra Low Power DC Sensing Circuit (Source: [23])

In [23] traditional NMOS transistors are used, along with a passive voltage multiplier, both designed and implemented using $0.18um$ CMOS technology. It presents a $f_{IN} = 2.4GHz$ RF/DC rectifier together with an innovating DC sensing circuit (figure 2.3) for the improvement of the circuit's sensibility. The rectifier is made with NMOS transistors and a voltage limiter on the output to limit the power amplitude when in the near field. The use of the DC sensing circuit, allows a sensibility as low as $-28dBm$, generating an output of $\approx 200mV$.

A special configuration for the diode connected MOSFET fabricated in a SMIC $0.18um$

CMOS process is shown in [24]. This paper includes a careful theoretical analysis on the rectifier's operation and compares the simulation output with these considerations, having obtained similar results in both cases. It uses a 3-stage charge pump rectifier, were the basic unit is the optimized diode connected CMOS of figure 2.4. The results presented show that for a $315mV$ turn-on voltage MOSFET, simulation efficiencies around 45% and output voltages of $\approx 4V$ are obtained for input power values of $-10dBm$.

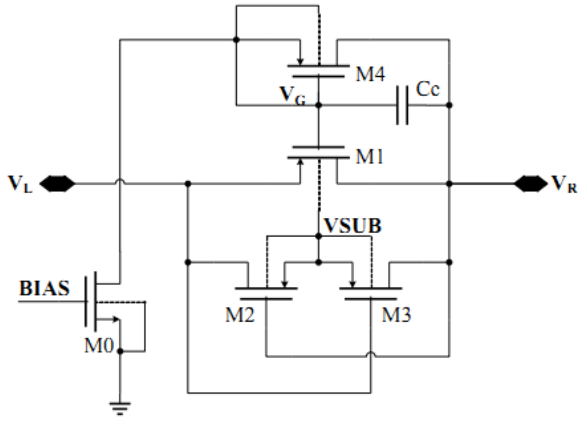

Figure 2.4: Schematic Diagram of Optimized Diode-connected CMOS (source [24])

Another modified version of the traditional CMOS voltage doubler can be found on [25], one that uses smart energy harvesting circuits for gathering energy from different sources, selecting the stronger source dynamically. This system claims it's main application to be the placement near RF sources such as wireless routers or fully charged mobile handsets so as to help charging other non-charged mobile handsets.

Finally on [26], a RF/DC rectifier for an UHF power harvester in the $915MHz$ band, fabricated in TSMC $0.18um$ CMOS process is presented. This voltage multiplier has a sensibility of $-9.5dBm$, for which generates an output voltage of $1.2V$, while generating $1.8V$ for an input power of $-7.8dBm$.

2.2 Rectifying Topology

To obtain higher output voltage values so as to power up commercial circuits, special rectifying topologies known as voltage multipliers must be used instead of the basic envelope detectors. The basic mechanism behind these multipliers is the charge-pump that was presented earlier, and uses capacitors as energy storage elements to create higher voltage power sources.

A careful study of the Dickson topology, the most commonly used on energy harvesting systems, is presented on [27], where analytical results that enable the estimation of the rise time of the output voltage and of the power consumption during boosting are provided. These results are in most agreement with the simulation results, proving it's validity, and it's usefulness as a tool in dimensioning voltage multipliers. A similar analysis is made on [28], were additional tools to find the best number of stages for specific applications are provided.

Concerning the application of these multipliers into RF/DC converters, in [29], a Dickson rectifier is used to harvest energy from a local radio station. It uses 6-stages and charges an

output capacitor with $520mV$, harvesting $60uJ$ per hour. This solution is viable for WSN that use a periodic awakening, and are not always being powered.

Another application of this multiplier is found on [30], were a study of the efficiency with the number of stages and load values is made. In this case the multiplier which is made of 5-stages works in accordance with a voltage boosting network, resulting in $Vo = 1V$ for an input of $-16.5dBm$.

Nevertheless, the most interesting results are found on [15] and [31], were both topologies cited above are considered and compared. The former studies the performance of both topologies with two stages, jointly with a resonant tank with high quality factor, having obtained very similar results.

In the latter two more configurations are added, the resonant Dickson and the resonant Villard, both adding a coil in series with the input. Although for the generic multipliers the results are again similar, in accordance with the previously exposed, for an input of $200mV$ experimental results denote a significant difference between the resonant circuits. With an open circuit, a voltage of $1.6V$ and current of $8uA$ are obtained for the resonant Villard, while the resonant Dickson obtains $2.75V$ with $3.5uA$. One last note for the flat answer of the generic structures in contrast with the resonant structures, where the response is highly frequency-dependent, presenting the maximum values for $f_{IN} \approx 1.6GHz$.

2.3 Bandwidth of the Energy Harvested

A further distinction between energy harvesting systems is the source of the harvested energy. It is possible to design a broadband system that gathers energy from multiple environmental sources of RF, or a narrowband system that is optimized for only one frequency source.

At first sight, the former option seems more logical, since it has many sources, and thus can harvest more energy at the same time, also being more independent on a specific emitter, however this is not quite that simple. The fact is that since the impedance of the rectifier circuit varies with the frequency, whilst the impedance of the antenna is kept more a less constant, it is almost impossible to match these two components for minimum reflected power, for a great variation of the input signal frequency. On the other hand, for a specific frequency adequate matching can be done, specially if the input power is more a less predictable, and so the insertion loss is minimized and the power delivered to the system is maximized

There are some solutions that will be presented further ahead that use more than one rectenna to harvest energy from different bands, and them combine the outputs with a DC combining system, such as [25] or [32], however most of the solutions proposed in the literature harvest energy from one specifically tuned frequency.

This is the case of almost all the solutions presented so far, which are generally tuned to the frequencies of $100MHz$, $863.8MHz$, $1.58GHz$ or $2.4GHz$, which represent the signal emitted mostly by FM radio stations, mobile communications and Wi-Fi, and so can be found almost everywhere with reasonable power values for harvesting.

An alternative to harvesting from remotely located emitters is the one used by RFID systems, where the receiver harvests from a local source. This is the case of [33] and [26], that employed a $950MHz$ wireless power transmission system with an interrogation range of $10m$ is employed. This approach might be useful for specific applications, such as RFID tags on public transportation tickets, however it does not guarantee a complete energy independence

essential for systems such as WSN, since the emitter has to be close and has to be powered up.

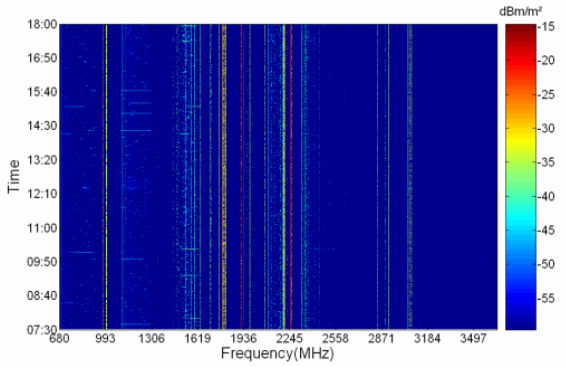

Figure 2.5: Measured RF Power Density (source: [34])

Lastly a comparison between a narrowband system at $1.8GHz$ and a broadband energy harvesting system can be found on [34], where the measurements of the outdoor RF power density were inclusively made in order to better tune the former. The harvested values were respectively $400pW$ and $12.5pW$, confirming the affirmations about the better performance of narrowband systems.

2.4 Other Techniques

Apart from choosing low turn-on voltage, fast turning devices and voltage multipliers there is still much to do to increase the efficiencies of RF energy harvesting circuits. Some further considerations on the already described solutions, as well as a few other state of the art solutions are to be presented next.

For starters, the method used in [23], that was shown previously, and consists on a regular NMOS rectifier with a DC sensing circuit (figure 2.3), that only consumes DC current when an input above a sensibility level is detected. This scheme receives radiation from a local emitting source, modulated as an OOK signal, and only wakes the system from deep sleep mode when the received identification code matches it's own. As advantage it doesn't need to use duty cycle scheduling as a power management scheme, since only consumes when queried, what simplifies the system.

Similarly to the DC sensing circuit, the solution on [24], was already presented, however here attention should be drawn for the alternative scheme of the diode-connected CMOS, that allows higher output voltages and smaller ripple values(figure 2.4).

The same idea of modifying the basic rectifying cell is employed in [35], where two techniques are used to increase performance of the system. The proposed converter employs diode-connected transistors with gate to drain bootstrapping capacitors so as to overcome the threshold voltage, and applies cross-couple bulk biasing to further reduce this threshold voltage and ensure faster turn on. Besides, the transistors are biased in triode region to improve the driving capability of the circuit while operating at lower input voltages. The results obtained show an efficiency of 18% for $P_{IN} = -10dBm$ generating $V_o = 1.1V$, while traditional methods have efficiencies around 6% for the same input power, and output voltages of $0.25V$.

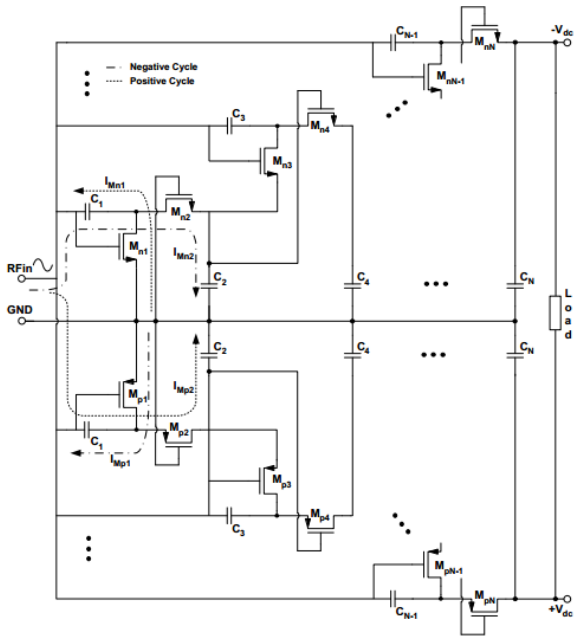

Figure 2.6: RF/DC Converter with Complementary Configuration (source: [35])

One last note to the employed complementary configuration, that generates both $+V_o$ and $-V_o$, what might be useful for some applications.

Another technique already refereed previously is the use of a DC combining section, as made in [32]. In this paper a ultra-wide band antenna that is used to gather energy from multiple sources, is connected to a series of circuits each containing a frequency tuned matching network and rectifying circuit. These are then connected to the combining section, thus generating an output power equal to the sum of the output of each rectification circuit. Although no results were presented in this work, the compromise between narrowband systems and energy gathered from many sources ought be a very well thought solution. A similar approach, briefly studied on [36] consists in separating the broadband antenna in an array of rectennas and then submitting the output of each to combining section, thereby using antennas that are optimized for the different frequencies.

Focusing on the matching network on the other hand, allows increased sensibility and voltage boosting by acting on the quality factor of the adaptation circuit. This is done for instance in [15], where a resonant tank is used both as matching network and as a voltage boosting mechanism that reduces the circuit sensibility by increasing the voltage at the input of the rectifying unit. A very useful formula is provided for this dependency with the quality factor, having figure 2.7 as a reference:

$$V_{out} = V_s \left| \frac{j\omega L + \frac{\omega L}{Q}}{j\omega L + \frac{\omega L}{Q} + \frac{1}{j\omega C} + R_s} \right| \tag{2.1}$$

Where an ideal quality factor implies:

$$V_{out} = \frac{1}{R_s}\sqrt{\frac{L}{C}}V_s \tag{2.2}$$

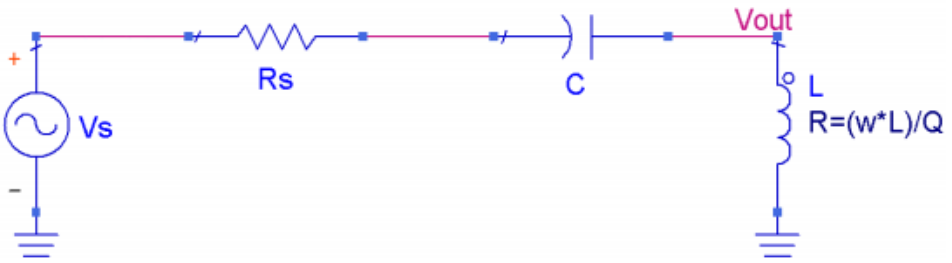

Figure 2.7: Simple Resonant Tank (source: [15])

In the results presented, although an input of $-20dBm$ implied a value of $32mV$ at the input of the rectifier, which is much lower than the diode threshold, the use of the matching network generated a voltage swing that was large enough to overcome the diode barrier. The high Q factor for this network was obtained through careful layout design, and allowed an output of $0.8V$.

A similar study to the former is made on [26] were an equation for the relationship between the input power at the antenna and the output voltage of an n-stage rectifier is provided.

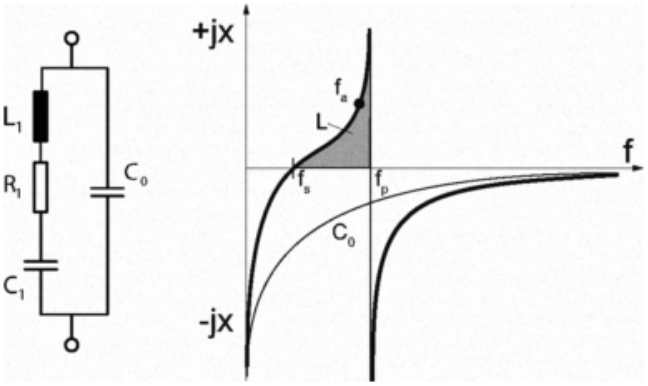

Figure 2.8: Crystal Equivalent Circuit and Frequency Response (source: [37])

A sharpest concept is used on [37], where the inductor is replaced with a quartz crystal resonator, thus providing an even higher quality factor. This element is characterized with two different resonances, f_p (parallel resonance) and f_s (series resonance), between which has inductive behaviour and is schematically pictured in figure 2.8. In this figure C_0 represents the static capacitor caused by the package and L_1, C_1 and R_1 custom components. The effective inductance value is given as:

$$L = \frac{2\Delta f}{f_s} L_1 \tag{2.3}$$

The careful matching of this circuit, using the quartz resonator resulted in a sensitivity of $-30dBm$ for a DC output voltage of $1V$ and an efficiency of more than 22%, which is rather satisfying in view of the low input power. Lastly, relating to high Q matching networks, a

bigger insight can be found on [38].

Finally, [39] explores the growth in efficiency achieved with the reduction of the dissipated power on the diode, by lowering it's series resistance. This is achieved by replacing the rectifying diode with two of the same in parallel, and so changing the overall series resistance to about the half. This investigation, being made with a basic rectifier circuit with the diode(s) in parallel with the load at $24GHz$ also presents two different solutions for the output filter, one made with a capacitor as the load and the other with a transmission line filter. As of experimental results efficiencies are approximately 52% and 66% for the capacitor and transmission lines solutions, respectively, however the power input values are not specified. One last note of attention for the fact that the parallelization of the diodes doubles it's junction capacitance effect, however the component used presented values of capacitance very low ($0.02pF$), so doubling this value was not critical.

2.5 Conclusion

Having made a review of the current state of the art techniques for the increase of electromagnetic energy harvesting efficiencies and sensitivities, an increased awareness on the current solutions in the literature was obtained. Although some of the studies have shown better efficiencies and output voltages than others, all the results shown have it's relative importance for the improvement of these systems, and so useful insights and lessons can be learned from them. Furthermore some of the mechanisms presented like the tuning of transmission lines or the use of resonant tanks can be inclusively applied to the work in question.

With this knowledge it is also possible to try to complement some of the solutions developed on this area, filling some gaps, as well developing new and useful techniques that may themselves be a part of the state of the art in the near future.

Chapter 3

Study of the Non-Linearities

The qualitative study of non-linear systems may seem an unattractive subject for engineers, something that may only be seen as an academic interest for mathematicians, for whom a large collection of references can be found [40, 41, 42]. Engineers are known to care for the quantitative aspects, to apply rules that are generally not even deduced from rigorous mathematical models, and to solve problems by following defined methods.

On the other hand the use of computer simulations as a tool for circuit design is becoming widespread, and it calls for something more than the application of well-defined procedures. The fact that most of the times this tool is used without a proper understanding of the involved processes, by the conduction of blind trial and error, is a serious limitation to the achievement of the best possible outputs.

Hence it becomes clear that in order to improve the results of circuit design simulations, one should do more than just enforcing the basic rules. A greater knowledge of the involved processes and of the inherent non-linear behaviours, even if just qualitative, may be used as guide for driving the simulation towards the right direction.

3.1 Description of NLS

A travelling signal is subjected to many interferences, either from the medium it crosses or from the devices it comes across, and thus can be deformed in numerous forms. Amongst this interferences the electromagnetic radiation from other external sources, attenuation of the cables, cross-talk from other transmitters, quantification noise from ADC and even the properties of the devices on its way.

Some of this effects can be prevented: transmission crosstalk between neighbouring pairs can be cancelled with twisted pair cables, electromagnetic radiation from external sources can be prevented by adequately shielding the cables, and quantification noise can be reduced by oversampling or increasing the ADC number of bits. However there are interferences that cannot be dissociated from the signal, such as the effect produced by the crossed devices, which may significantly change the signal's form.

This last effect is commonly refereed to as distortion and can be classified either as linear or non-linear phenomena. While the former affects only the gain, changing the amplitude of the signal, the latter can change both the signal amplitude and form, thus deforming the original signal to a completely different one. Systems which comprise devices that exhibit this non-linear behaviour are usually known as Non Linear Systems (NLS).

The two types of distortion have different effects and weights depending on the specific features and goals of the system. For instance, for an instrumentation system the undesired change on a signal's amplitude (linear distortion), invalidates any measurement, while on a radio-frequency receiver changes to the amplitude of the input signal are not critical if an Automatic Gain Control (AGC) is available to correct the input level. A non-linear distortion on the other hand invalidates a signal arriving to a telecommunications system, since changing it's form changes it's content. Non-linearities have however many practical uses, for example in RF/DC converters, mixers and modulators, since they allow for the information to change from one frequency to another.

Due to the amount of so said linear systems studied in every field of engineering and science (for example), it can be mistakenly assumed that these consist in the great majority of systems. In fact this is not true, and every device, active or passive, low-power or high-power, shows non-linear characteristics of some degree ([43] and [44] make this study for passive and active devices, respectively). Thus, the question to be answered is not if the device is non-linear but how strongly it is.

The fact that many sciences don't use non-linear models and equations to approach the real behaviours of the systems relates to the complexity of the available mathematical tools which are generally not practical or non-existent. Very often the non-linearity of the devices is rather small for a specified range of operation, and can perfectly be replaced with linear operators, thus resulting in local linear systems. There are other cases where a global linear operator is used to achieve a complete description of a particular system.

Part of the inherent simplicity of using linear operators is that a particular input can be used to generalize the response for all other inputs. Typically an unit-impulse is used and a response named a Weighting Function (WF) obtained, providing all modes of functioning. This useful concept justifies the approximations, since it does not apply to NLS, due to the variety of responses and change of behaviour under the characteristics of the input.

The diagram and analysis of a typical transceiver link subjected to many forms of distortion can be found on [45, Ch. 1, p. 2].

3.2 Methods for the study of NLS

A rather large collection of techniques to study the performance of non-linear systems can be used, allowing a selection accordingly to specific characteristics. Since each one of this techniques has advantages and disadvantages that make them suitable for different practical contexts they must be studied together to provide a larger insight on how to approach a specific problem. Nevertheless the differences, a common characteristic to all of them is their usefulness on the design of practical non-linear systems.

The methods hereby presented are the more frequently know and used, and can be regarded in further detail in [45]:

Prototype has the obvious advantage of obtaining a real system, therefore making an exact analysis of it, but also bears many disadvantages. The costs associated with this technique are larger comparing to the others, as expected, as well as the time to prepare and conduct the respective trials. Building and testing an unknown prototype may also be dangerous and unpredictable. On the bright side a prototype construction avoids the selection of mathematical models for the system and it's complex study.

Simulation in a computer avoids the cost of prototypes and the time expended in the trials. However blindly designing a system without concern for a mathematical model of some sort may take an immense amount of time to reach desired results. This method is better suited as an optimizing tool, used as a final step before the assembling of the hardware, allowing the changes in the system that will lead to the desired response. An important requisite of a simulation is that the computer has enough processing ability to conduct simulations in reduced time.

Closed-Form and Phase-Plane Solutions are two more theoretical approaches to the problematic of the non-linear systems. However they can only be of use in a very restrict number of systems, where exact solutions for non-linear differential equations can be found.

Lyapunov's Direct Method is another theoretical technique that is used to analyse the stability of a system without concern for the system responses. It checks if the solution tends in a generalized sense to a balance point. Since for NLS this method requires a try and error technique to find an adequate functional method, this may prove to be very exhausting and inefficient.

Series Expansion has several types such as Taylor series, MacLaurin series or Fourier Series. This method is regularly used and refereed to since it adapts to many systems, however in order to work it has to guarantee convergence, what not always happens. It can be proved that the more non-linear a system gets, the longer it takes to converge.

Linearisation greatly simplifies the analysis of non-linear systems, at the cost of a rough approximation, by replacing each non-linear operator with a similar linear one. As expected the applicability is restricted to systems whose non-linearity is reduced, or to small departures of the variables from the nominal value (this explains the terminology "small signal approach"). This method can be used as a piece-wise approximation where different linear operators are used for different regions of operation.

Quasi-Linearisation relives the small signal approximation of the linearisation, by mimicking the response of the NLS in different regions. It diverges from the linearisation in the fact that characteristics change with the signal. Since it works for any magnitude of input signal it presents itself as a much more useful and encompassing method for the study of the systems in question. A non-linearisation technique known as Describing Function(s) (DF) will be described in further detail in the next pages.

In the next section, only three of this methods will be presented in more detail, since they represent the most of the practical choices. Those are the linearisation, the series expansion and the quasi-linearisation methods, particularized with the describing function.

3.2.1 Linearisation and Series Expansion Methods

As stated before both the linearisation and series expansion methods can be used to provide solutions to non-linear systems, where the former can be considered a particular case of the latter with truncation. In the following paragraphs a brief analysis to the response of a NLS approximation to a sinusoidal input by both methods will be provided. Selecting a sinusoidal input is justified by the fact that in many practical systems the input has a sinusoidal

characteristic, and so a solution to a sinusoidal input provides a response that can be extended to real systems.

The input, given by equation 3.1, is assumed a sinusoidal signal with time-varying amplitude and phase:

$$x(t) = A(t)cos\left[\omega_c t + \theta(t)\right] \tag{3.1}$$

If this signal is passed through a non-linear device it will generate a response that can be approximated by either a linear response ($y_L = F_L\left[x(t)\right]$) or a polynomial/series expansion response ($y_{NL} = F_{NL}\left[x(t)\right]$).

The general polynomial solution is given in equation 3.2 and while the linear response to the input is given considering only the first term, in equation 3.3, the selected polynomial response considers up to the third order, in equation 3.4.

$$y_{poly}(t) = a_1 x(t-\tau_1) + a_2 x(t-\tau_2)^2 + a_3 x(t-\tau_3)^3 + ... + a_n x(t-\tau_n)^n \tag{3.2}$$

$$y_L(t) = a_1 A(t-\tau_1)cos\left[\omega_c t + \theta(t-\tau_1) - \omega_c\tau_1\right] \tag{3.3}$$

$$\begin{aligned} y_{NL}(t) = {} & a_1 A(t-\tau_1)cos\left[\omega_c t + \theta(t-\tau_1) - \omega_c\tau_1\right] \\ & + a_2 A(t-\tau_2)^2 cos\left[\omega_c t + \theta(t-\tau_2) - \omega_c\tau_2\right]^2 \\ & + a_3 A(t-\tau_3)^3 cos\left[\omega_c t + \theta(t-\tau_3) - \omega_c\tau_3\right]^3 \end{aligned} \tag{3.4}$$

It should be noted that a pre-requisite for the linear approximation is that $x(t) >> x(t)^2/x(t)^3$, implying that the first term of the polynomial is much larger than the following.

Now, particularizing to an input signal with slowly varying phase and amplitude both equations 3.3 and 3.4 turn into 3.5 and 3.6, respectively.

$$y_L(t) = a_1 A(t)cos\left[\omega_c t + \theta(t)\right] \tag{3.5}$$

$$\begin{aligned} y(t) = {} & a_1 A(t)cos\left[\omega_c t + \theta(t)\right] \\ & + a_2 A(t)^2 cos\left[\omega_c t + \theta(t)\right]^2 \\ & + a_3 A(t)^3 cos\left[\omega_c t + \theta(t)\right]^3 \end{aligned} \tag{3.6}$$

Finally, a further development of the polynomial solution applying proper trigonometric identities results in equation 3.7:

$$\begin{aligned} y(t) = {} & a_1 A(t)cos\left[\omega_c t + \theta(t)\right] \\ & + \frac{1}{2}a_2 A(t)^2 + \frac{1}{2}a_2 A(t)^2 cos\left[2\omega_c t + 2\theta(t)\right] \\ & + \frac{3}{4}a_3 A(t)^3 cos\left[\omega_c t + \theta(t)\right] \\ & + \frac{1}{4}a_3 A(t)^3 cos\left[3\omega_c t + 3\theta(t)\right] \end{aligned} \tag{3.7}$$

From the analysis of this equations, specifically the last one, a couple of conclusions can be drawn. While in the linear approximation there is only information in the original frequency ω_c, the polynomial output has components both in the original frequency and in it's multiples $2\omega_c, 3\omega_c$ as well as in $0Hz$. This image frequencies are called harmonics and are characteristic of non-linearities, which modify the signal spectrum, creating new components.

For a system with more than one input signal, this output becomes more complex, comprising both the multipliers of the fundamental frequencies and the mixture of the input signals. Some of this spectrum replicas are located very close, or on top of the original signal (in-band distortion) and are therefore undistinguishable from it, but many other are located in different parts of the spectrum and can be filtered (out-of-band distortion). When using a multiple input system the frequency mixing products generated by the non-linearity can be counted and put to evidence by adequate analysis such as the one used on [45, Ch. 1, p. 16].

Ending this short analysis of NLS under the methods of series expansion and linearisation it should be kept in mind that both this methods have restricted applicability and the first step should be to evaluate their applicability to the system in cause.

3.2.2 Describing Functions (DF)

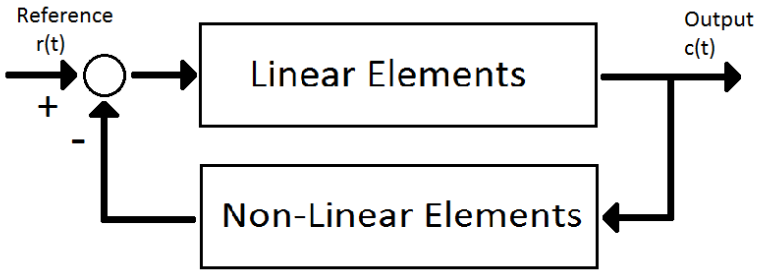

Figure 3.1: Typical Control System Block Diagram

As stated previously, a particular case of quasi-linearisation are the DF. This technique, which represents a powerful mathematical approach for understanding and improving the non-linear systems, assumes a system configuration composed of an interconnection of separable linear and non-linear parts with a feedback element, which is typically represented as in figure 3.1.

In order for this method to succeed the input form of the signal has however to be predicted, since it depends on both the reference and feedback signal which is highly unpredictable. This prediction is generally made assuming three general types of signals:

Bias stands for the constant component of the signal, or the combination of constant components;

Sinusoidal is the most common signal, since all periodic signals in feedback systems with a low pass filter tend to a sinusoid after propagation through the linear part;

Gaussian Processes represents the tendency of any random signal after filtration, similarly to what happens to the sinusoid.

The only restriction to the applicability of the DF method is, as expected, the adequateness of these signals to the real input. Nevertheless, proper filtering virtually guarantees that input signals degenerate into one or more of the previous signals, meaning that the filter behaviour is essential for the validity of this method. Another advantage of this method is that the order of the system does not exponentially increases the difficulty of finding a solution, as is the case of other methods, and in some cases large order systems are similarly solved to low order systems. It is due to this advantages that this method is of great assistance in the practical design of non-linear systems.

As of the structure behind the DF, it uses quasi-linear approximators for non-linear operators, setting them up in parallel with their respective WF ($w_i(t)$), as pictured in figure 3.2.

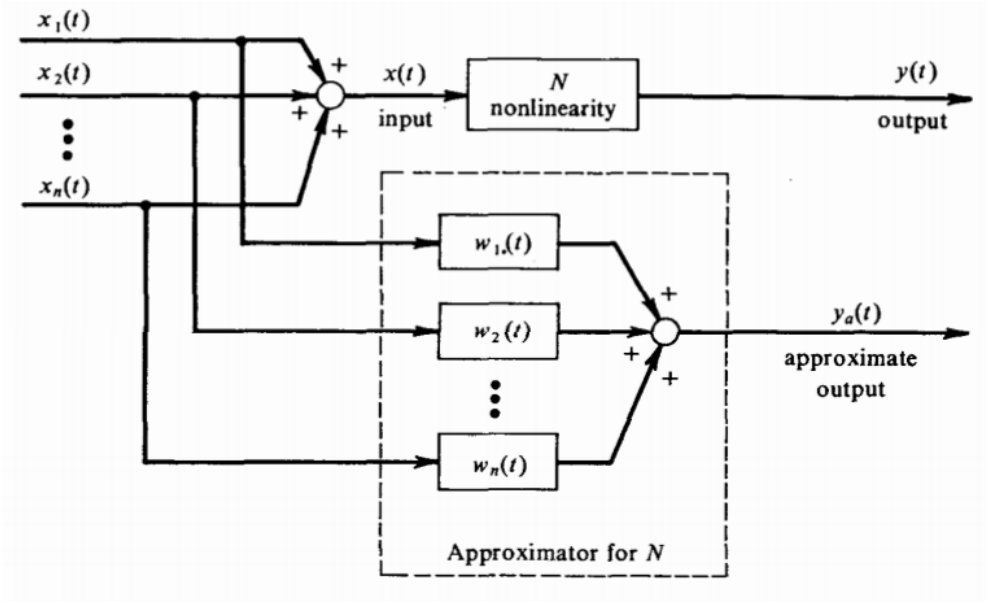

Figure 3.2: General Linear Approximator for a Non-linear Operator (source: [46])

Having a structure for the calculation of the approximate output lacks still the quantification of the committed error, something that can be done by evaluating the minimum mean-squared error, as in equation 3.9:

$$\overline{e(t)} = \overline{y_a(t)} - \overline{y_t(t)} \tag{3.8}$$

$$\overline{e(t)^2} = \overline{y_a(t)} - \overline{2y_a(t)y(t)} + \overline{y(t)^2} \tag{3.9}$$

Being the approximated output given by equation (3.10), where $w_i(\tau)$ are the WF and $x_i(t)$ the input components, the latter being one of the three types of inputs presented previously.

$$y_a(t) = \sum_{i=1}^{n} \int_0^{\infty} w_i(\tau) x_i(t-\tau)\, \mathrm{d}\tau_2 \tag{3.10}$$

This equation can easily be related with figure 3.2.

This minimization of the mean-squared error is used as the basic mechanism to retrieve the DF for specific input forms, as studied in detail in [46, Ch. 1, p. 20], and presented in the next section.

To obtain these specific forms, the pre-requisite is that the WF are chosen so as to respect the condition $\Delta|e(t)|^2 = 0$, or equivalently equation (3.11), where $\phi_{ii}(\tau_1 - \tau_2)$ stands for the correlation between the signals.

$$\sum_{j=1}^{n} \int_0^\infty w_{0j}\phi_{ij}(\tau_1 - \tau_2)\,\mathrm{d}\tau_2 = \overline{y(t)x_i(t-\tau_1)}, \quad \tau_1 >= 0, i = 1, 2, ..., n \tag{3.11}$$

DF of specific input forms

Recalling the three categories of input signal forms previously defined, the respective DF, deducted in [46, Ch. 1, p. 20] will hereby be described:

Bias For a stationary input the DF is denoted simply with a constant, that uses the mean value of the output:

$$N_B = \frac{1}{B}\overline{y(0)} \tag{3.12}$$

Sinusoid In this case, which will be studied in further detail ahead, the amplitude and frequency are deterministic, having only undetermined phase randomly distributed between 0 and 2π radians, with the DF being given as:

$$\begin{aligned} N_A =& n_p + jn_q \\ n_p =& \frac{2}{A}\overline{y(0)sin\theta} \\ n_q =& \frac{2}{A}\overline{y(0)cos\theta} \end{aligned} \tag{3.13}$$

Or, equivalently:

$$N_A = \frac{1}{\pi A}\int_0^{2\pi} y'(Asin\theta)sin(\theta)\mathrm{d}\theta \tag{3.14}$$

Random The random signal DF is also just a static gain, and is given by equation 3.15, where σ^2 is the variance of the input:

$$N_R = \frac{1}{\sigma^2}\overline{y(0)r(0)} \tag{3.15}$$

With this representations in mind, in order to represent complex signals a very useful consideration can be taken, which is that any signal can be represented as a combination of these three, as long as the following sentences are respected:

- Bias signals are undistinguishable, and therefore can be combined into a single value, whose value is the corresponding mean;
- Gaussian inputs enjoy equal properties where the total variance is the sum of the singular variances;
- Sinusoidal signals cannot be combined and must be analysed individually.

In mathematical therms this ultimately means that any signal $x(t)$ can be written as:

$$x(t) = B + r(t) + A_1 sin(\omega_1 t + \theta_1) + ... + A_n sin(\omega_n t + \theta_n) \tag{3.16}$$

In the next section a greater insight on the Sinusoidal Input Describing Function (SIDF) will be provided, however for a further investigation on other DF [46] should be consulted.

Sinusoidal Input Describing Function

The SIDF is the most used and applied DF, since it adapts to many real system inputs. Besides the output of a real system can generally be decomposed in the sum of the SIDF with a residual value that gets smaller as the input signal approaches the reference sinusoid.

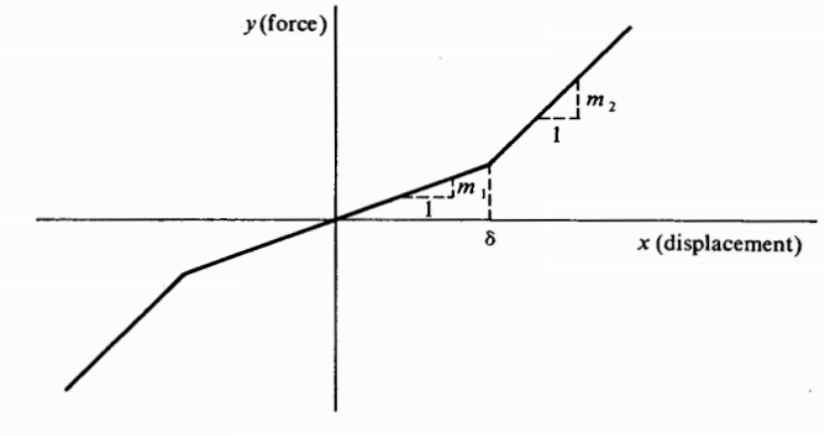

Figure 3.3: Gain-Changing Element Characteristic (source: [46])

Assuming a symmetrical gain-changing element with two slope discontinuities such as the one on figure 3.3, and selecting the independent variable as the phase (ϕ_1), where:

$$\begin{aligned} Asin\phi_1 &= \delta \\ \phi_1 &= sin^{-1}\frac{\delta}{A} \end{aligned} \tag{3.17}$$

The regions of operation for this system can be defined as:

$$\begin{aligned} 0 < \phi \leq \phi_1, &\qquad y = m_1 x \\ \phi_1 < \phi \leq \frac{\pi}{2}, &\quad y = (m_1 - m_2)\delta + m_2 x \end{aligned} \tag{3.18}$$

Combining 3.14 with 3.17, as done in more detail in [46, Ch. 2, p. 56], results in the describing function:

$$\begin{aligned} N(A) &= \frac{4}{\pi A}\int_0^{\frac{\pi}{2}} y(Asin\phi)sin(\phi)\mathrm{d}\phi \\ &= \frac{2(m_1 - m_2)}{\pi}\left(\phi_1 - \frac{1}{2}sin2\phi_1 + 2\frac{\delta}{A}cos\phi_1\right) + m_2 \\ &= \frac{2(m_1 - m_2)}{\pi}\left[sin^{-1}\frac{\delta}{A} + \frac{\delta}{A}\sqrt{1 - \left(\frac{\delta}{A}\right)^2}\right] + m_2 \end{aligned} \tag{3.19}$$

From the observation [46, Ch. 2, p. 58, fig. 2.3-3], where DF for different systems such as the gain-changing element, saturation or the dead zone are shown, a single functional form is observed to be recurrent. This structure is named the saturation function, $f\left(\frac{\delta}{A}\right)$, is depicted

in figure 3.4, and can be used, with adjustments, to represent many different DF, being the standard model used for a normalized saturation describing function.

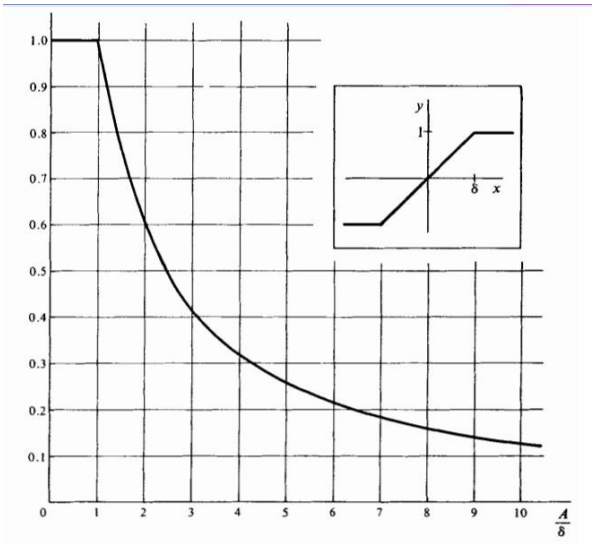

Figure 3.4: Saturation Function (source: [46])

It can be defined as:

$$f\left(\frac{\delta}{A}\right) = \begin{cases} f\left(\frac{\delta}{A}\right) = \frac{2}{\pi}\left[sin^{-1}\frac{\delta}{A} + \frac{\delta}{A}\sqrt{1-\left(\frac{\delta}{A}\right)^2}\right] & for \ \frac{\delta}{a} \leq 1 \\ 1 & for \ \frac{\delta}{a} > 1 \end{cases}$$

As an example of it's applicability, we have:

Gain-Changing :

$$N(A) = m\left[1 - f\left(\frac{\delta}{A}\right)\right] \tag{3.20}$$

Dead Zone :

$$N(A) = m\left[1 - f\left(\frac{\delta}{A}\right)\right] \tag{3.21}$$

General Saturation :

$$N(A) = mf\left(\frac{\delta}{A}\right) \tag{3.22}$$

These functions can be used to approach a real system, by using the very rough approximation of dividing it into 3 operation regions, as for example a diode can be approximated by the Gain-Changing Element, however a most customizable technique can be used, and is presented next.

Piecewise-Linear Non-Linearity

This final approach relives the system from have to adapt to predefined forms, and uses a piecewise-linear non-linearity to adapt to it, as exemplified in figure 3.5 in a typical four segment characteristic.

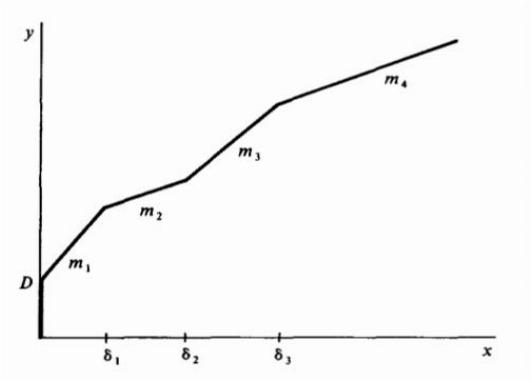

Figure 3.5: General Piecewise-linear Non-linearity (source: [46])

The output in therms of the input can be written as:

$$\begin{aligned} 0 < x \leq \delta_1, &\quad y = m_1 x + D \\ \delta_1 < x \leq \delta_2, &\quad y = (m_1 - m_2)\delta_1 + m_2 x + D \\ \delta_2 < x \leq \delta_3, &\quad y = (m_1 - m_2)\delta_1 + (m_2 - m_3)\delta_2 + m_3 x + D \\ \delta_3 < x, &\quad y = (m_1 - m_2)\delta_1 + (m_2 - m_3)\delta_2 + (m_3 - m_4)\delta_3 + m_4 x + D \end{aligned} \tag{3.23}$$

By applying a sinusoidal input, as before, the describing function, that can be conveniently described in therms of the saturation function, $f\left(\frac{\delta}{A}\right)$, is given as:

$$\begin{aligned} N(A) = \frac{4D}{\pi A} + (m_1 - m_2) f\left(\frac{\delta_1}{A}\right) + \\ + (m_2 - m_3) f\left(\frac{\delta_2}{A}\right) + (m_3 - m_4) f\left(\frac{\delta_3}{A}\right) + m_4 \end{aligned} \tag{3.24}$$

Thus, a rather simplified model for adapting to any kind of system is obtained, where the complexity growth only implies adding more breakpoints and slopes, and so can be easily used in practice.

3.3 Conclusion

In this chapter, the non-linearities were carefully considered and explained in a practical way, in order to simplify the understanding of the phenomena involved in the operation of the studied circuits.

Although an introduction was made to a large number of the methods available to address this issue, only a couple of them were viewed in further detail, those which presented a more practical feature being of simple and rather automatized application, given that the intention here was to simplify the analysis, and not increase it's complexity.

As of lighter non-linearities these were shown to be of possible approximation by the series expansion method, or by linearisation, specially for limited regions of operation. This section also highlighted the frequency generation process involved in the non linearity, that is behind the conversion of the energy from the fundamental input frequency to DC.

For devices with high non-linearities the describing functions, that consist in a quasi linearisation particular case, were advised for successful analysis. This method, which might use pre specified and simplified forms to adapt to the system, also provides a much more customizable solution trough the use of a piecewise linear DF, where the division of the approximator in multiple sections permits a very detailed mimicking of the system behaviour.

Chapter 4

Rectifier Design

The main objective of this research is, as stated before, to find techniques for the improvement of rectifying circuits efficiency. One way to do so is finding the regions of operation that result in higher DC output for the same input, or equivalently, the regions that maximize the second harmonic value (this last consideration will be very useful further ahead). Alongside, minimizing the reflections and respective insertion loss in the circuit is also essential for the achievement of higher efficiencies.

To obtain desirable outputs, a careful study of the involved non-linear devices must be made, so that a good understanding of the concerned processes and it's non-linearities can be reached, which is why a brief introduction to this matter was made in a previous chapter.

This analysis could have been done by applying some of the analytic methods introduced previously, such as the series expansion method or the describing functions, however various simulations where made instead, due to the lower complexity and extra functionalities it presents. This simulations were nevertheless associated with the qualitative study of the circuit in cause with these analytic tools.

4.1 Simulation Tools

To obtain valuable results from these simulations, a tool that allowed for a complete characterization and optimization of the circuits under various conditions was required. The choice, which relied on Advanced Design System (ADS), was used in partnership with the Harmonic Balance (HB) method, the two being shown in more detail in the following lines.

4.1.1 Advanced Design System (ADS)

ADS, a tool produced by Agilent Technologies, is a powerful and versatile design automation software, that provides an integrated design environment and is suitable for Radio-Frequency (RF) and Micro-Wave (MW) applications, as well as high speed digital applications. It permits simulations in both frequency-domain and time domain as well as electromagnetic field simulation.

It has a structure based in workspaces with four main types of windows. The first three are design windows, and the last one is used for the visualisation of the simulation design output:

Schematic design of the circuits to be simulated, either simple or complex. Can contain components described by the Symbols window;

Layout practical implementation of the schematic circuit or a custom circuit;

Symbol design of elemental circuits that describe particular components;

Data Display representation of data in a variety of plots and formats, as well as mathematical equations.

The learning curve of this software is not very short, since it has many options and hard to reach advanced options, however once this initial phase is surpassed, a very complete and full of options software proves to be immensely useful to the needed measurements and conclusions, providing a great level of detail and customization.

4.1.2 Harmonic Balance (HB)

ADS has, as well as many other similar tools, more than one method for obtaining simulation results, such as the transient analysis or the harmonic balance. While the first uses the circuit's equations, computing all the calculations over time that lead the circuit from the transient to the stationary regime, the second behaves in a very distinct way and shall herein be discussed in more detail.

HB is a frequency domain analysis technique for simulating non-linear circuits and systems that requires inputs consisting in sinusoidal, quasi-sinusoidal or sinusoidal combinations. It generates an output that might be expressed as the sum of steady state sinusoids, whose frequency comprises both the input frequencies and the harmonics generated by the non-linear elements.

This method is based on the calculation of the node's current and voltages by the application of the Kirchoff's Current Law (KCL) and by dividing the circuit into two parts, the linear and the non-linear. The calculations on the former are made resorting to basic frequency-domain linear analysis for which different techniques exist, while the latter current and voltage calculations are made in time-domain and with finite Fourier Series, respectively. It should be noted however that these values represent only iterations and not the real value, so many iterations for the non-linear elements is needed until the KCL sum is a close to zero as an established tolerance.

The main HB advantages and limitations over other methods such as the transient can be defined as:

Advantages :

- Linear devices with different frequency responses can be easily and quickly modelled;
- Time domain convolution is replaced with easier frequency domain multiplication;
- Provides the steady-state solution without waiting for the transient solution (this could result in long waiting periods for high frequencies or high Q circuits).

Limitations :

- Input signal has to be quasi-periodic;

- Input must be represented in a sum of N discrete tones;
- Large value for N increases memory requisites up to an excessive level (this might be a quadratic or linear dependency depending on the iteration scheme).

The fact that harmonic balance has so many advantages relatively to the conventional time-domain analysis, is why it is a method of choice for simulating many analogue RF and MW problems. It's high frequency characteristic and steady-state behaviour output, are generally what is needed to address this type of problems, since using conventional transient methods would require integration over an enormous number of periods for the higher frequency components. Referring to [47]: "Simulation in the frequency domain avoids many of the severe problems experienced when traditional time-domain simulators such as SPICE are used to find the steady state behaviour of microwave circuits". Besides, many linear models are best represented in the frequency domain, and so problems that are inherent to the time analysis such as losing accuracy, causality, or stability, are avoided. Extra information on the HB method can be found on [47] or [48].

Amongst the devices that are generally suited for this analysis are mixers, frequency multipliers, modulators or rectifiers under large signal sinusoidal inputs, the last one being the type of device that is to be considered in this work.

4.2 Lighting System

One of the main objectives of this work was to power up a lighting system without an external power source, thus generating no-cost illumination, for which adequate electromagnetic energy harvesting systems were studied, developed and implemented.

However a bigger insight must exist over the actual system, so as to characterize it's electrical needs and characteristics, in order to optimize the rectifier to it's needs, so a brief study was made on the issue. The system consisted in a stripe of LEDs, organized in cells with 3 components, in parallel with each other, with very low consumption needs.

So as to properly characterize both these cells and individual LED units an experimental trial was made to obtain both the IV characteristic curves and the voltage and power needs to effectively generate light. The characteristic plots are found in figures 4.1 and 4.2, for the single and triple components, respectively.

The information gathered in these graphics, together with the perception of generated light, leads to the following conclusions:

Single LED unit :

- Minimum voltage: $\approx 2.65V$
- Current value: $0.5mA$
- Required power: $1.22dBm$

Triple LEDs cell :

- Minimum voltage: $\approx 8V$
- Current value: $0.5mA$
- Required power: $6.02dBm$

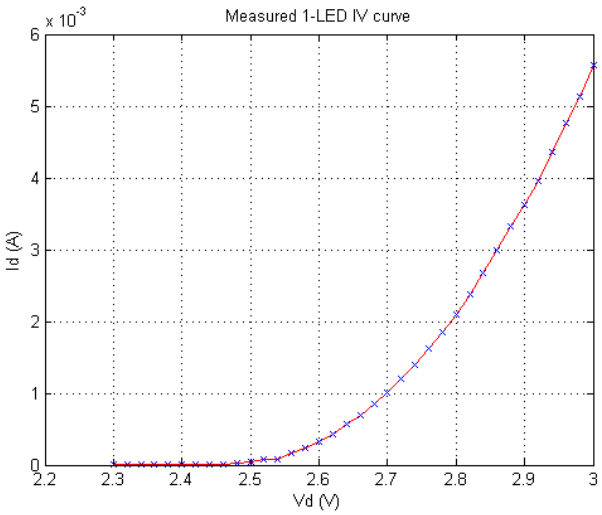

Figure 4.1: 1-LED IV Curve

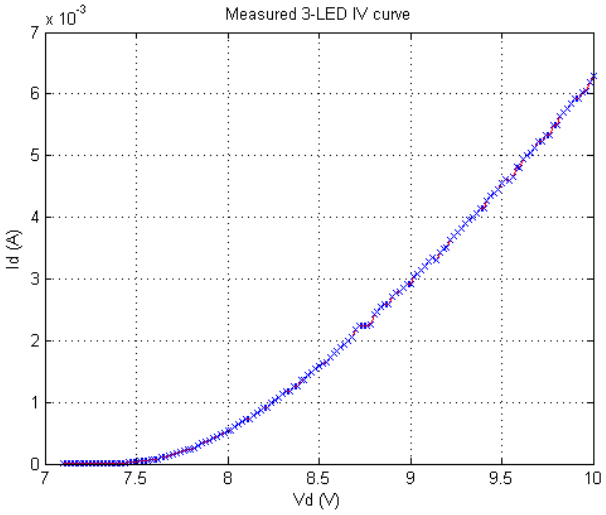

Figure 4.2: 3-LED IV Curve

The previous results show that the value of current for lighting up the LEDs is about $0.5mA$, while the voltage applied varies since the elements are in series. Additionally this means that if a power of $10dBm$ is received by the rectifying circuit, efficiencies larger than 12% and 60% would be necessary, for the systems with 1 and 3 LEDs, this together with the adequate voltage values.

Although even the best case, consisting in 3 LEDs may seem a very scarce source of light to be useful in practical situations, the fact that the whole rectifying circuit is rather small and low cost, allows the deployment of many of these systems together in the same area, increasing the amount of light produced.

Finally it should be noted that not all the developed systems will be adequate for this application, because even though they may present very high efficiencies they will lack in the

voltage output level, which is why later a different type of circuit from the simple rectifier will be discussed.

4.3 Rectifier with Polarization Source

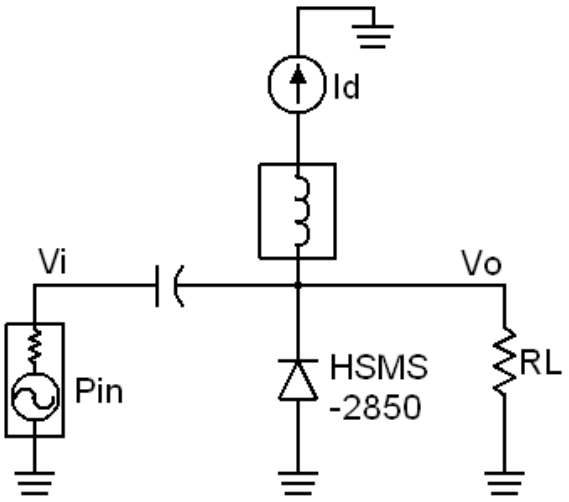

Figure 4.3: 1-Stage Simple Rectifier with Polarization Source

The first circuit considered, which is depicted in figure 4.3, consisted basically in a simple rectifying circuit containing a non-linear device, a high-frequency and low forward voltage diode, in parallel with the load. The motive for using a parallel element instead of a series one is related to the feasibility of the polarization network, and will be explained in detail further ahead. This network is supposed to place the diode in a region where the circuit's efficiency can be maximized, therefore using an innovative approach to the rectifying circuits problematic.

Besides this non-linear device and respective current biasing source, the circuit contained a power supply, a load resistance and two energy storage elements: a capacitor and a coil. A couple of this elements are described next:

Power supply provides the adequate voltage that generates the selected power, with a source resistance of 50Ω.

Diode HSMS-2850 non-linear device used for the conversion of RF to DC by the generation of the harmonics. It must have low parasitic capacitances and forward voltage to obtain the best results at high frequencies. More details can be found on the device's datasheet, [14];

Load resistor has a large value, so that it doesn't interferes with the diode's polarization. Ultimately it may not exist and trials can be made without it;

Current source places the diode in a specific region of operation as stated. The current must go mostly to the diode and not to the other branches of the circuit;

Energy storage elements separate the polarization from the small-signal, so that the energy from the power source doesn't ends up leaking to the current source and vice-versa.

At this point no matching network was used, what explained the low efficiency results obtained, due to the reflection losses. The output of this particular circuit is composed of both the desired DC value and the other frequencies components, since no filtering exists. The purpose of this is to allow the study of the second harmonic, that will be explained latter.

Furthermore there is the possibility of swapping the current source with a voltage source, thus polarizing the circuit in voltage.

4.3.1 Problems and Limitations

The circuit design and graphical outputs have significantly changed during the trials, to address the multiple problems found. In the results section only the final graphics, those from which the key conclusions were drawn, are presented, nevertheless the intermediate steps to reach them are shown next.

As the awareness for the non-linear behaviours grew with the holding of distinct trials, the circuit's problems were more easily detected and corrected, thus allowing a greater focus on the optimization of the system efficiency

Merely to justify some options it should be mentioned, first of all, that an alternate scheme to figure 4.3 was considered. This circuit consisted in a diode in series with the load resistor instead of in parallel and had a DC returning network in parallel with the load, so the polarization wouldn't affect the output level.

It's main problem was that the returning network was driving both the desired output and polarization to the ground, and thus was not generating any output.

Back to circuit 4.3, a voltage polarization was firstly considered. With this a region of operation could be fixed, however the output signal would be hanging in the polarization since no returning bias network was implemented. The output level would depend more on the polarization than on the harvested signal itself, therefore creating a highly undesirable situation to the analysis of the system behaviour.

Due to the apparent impossibility of biasing in voltage, current polarization was considered, which is more difficult to implement, but would suffice for the drawing of conclusions. Although no DC voltage was present now, the output kept changing linearly with the current. This was due to the diode's parasitic resistance, which kept generating a voltage proportional to the feeding current, thereby invalidating the outlet.

Mathematically this problem can be verified by the application of the KCL together with a series expansion analysis on the diode's behaviour (figure 4.4):

$$I_{ac}(t) + I_{DC} = I_{out}(t) + I_d(t) \tag{4.1}$$

Taking into account that the load resistor is very large $R_L = 1M\Omega$, $I_{out} \approx 0$ and so:

$$I_d(t) \approx I_{ac}(t) + I_{DC} \tag{4.2}$$

Applying the series expansion method to the diode's voltage and truncating it to the third order:

$$v_d(t) \approx k_1 I_d(t) + k_2 I_d(t)^2 + k_3 I_d(t)^3 \tag{4.3}$$

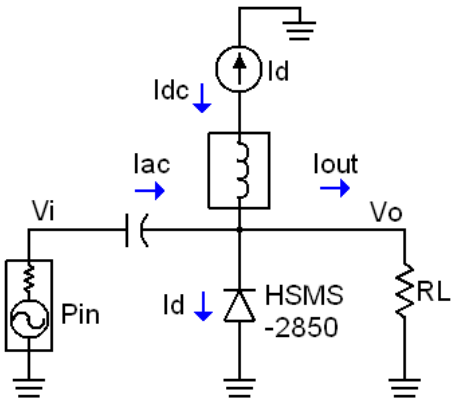

Figure 4.4: Application of KCL to the Circuit

The combination of (4.2) with (4.3) results in:

$$v_d(t) \approx k_1(I_{ac}(t) + I_{DC}) + k_2(I_{ac}(t) + I_{DC})^2 + k_3(I_{ac}(t) + I_{DC})^3 \tag{4.4}$$

Gathering all DC values under the same term:

$$V_{DC} = k_1 I_{DC} + k_2 I_{DC}^2 + k_3 I_{DC}^3 \tag{4.5}$$

Resulting in:

$$v_d(t) \approx V_{DC} + k_1 I_{ac}(t) + k_2 I_{ac}(t)^2 + k_3 I_{ac}(t)^3 \tag{4.6}$$

Now, if we take a simple sinusoidal input current of $I_{ac}(t) = A_{ac} cos\left[\omega_c t + \theta\right]$ and apply a low-pass filter at the output of the system, we have that $v_d(t)$, or equivalently, $v_o(t)$ can be seen as:

$$v_{o(filtered)}(t) \approx V_{DC} + \frac{k_2 A_{ac}^2}{2} \tag{4.7}$$

So, it is proven that the DC for this circuit topology is dissociable from the polarization value, since the rectified voltage will be mixed with the biasing V_{DC}.

A partial solution for studying the harvested energy behaviour with polarization, that avoids the issues described above, is considering the second harmonic instead of the fundamental value. This could be done since, recalling equation 3.7, both frequency components depend equally on the input, and so exhibit the same behaviour. To obtain this signal, it should be reminded however that no load capacitor or similar filtering component should exist, because of undesired harmonic frequency filtering. It should be noted still that this solution is as applicable to voltage polarization, as it is for current, which is why simulations were made for both cases. All the graphics and conclusions for this simulations can be found on the results section.

4.4 Rectifier with Matching Network

Although many conclusions could be drawn from the analysis of the previous circuit results, the miserable efficiencies obtained compromised it's usefulness, simply because there is no

point in polarizing a diode in a specific operation point whose best efficiencies are still orders of magnitude bellow the results found in the literature. Furthermore it would carry no interest to physically implement a circuit to achieve this kind of output.

If the efficiency is to low, the justification is simple: only a fraction of the input power is being converted to the usable output. This leakage has two sources, the reflected power in the various parts of the circuit, and the dissipated power on the circuit's components. While the latter is essentially due to the diode resistance as well as any conductor losses, and can hardly be altered, the former can be greatly reduced by the use of a well-designed matching network.

For this study two simple rectifying circuits were considered, one with a NLE in parallel with the load resistance, and another with this element in series. This circuits are depicted on figures 4.5 and 4.6, respectively. Now only the DC component is considered, as can be concluded from the presence of the low-pass filters, and none of the circuits has a polarization network.

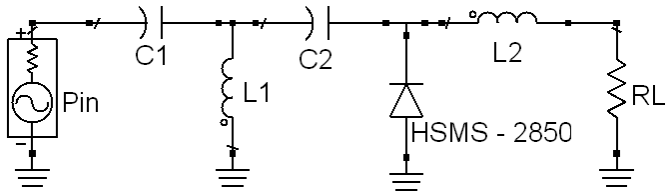

Figure 4.5: Parallel Diode Rectifier with Matching Network

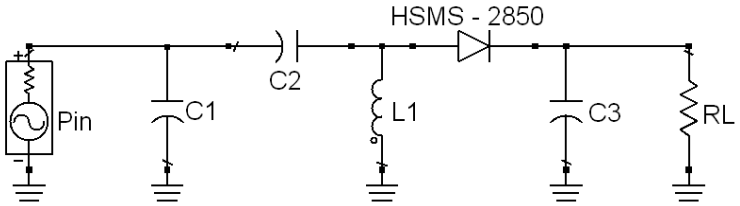

Figure 4.6: Series Diode Rectifier with Matching Network

In addition to the diode each of the circuits contains a few more components, whose function is as follows:

Parallel Diode Rectifier :

- C_1 and L_1 are used for matching network purposes, and their value is optimized for specific input power P_{IN} and load resistance R_L;
- C_2 prevents the DC signal from returning to the source thus separating it from the RF signal, working as an open circuit for it;
- L_2 in conjunction with R_L creates a low-pass filter, to obtain only the DC value of the rectified signal.

Series Diode Rectifier :

- C_1 and C_2 are used to minimize reflections as the matching network, and are also tuned for specific input power P_{IN} and load resistance R_L;
- L_1 is the element that prevents the return of DC signal to the input, shortening it;

- The low-pass filter is in this case the responsibility of C_3 and the series resistance of the diode;
- R_L is exclusively used as the load here.

The matching network, and respective components were obtained through simulation with the source-pull mechanism and are detailed in the next pages.

4.4.1 Source-Pull Mechanism

The low efficiencies obtained for the circuit shown in the beginning of this chapter (figure 4.3) raised the need for source adaptation, so as to reduce it's insertion loss, that is, improving the power delivered to the circuit in detriment of the reflected fraction.

For an ideal circuit this can be achieved by simply matching the source impedance to the input impedance. Assuming known circuit S parameters, as well as load value (Γ_L), this is done simply by making $\Gamma_s = \Gamma_{in}^*$, where:

$$\Gamma_{in} = S_{11} + \frac{S_{12}S_{21}\Gamma_L}{1 - S_{22}\Gamma_L} \tag{4.8}$$

However this procedure is only valid if the input impedance is independent of the input power, which is not the case. Due to the highly non-linear behaviour of the Schottky diode, the impedance is indeed altered for different input values. The dependence of the circuits input impedance with the power is shown in table 4.1, where the S parameters were taken from a Large Signal S Parameters (LSSP) simulation on ADS.

Diode in Parallel			
$P_{IN}(dBm)$	S_{11}	S_{21} and S_{12}	Γ_{in}
-20	$0.49\angle -115.2°$	≈ 0	$0.49\angle -115.2°$
-10	$0.367\angle -106.8°$	≈ 0	$0.367\angle -106.8°$
0	$0.28\angle -99.2°$	≈ 0	$0.28\angle -99.2°$
10	$0.25\angle -94.4°$	≈ 0	$0.25\angle -94.4°$
20	$0.24\angle -91.2°$	≈ 0	$0.24\angle -91.2°$
Diode in Series			
$P_{IN}(dBm)$	S_{11}	S_{21} and S_{12}	Γ_{in}
-20	$0.97\angle -139.7°$	≈ 0	$0.97\angle -139.7°$
-10	$0.95\angle -139.7°$	≈ 0	$0.95\angle -139.7°$
0	$0.93\angle -139.8°$	≈ 0	$0.93\angle -139.8°$
10	$0.91\angle -139.7°$	≈ 0	$0.91\angle -139.7°$
20	$0.90\angle -139.6°$	≈ 0	$0.90\angle -139.6°$

Table 4.1: S Parameters

The option chosen to circumvent this situation was the source-pull method, a variation of the more often referred method of load-pull. Referring to [49], "This method is important for large signal, non-linear devices where the operating point may change with power level or tuning. Load or source pull is not usually needed for linear devices, where performance with any load can be predicted from small signal S-parameters".

Basically, this technique works by systematically varying the impedance presented to Device(s) Under Test (DUT), in this case a Schottky diode, in order to assess it's performance under this variation and thus computing the best out of it.

This type of mechanisms is very commonly used to optimize systems ensuring best performance trade-off. For example, with it it's possible to design a fully optimized final stage for GSM applications in less than a day, thereby dramatically reducing the design cycle-time. For more information on this adaptation method [49] is available.

For the particular case of this work, a series of equations over the Data Display Window (DDS) window of ADS were created, in order to plot constant efficiency circles, as well as constant output voltage circles in Smith Charts representing the input impedance. A picture of the typical configuration used is found on figure 4.7. This analysis was made for both circuits 4.5 and 4.6, having resulted in similar results for both cases, as well as in posterior circuits.

The values of P_{IN} and R_L that originated these circumferences were chosen dynamically, to improve the results for specific purposes.

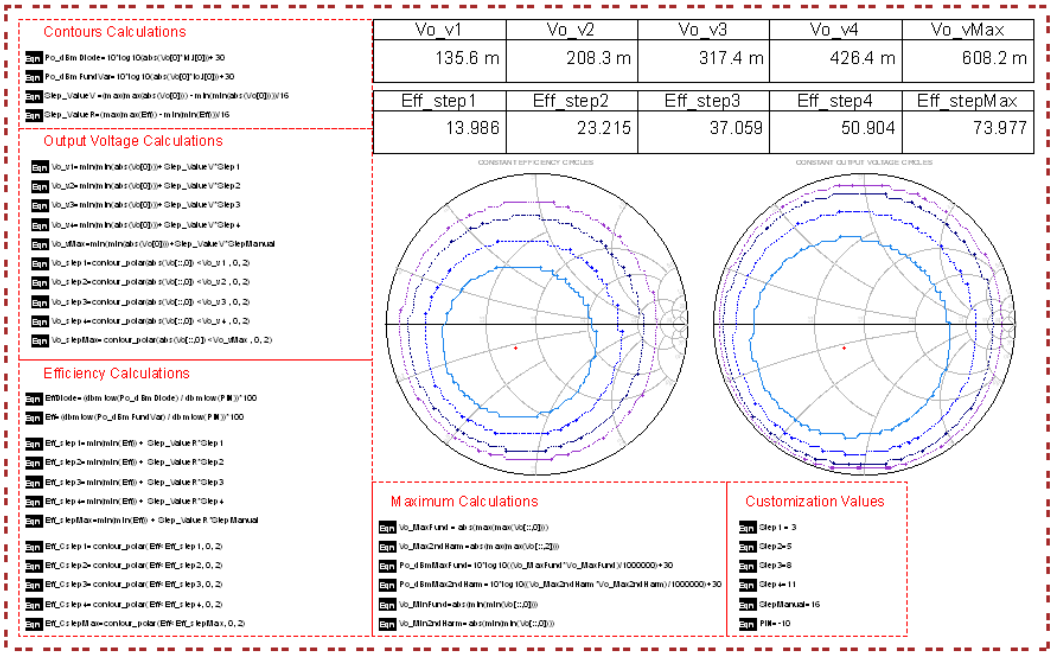

Figure 4.7: Equations and Smith Charts on DDS

Additionally an analysis of the efficiency dependency on the load resistor for specific matching networks is also present in the results section.

4.5 3-Port Network Analysis

A different approach from the previous study of the input impedance variation, was undertaken using a network with three terminals. It consisted in evaluating the relationship between the voltage values in the different parts of the circuit, for variable passive components, and was made for the basic rectifying cell with the diode in parallel.

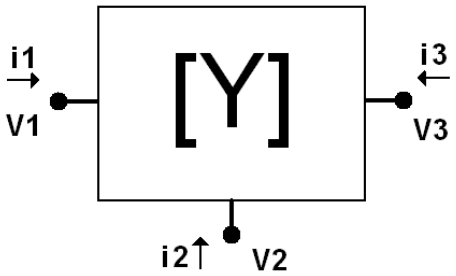

Figure 4.8: Generic 3-Port System

This method was only applied to the parallel rectifier (figure 4.5), since such a straightforward decomposition in a 3-port system wouldn't be possible for the series rectifier.

The characterization was made trough it's admittance parameters, $[Y]$, for which the basic representation can be found in figure 4.8, and mathematically representation in the following equations:

$$\begin{bmatrix} Y_{11} & Y_{21} & Y_{31} \\ Y_{21} & Y_{22} & Y_{23} \\ Y_{31} & Y_{32} & Y_{33} \end{bmatrix}$$

The relationship between the current and voltage values in the circuit is given as:

$$I_1 = Y_{11}V_1 + Y_{12}V_2 + Y_{13}V_3 \tag{4.9}$$

$$I_2 = Y_{21}V_1 + Y_{22}V_2 + Y_{23}V_3 \tag{4.10}$$

$$I_3 = Y_{31}V_1 + Y_{32}V_2 + Y_{33}V_3 \tag{4.11}$$

At first sight one could ask why choosing a 3-port system when only the relationship between the input and the output is necessary, thus increasing the complexity. The answer has to do with the non-linearities of the diode, which appear at port 2, and are not feasibly represented by the Y parameters which contain only passive components, so the diode's voltage dependent current source has to be added externally.

However before transforming the diode passive elements (obtained from [14] and [50]) in the desired system, a couple of simplifications had to be made over it's equivalent circuit (figure 4.9):

- The low capacitances, together with the not very high frequency, result in high impedance values;
- The values are approximately $-20Ki\Omega$ and $-27Ki\Omega$ for C_c and C_p, respectively;
- $C_1 \approx 0$, and so Z_{C1} is even larger than the other impedances;

With these simplifications in mind, the system could be reduced to the represented on figure 4.10, where R_y and L_y are the equivalent model values of R_s and $2L_l + L_b$, and the matching network is composed of C_m and L_m.

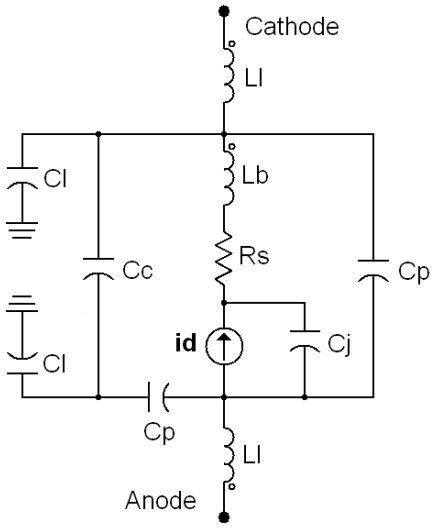

Figure 4.9: HSMS-2850 Model with Parasitic Elements

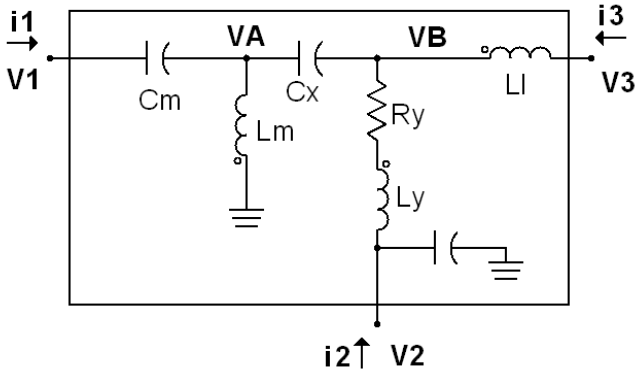

Figure 4.10: 3-Port Network for Diode in Parallel

As of the Y parameters, only the most significant where calculated, those which represent the port input admittances, and the relationship between the input and output and the input and the diode port, while the rest was obtained only through ADS simulation. Another note for the fact that the admittances are only symbolically represented, so as not to overcomplicate it's representation.

The input admittances are given as:

$$Y_{11} = \frac{1}{ZC_m + ZL_m \parallel [ZC_x + (ZR_y + ZL_y) \parallel ZL_l)]} \tag{4.12}$$

$$Y_{22} = \frac{1}{ZC_j \parallel (ZL_y + ZR_y + ZL_l \parallel [ZC_x + ZL_m \parallel (ZC_m)])} \tag{4.13}$$

$$Y_{33} = \frac{1}{ZL_l + (ZR_y + Z_L y) \parallel [ZC_x + ZL_m \parallel ZC_m]} \tag{4.14}$$

As of the calculation of the other Y parameters of interest, it's a bit more complicated. For Y_{21}:

$$\frac{V_B}{i_2} = -(ZL_y + ZR_y) \tag{4.15}$$

$$\frac{V_A}{V_B} = \frac{ZC_x + (ZR_y + ZL_y) \parallel ZL_l}{(ZR_y + ZL_y) \parallel ZL_l} \tag{4.16}$$

$$\frac{V_1}{V_A} = \frac{ZC_m + ZL_m \parallel [ZC_x + (ZR_y + ZL_y) \parallel ZL_l]}{ZL_m \parallel [ZC_x + (ZR_y + ZL_y) \parallel ZL_l]} \tag{4.17}$$

$$Y_{21} = \left(\frac{V_1}{V_A}\frac{V_A}{V_B}\frac{V_B}{i_2}\right)^{-1} \tag{4.18}$$

A similar study is made to obtain the value of Y_{31}:

$$\frac{V_B}{i_3} = -ZL_l \tag{4.19}$$

$$\frac{V_A}{V_B} = \frac{ZC_x + (ZR_y + ZL_y) \parallel ZL_l}{(ZR_y + ZL_y) \parallel ZL_l} \tag{4.20}$$

$$\frac{V_1}{V_A} = \frac{ZC_m + ZL_m \parallel [ZC_x + (ZR_y + ZL_y) \parallel ZL_l]}{ZL_m \parallel [ZC_x + (ZR_y + ZL_y) \parallel ZL_l]} \tag{4.21}$$

$$Y_{31} = \left(\frac{V_1}{V_A}\frac{V_A}{V_B}\frac{V_B}{i_3}\right)^{-1} \tag{4.22}$$

Lastly, for Y_{32}:

$$\frac{V_2}{V_B} = \frac{ZR_y + ZL_y + ZL_l \parallel [ZC_x + ZL_m \parallel ZC_m)]}{ZL_l \parallel [ZC_x + ZL_m \parallel ZC_m]} \tag{4.23}$$

$$\frac{V_B}{i_3} = -ZL_l \tag{4.24}$$

$$Y_{32} = \left(\frac{V_2}{V_B}\frac{V_B}{i_3}\right)^{-1} \tag{4.25}$$

Now having the relationship between the 3 ports, and considering the current at the second port as $I_2 = I_s e^{\frac{V_2}{Vt}}$, as in figure 4.11 it can be written:

$$\frac{V_s - V_1}{R_s} = Y_{11}V_1 + Y_{12}V_2 + Y_{13}V_3 \tag{4.26}$$

$$I_s e^{\frac{V_2}{Vt}} = Y_{21}V_1 + Y_{22}V_2 + Y_{23}V_3 \tag{4.27}$$

$$-\frac{V_3}{R_l} = Y_{31}V_1 + Y_{32}V_2 + Y_{33}V_3 \tag{4.28}$$

The results of this analysis were obtained both with the help of Matlab and the solve command, which computes a solution iteratively for the output voltage, and with corresponding ADS simulations, the latter having generated a couple of interesting graphics present in the next chapter.

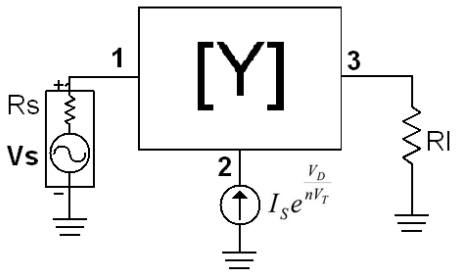

Figure 4.11: Complete 3-Port System

4.6 Voltage Multipliers

The voltage multipliers are a specific type of circuit that uses the charge-pump mechanism to increase the voltage output of a specific circuit. In this section however, only RF-DC converters will be addressed, since these circuits are to be used as rectifiers.

The chosen circuits, which were selected to address the needs of the lighting system, were already introduced earlier and consisted in Villard (or Cookroft-Walton) and the Dickson voltage multipliers, being each represented in figures 4.13 and 4.12.

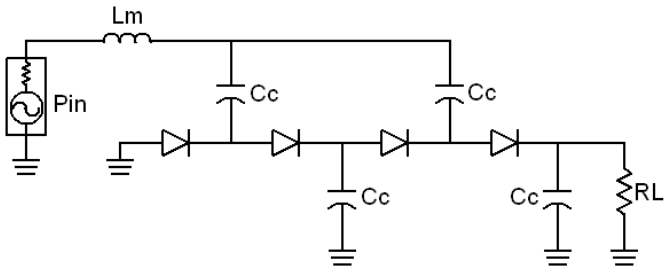

Figure 4.12: Villard Voltage Multiplier with 2-Stages

Here particular attention should be drawn to the inductor present in the input of the circuit, whose main objective was to improve the overall results of the circuit by increasing the input voltage value of the multipliers. Besides, this component alone took care of matching the circuit and reducing the reflections at the input, thus simplifying the matching network. Attention should be drawn however to the importance of having inductors with low tolerances and high quality values, so as to not jeopardise the desired results, and guaranteeing experimental results close to simulation counterparts.

As of the number of stages empirical studies showed that two would suffice the necessary output voltage and power, and although more stages could generate better voltage values the additional components would increase the power dissipation and reflections at the various points of the circuit.

The study of these multipliers was initially made in a similar fashion to the series rectifiers, using the source-pull mechanism and ADS optimization to obtain the best results, and then measuring the system response with the help of a frequency synthesiser. However in a posterior phase, having obtained sufficient voltage for the 3-LEDs cell characterized previously (namely with the Dickson voltage multiplier) a similar circuit with the necessary changes was developed.

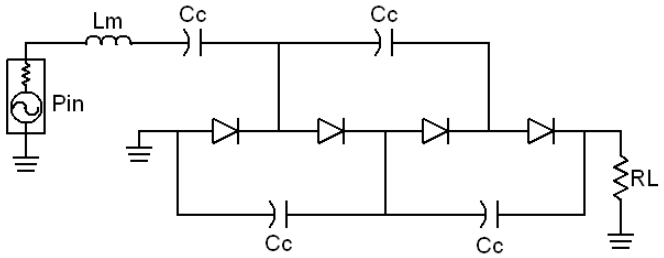

Figure 4.13: Dickson Voltage Multiplier with 2-Stages

Besides the multiplier elements at all equal to the previous studies on the selected topology, 3 LEDs and respective resistance were added to the set, consisting in the illumination cell which is the fundamental unit of the LED strip studied before.

Furthermore, considering that the placement of this unit in parallel or in series with the load would substantially change it's value, reducing the matching and efficiency, yet another component was added between the load and the lighting elements, a Schmitt-Trigger buffer (SN74LVC1G17 from Texas Instruments). This component served to preserve the load viewed by the rectifier, since it has a very large input impedance, a very low power consumption current of $10uA$ and a good supply voltage range. The final circuit is pictured in figure 4.14 and comprises both the basic system and the components added after the load, described above.

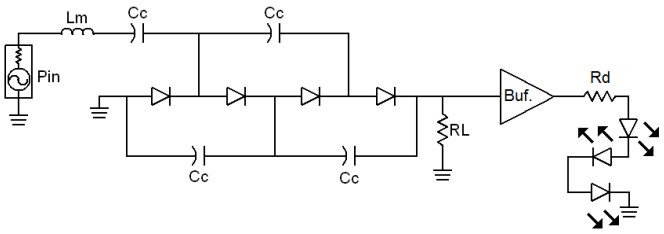

Figure 4.14: Dickson Voltage Multiplier with 2-Stages

With this system many experiments were made, being that for this case besides the same laboratory measurements as before, the system was actually tested in outdoor conditions, harvesting from a Radio emitting antenna. For this purpose a very simple Yagi antenna was developed to prove the concept. Before this however, a trial involving a simple monopole connected to a frequency synthesiser and the built receptor was also made to verify the correct operation of the system. All these situations, respective results and other considerations are found in the next chapter.

4.7 Conclusion

This chapter consisted in the problems that had to be addressed and in the proposed solutions for them, in the perspective of highly efficient energy harvesting circuits. Here the development of the work as a flow can be perceived, since subsequent approaches were made

to complement/improve previous attempts.

Beyond the rectifying systems, here the main simulations tools are introduced, consisting in the Advanced Design System, the automation software where the circuits were implemented and tuned, and in Harmonic Balance, the iterative simulation mechanism used in accordance with ADS. Both these tools were essential for this work since permitted a deep study over the circuit's characteristics and behaviours, and so a great level of detail on the design.

Also contained in this chapter are the lighting system electrical needs, which were obtained experimentally, and permitted and optimized development of the latter rectifying circuits.

As of the rectifying systems, the study started with the intention of polarizing (both in voltage and in current) a parallel non-linear element in a zone of maximized DC output for an RF input. A variety of problems (explicitly mentioned in the next chapter) however changed the course of the investigation, and methods for reducing the energy reflections in the circuit became priority. For this purpose a source-pulling study was made over the previous circuit without polarization, and over a rectifier with a non-linear element in series, settling over a graphical tool developed to observe circles of constant efficiency and voltage for varying input impedance.

Subsequently a mathematical study was also made on the parallel circuit consisting in replacing it's passive equivalent with a 3-port network, and placing the voltage dependent current source externally. The admittance values of this network were computed both from ADS simulation and analytically with the help of Matlab, the same being told for the output-input voltage ratio.

In a final stage voltage multiplier circuits, using both the Dickson and the Villard configuration were studied and developed to adapt to the lighting system electrical needs, whose final prototype was also briefly introduced here.

Chapter 5

Simulations and Experimental Results

Having studied the non-linear behaviours of the NLE and respective circuits, the proposed circuits were carefully designed for the simulations and purpose-specific graphics were obtained.

The first set of results had a bigger insight on the circuit behaviour, and on the dependency with the polarization, but presented very low efficiencies. Posterior simulations had much better efficiency results and therefore the circuits were actually built and measured in adequate laboratory conditions.

So as to perform suitable dimensioning and obtaining experimental results as close to simulation as possible, all elements from the circuits were inserted into the simulation, as is the case of the micro-strip lines length and width used to interconnect the elements.

In this section the results all the both simulations and tested circuits are present together with some inferences and conclusions.

5.1 Rectifier with Polarization Source

Before addressing the results of the circuit from figure 4.3 themselves, a couple of considerations are to be made about it:

- The components simulated were the generic ones provided by the ADS libraries, except for the diode, whose SPICE model was directly taken of the device datasheet so that it could be accurately characterized;
- The simulations used many parameter sweeps so that the operation of the device could be analysed from different points of view;
- The circuit was polarized in both voltage and current, separately, however results without parasitic resistance and for efficiency only consider the current polarization for simplicity;
- HB was used considering a number of harmonics equal to nine ($N = 9$), due to the high non-linear behaviour of the diode;
- The electrical parameters used in the simulations were mostly selected to obtain the best graphical results, however it's selection can be justified as following:

  Current Polarization : $[-10mA, 10mA]$, since this is the region were the device is supposed to operate and where important behaviours can be seen;

Voltage Polarization : $[-1V, 1V]$, for the same reason as the previous;

Input Power : $[-10dBm, 10dBm]$, although in practice those values for the final purpose, specially the upper limit, are too high, they are useful to understand the circuit's performance under power variation.

- The graphics selection was made dynamically, accordingly to the values that were of interest, and by it's usefulness for the conclusions.

5.1.1 Current Polarization

The first set of results presented here correspond to the current polarization case, that is the same circuit that was presented in figure 4.3.

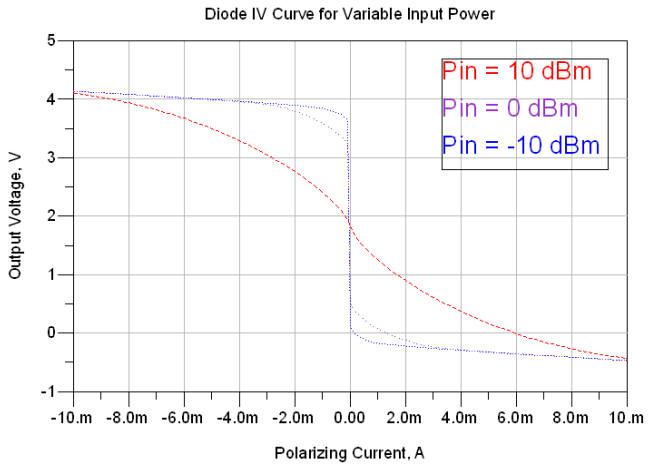

Figure 5.1: Diode IV Curve for Discrete Input Power

Analysing the diode characteristic in figure 5.1 a couple of considerations can be drawn:

- There is a slope in every curve when the magnitude of the current increases, instead of a constant voltage value as might be expected. This is caused by the parasitic resistance of the diode, which for a certain amount of current makes the device start acting as a resistance;
- For an increased input power the curves start acting like straight lines for the entire range of current, since the device puts itself into an equivalent biasing point;
- When the diode is directly polarized with small signal, it generates an output of around $-0.5V$, and when inversely it outputs just above $4V$;
- Any change in current, even if very small, places the device either in the forward region, or in the breakdown. Actually with $I_{pol} = 0A$ the device is already in the forward region.
- This device only properly behaves as a diode between the values of $I_{pol} = [-2mA, 2mA]$.

The second harmonic, which allows us to draw conclusions about the dependence of the 2^{nd} harmonic value with the polarization can be found in figure 5.2.

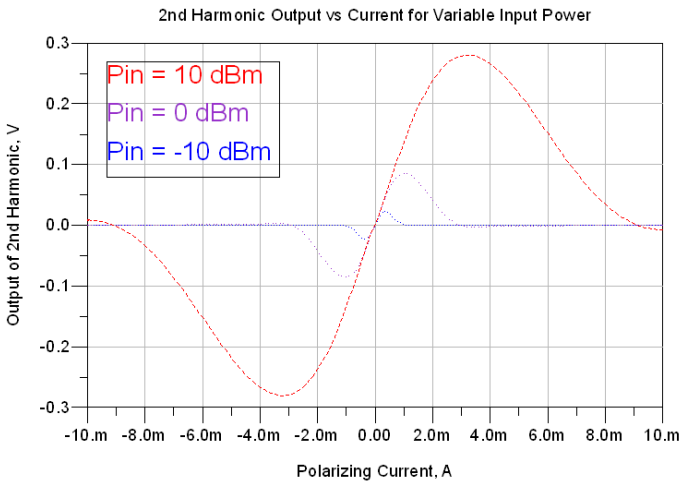

Figure 5.2: 2nd Harmonic Output vs Polarizing Current for Discrete Input Power

---

- The output voltage rises with the power as expected since there is more energy in the system to be handled to the harmonics;
- The output also depends on the current, by the existence of maximal and minimal values;
- This dependence is not absolute for every polarization, since the maximum changes with the input power.
- For an input of $P_{in} = 0dBm$ the device should be polarized with $I_{pol} \approx 1mA$, while for $P_{in} = 10dBm$ the best value is $I_{pol} \approx 3mA$.

Another possibility is to plot the curve of the output voltage against the input power for discrete values of current polarization, as in figure 5.3, which carries that:

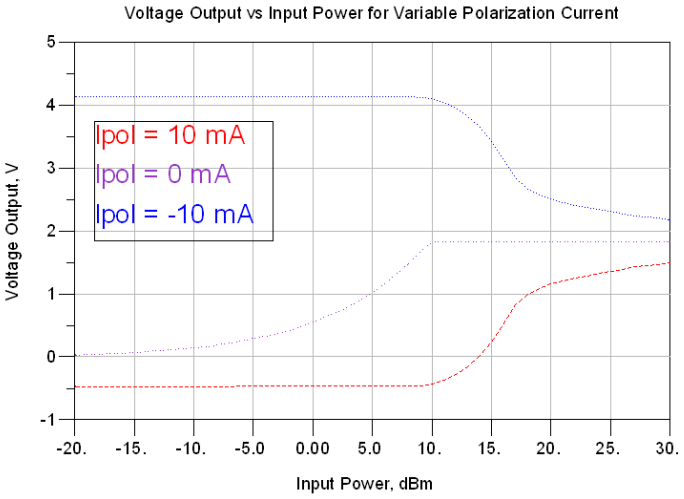

Figure 5.3: Voltage Output vs Input Power for Discrete Polarization Current

- As stated before, a current of $0mA$ directly polarizes the diode, and for small signals the output is either ≈ -0.5 or $\approx 4V$;
- Increasing the input power to values larger than $25dBm$ the output tends to approximately $1.5 < V_{out} < 2.1V$. This value represents the equivalent polarization and is approximately equal to half of the limits sum;
- Without input and with polarization, the output is different from zero due to the influence of the biasing current in the DC output;

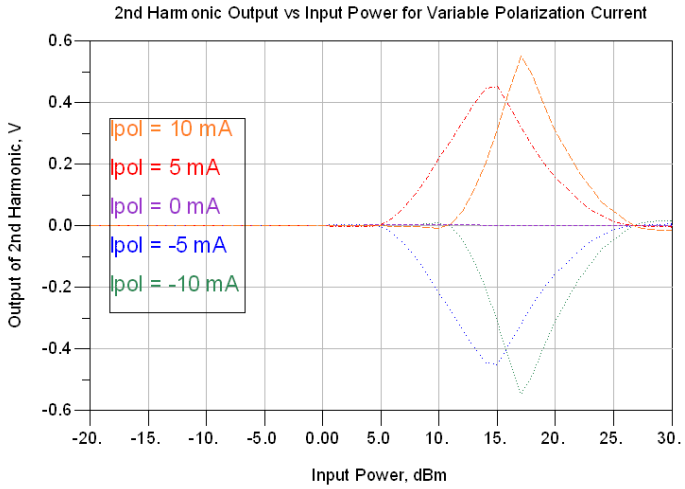

Figure 5.4: 2nd Harmonic Output vs Input Power for Discrete Polarization Current

Plotting the second harmonic instead of the fundamental mode generates the results of figure 5.4, which show that:

- No polarization results in no output value;
- For a certain input power the output is maximized;
- This maximum voltage also depends on the current, since it's increase in absolute value causes the maximum point to be moved to a higher power;
- With an $I_{pol} = 5mA$, the highest output occurs for $P_{in} \approx 15dBm$ while $I_{pol} = 10mA$ increases this value for a $P_{in} \approx 17dBm$.

5.1.2 Voltage Polarization

Subsequently, by replacing the current source in the circuit with a voltage source, voltage polarization was obtained, and a couple of simulations made. In this case the fundamental mode simulation carried no useful information, because it's representation was just a curve with a slope different than zero, since the output DC level is directly dependent on the DC bias.

The second harmonic however carries important information, and can be seen in figure 5.5. Essentially it shows that:

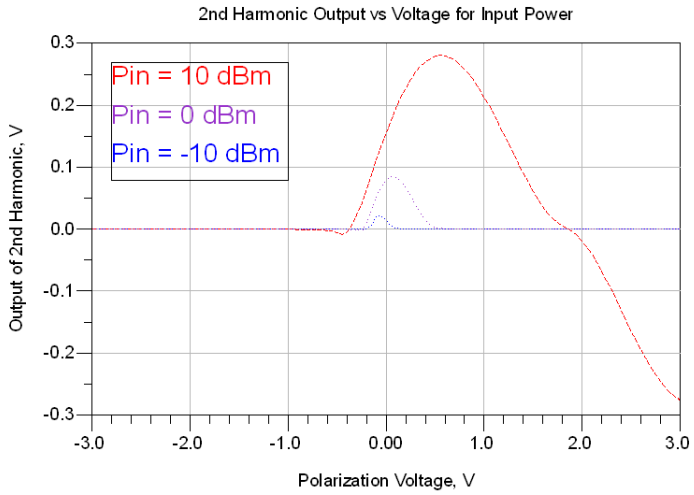

Figure 5.5: 2nd Harmonic Output vs Polarizing Voltage for Discrete Input Power

---

- Similarly to the previous cases the output increases with the power provided to the system;
- Also similar is the dependence of the output maximum value with this power;
- Any value of polarization outside the values $V_{pol} = [-0.5, 2.0]V$ for less than $10dBm$ is worthless;
- Again, while for $P_{in} = 0dBm$ the preferable biasing voltage is $V_{pol} \approx 0.05V$, for $P_{in} = 10dBm$ it changes to $V_{pol} \approx 0.5V$.

The second graphic for the voltage polarization method is depicted in figure 5.6 and adds, or reinforces the following considerations:

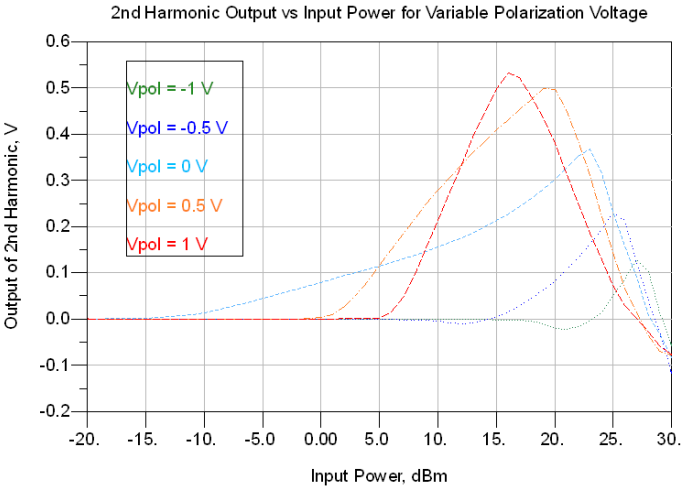

Figure 5.6: 2nd Harmonic Output vs Input Power for Discrete Polarization Voltage

- The maximum efficiencies are obtained for high input powers ($P_{in} > 15dBm$);
- This maximum values depend a lot on the polarization;
- For instance, $V_{pol} = 0V$ is a very good choice for $P_{in} < 5dBm$ but not so much for $P_{in} = 15dBm$ where $V_{pol} = 1V$ is clearly the best option.

5.1.3 Parasitic Resistance equal to Zero

Removing the diode's resistance from the SPICE model and running the same simulations for the current polarization, the graphics from figures 5.7 and 5.8 were obtained.

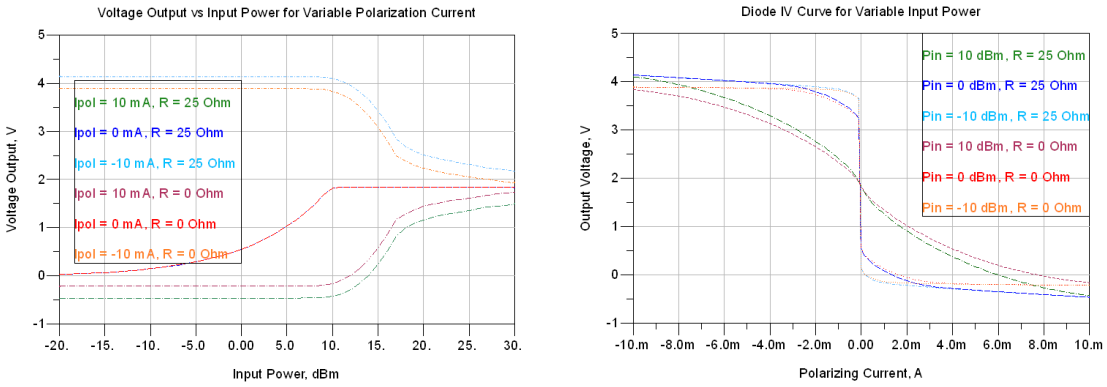

Figure 5.7: Figures 5.1 & 5.3 with and without R_s

In figure 5.7, that shows the fundamental mode for two different plots, it is shown that without the parasitic resistance:

- The diode's IV curve behaves more like an exponential, which means that for higher power inputs the linear dependence of the output with the current is almost absent;
- There is a better convergence for the equivalent polarization point, because for a larger input signal the output is fixed on either $V \approx 4.1$ or $V \approx -0.5$, not changing for an increased current biasing.

As for the second harmonic results, which are plotted in figure 5.8 the unique important conclusion is that R_s is responsible for changes in the output maximum values.

Although in general the removal of this resistance would improve the behaviour of the circuit, this is an inherent parameter and little or nothing can be done about this.

Another curious effect of the presence of the resistance can be taken from the time domain signal present in figure 5.9, where $P_{in} = 30dBm$ and $I_{pol} = 10mA$. The square shape for a $R_s = 0\Omega$ means that the diode clamps either positively or negatively, thus saturating, which is the desirable outcome.

On the other hand, with $Rs = 25\Omega$ there is a resistance-like behaviour of the diode for high power input signals. This contradicts the former, and is pictured as a sinusoidal output. Finally, both curves have a mean value of $V_{out} \approx 2V$, which is the polarization equivalent point, and represents the expected value for large signals.

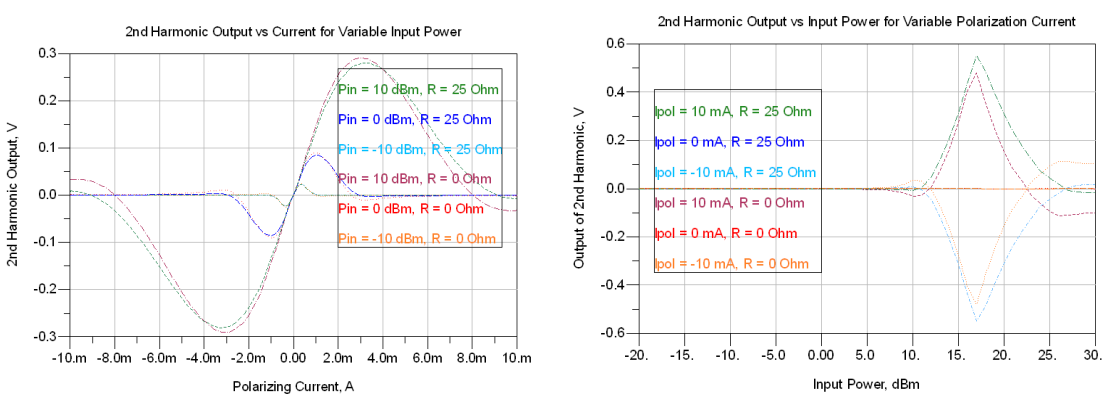

Figure 5.8: Figures 5.2 & 5.4 with and without R_s

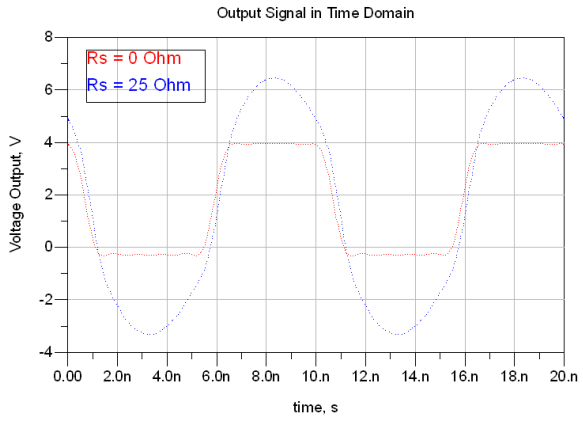

Figure 5.9: Output Signal Forms with and without R_s

5.1.4 Circuit Efficiency

A very important concept in energy harvesting circuits is the quantity of input energy that is the transformed into useful energy to the output.

This parameter, named efficiency, is mathematically defined as:

$$\eta = \frac{P_{DC}}{P_{RF}} \tag{5.1}$$

For the purpose of evaluating the efficiency of the circuit in question two approaches were used, both recurring to current polarization. One the one hand it was calculated the ratio between the input power and the DC component.

This measure which was done without polarization current, since otherwise the output would not be just dependent on the input signal, is shown in figure 5.10, and carries a maximum efficiency of $\eta = 0.035\%$ for an input power of $10dBm$. This value which is extremely low, can be partly explained with the absence of matching networks.

On the other hand, two simulations were made for the ratio between the power in the second harmonic and the input signal, resulting in figure 5.11. This output should be studied under a qualitative point of view and not quantitative since the output power belongs to an harmonic and not to a DC value.

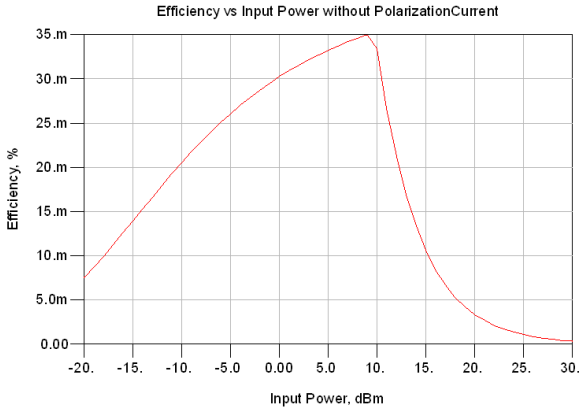

Figure 5.10: Efficiency for DC without Polarization

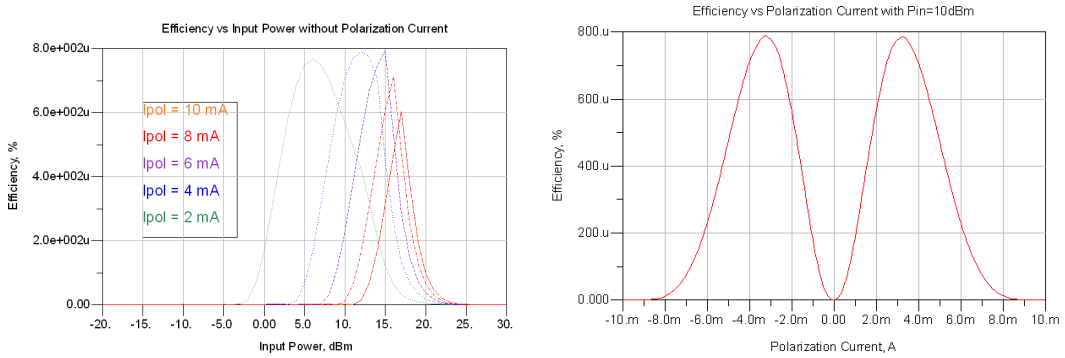

Figure 5.11: Efficiency for the 2nd Harmonic

While in the first figure the efficiency is evaluated for a variable input signal and discrete biasing values, in the second an input power of $P_{IN} = 10dBm$ was fixed and the device was polarized in different regions.

Both this graphics present maximum values, which should be examined qualitatively. The first graphic states the same as the DC efficiency plot, which is that the maximum points of efficiency change with P_{in}. On the second graphic a dependence of this point with current is observed. Furthermore a very low efficiency for $I_{pol} = 0A$ is displayed which may help explaining the low efficiency values of figure 5.10.

5.2 Rectifier with Matching Network

As just seen the obtained efficiencies for circuit 4.3 were very low, which demanded alternative solutions, so circuits 4.5 and 4.6 were considered. Effectively these presented much better results, that will hereby be exposed and discussed on the form of graphics.

5.2.1 Source-Pull Mechanism

On each figure presented in this section two smith charts condense the information about the efficiency and output voltage, via constant valued circles and respective values of the

measured magnitudes through the application of the source-pull method.

The process of choosing the load was based on a try and error method, by the observation of the efficiencies for each resistance value, therefore there was always a certain inaccuracy. To obtain the best possible value out of these experiments, a 3D Smith Chart that allowed to sweep this component at the same time as the input impedance was changed would be preferable, but this technique would consume an enormous quantity of a processor resources.

Furthermore since the values of all the components on the circuit suffer from some uncertainty, optimizing the simulation down to the smallest detail would generate unachievable results for real circuits.

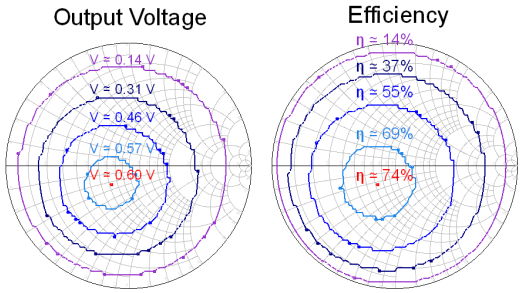

Figure 5.12: Voltage and Efficiency for the Diode in Parallel with $P_{IN} = -10dBm$

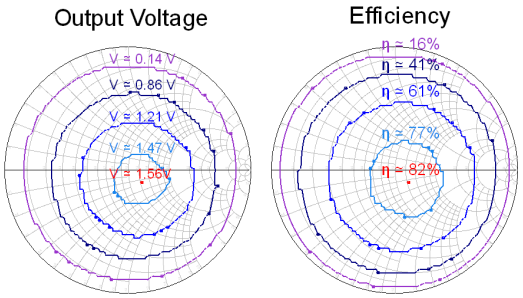

Figure 5.13: Voltage and Efficiency for the Diode in Parallel with $P_{IN} = 0dBm$

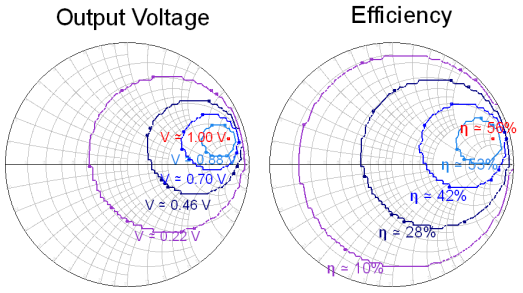

Figure 5.14: Voltage and Efficiency for the Diode in Parallel with $P_{IN} = 10dBm$

Figures 5.12 to 5.14 contain the values of interest for the first circuit, with the diode in parallel for the discrete values of input power.

The chosen values of the load resistances were $R = 5K\Omega$, $3K\Omega$ and 180Ω for the input

power values of $P_{IN} = -10dBm$, $0dBm$ and $10dBm$, respectively.

Analysing these first graphics, a couple of inferences can be drawn:

- The circles of constant output voltage are relatively coincident with the efficiency circles, as would be expected, since the output power is only dependent on the voltage and on the resistor that is maintained constant for each essay;
- The constant circles and maximum point values are dependent on the input power, since they rotate their location for different P_{IN};
- The maximum efficiency, and voltage are obtained for an input power of $P_{IN} = 0dBm$.

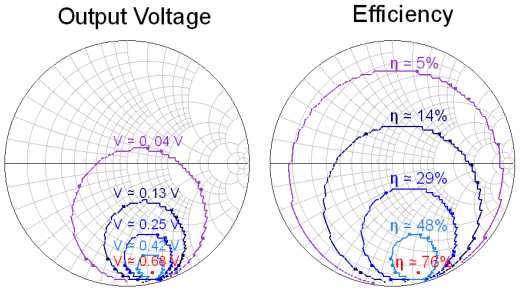

Figure 5.15: Voltage and Efficiency for the Diode in Series with $P_{IN} = -10dBm$

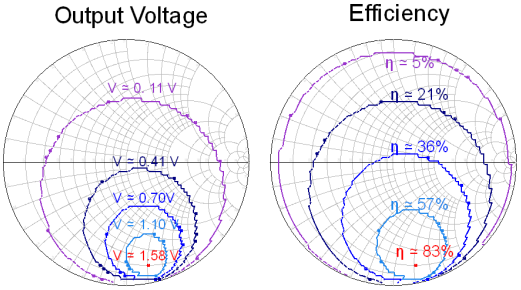

Figure 5.16: Voltage and Efficiency for the Diode in Series with $P_{IN} = 0dBm$

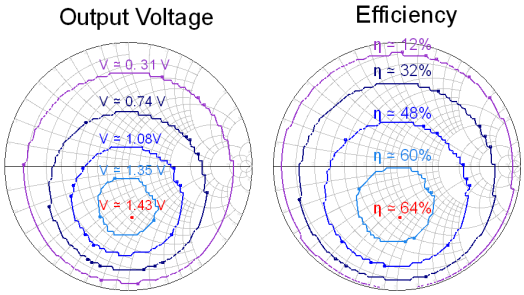

Figure 5.17: Voltage and Efficiency for the Diode in Series with $P_{IN} = 10dBm$

Putting the diode in series, the results do not change dramatically, however some changes are observed analysing figures 5.15, 5.16 and 5.17 in comparison with the previously presented graphics. With respect to these results:

- While the maximum values don't significantly change, this configuration has worse efficiencies when considering source impedances near the Smith Chart border. For instance for $P_{IN} = 0dBm$ the efficiency lowers from $\eta \approx 16\%$ to $\approx 5\%$;
- The constant circles depend whether the diode is in parallel or in series, something that can be clearly seen by placing $P_{IN} = 10dBm$ in both circuits and observing the best source impedance;
- The deductions about the dependency of the circles with the power and the maximum efficiency are also valid for this case.

In general this method of efficiency analysis intuitively allows a careful tuning of the circuit components, and being a graphical technique is of simply understanding. It might be applied to a great variety of other circuits without significant changes, and inclusively can work as load-pull method by sweeping the load impedance instead of the source value.

Finally the energy storage elements of the circuit, can and in fact were, subjected to small adjustments so as to increase the overall results.

5.2.2 Fixed Matching Network

Dropping the source-pull optimization by fixating the input impedance to the maximum efficiency location for different input powers results in a degree of freedom, that may be used to further study the dependence of the efficiency with the load resistor.

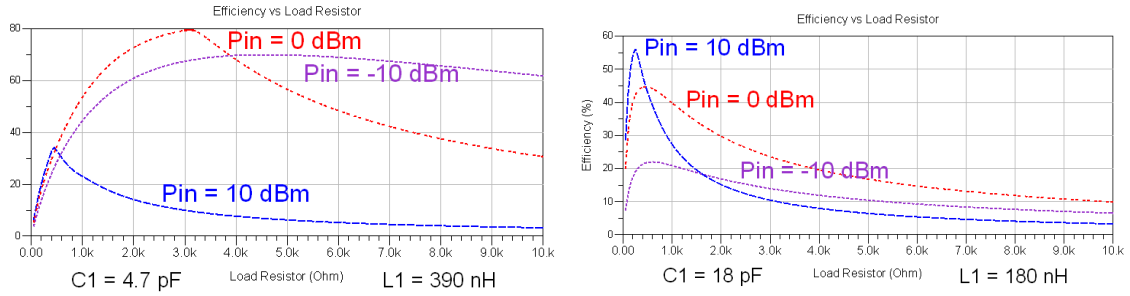

Figure 5.18: Diode in Parallel with Different Matching Networks

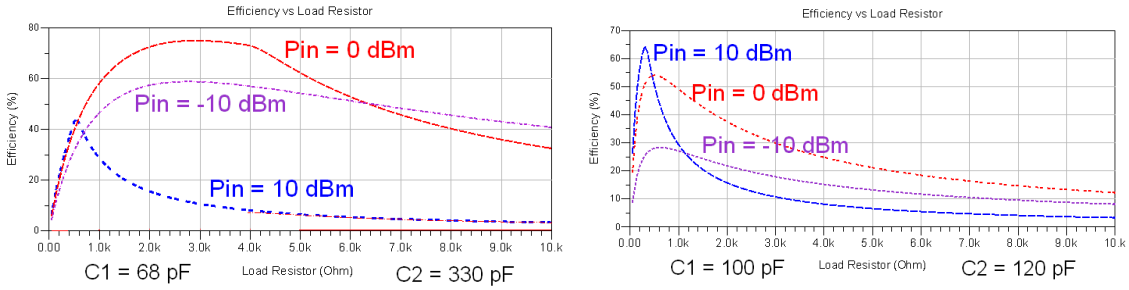

Figure 5.19: Diode in Series with Different Matching Networks

That said, the results of figures 5.18, and 5.19 are introduced, were two sets of matching networks were tested for each configuration, resulting in distinct values of efficiency for different

values of P_{IN}. It should be noted also, that the location of components shown in the graphics (C_1, C_2 and L_1) is properly identified in 4.5 and 4.6.

The obtained results from these simulations corroborate some of the made deductions and introduce a few others:

- For lower values of P_{IN} the variation of the load resistor has less influence on the efficiency;
- An input power of $0dBm$ is less influenced by changes to the matching network;
- The best results are obtained for this value of P_{IN};
- Both circuits show similar behaviours in relation to the change on the matching and power.

In contrast to the polarized circuit the efficiencies are now very good, above 60% for every input power simulated, and therefore allow the further step of designing the layout for real circuit. This process and respective results are presented in the next section. [51]

5.3 3-Port Network Analysis

This analysis which was made to complement the previous, was made both mathematically through Matlab and by simulation with ADS. Into the Matlab script the equations that represent the admittance values and the output/input ratio were inserted, while for the simulation the circuit of figure 5.20 was implemented.

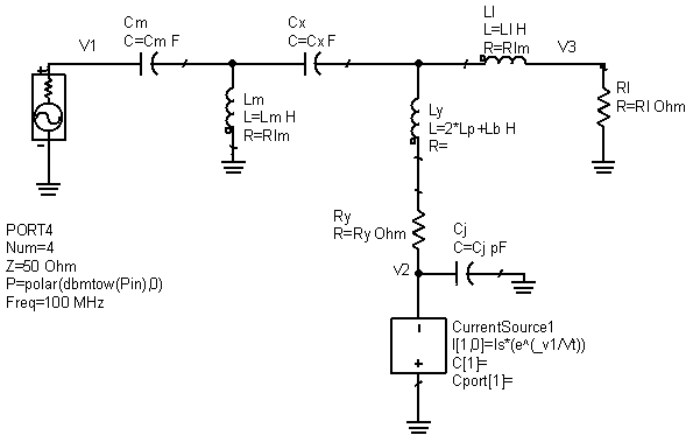

Figure 5.20: ADS Simulated Circuit

This circuit, which consists in the 3-port network with a power source input, a load in the output and a Symbolically Defined Device (SDD) with the diode's equation in port 2, uses the same components as in the built parallel circuit which will be presented further ahead, that is: $C_m = 5.1pF$, $L_m = 330nH$, $C_x = 10nF$, $L_l = 100uH$ and $R_l = 3300Ohm$. Running the Matlab script, and complementing with the ADS, the Y matrix bellow is obtained.

$$\begin{bmatrix} 3.2m\angle 85.5 & 3.2m\angle -87.7 & 1.3u\angle -174.8 \\ 3.2m\angle -87.5 & 1.5m\angle -87.5 & 15.8u\angle 92.3 \\ 1.2u\angle -174.8 & 15.8u\angle 92.3 & 15.9u\angle -90.0 \end{bmatrix}$$

It should be noted, that although not all the parameters were calculated in Matlab, those which were effectively presented the same values as the ones obtained from the ADS, which proves that the circuit was successfully analysed.

As of the voltage voltage values on the three ports, for an input power of $0dBm$, these are depicted in figure 5.21, having been obtained with the ADS simulations.

It can be seen that the output value is a DC value ($\approx 1.4V$), and the efficiency obtained for this configuration is around $\approx 58\%$, what agrees with the results that were obtained for the tested parallel circuit that will be presented in the next section. A more careful selection of components instead of the components that were chosen for the practical circuit, would take these results to be in more in concordance with the source-pull study however these provide a more realistic overview.

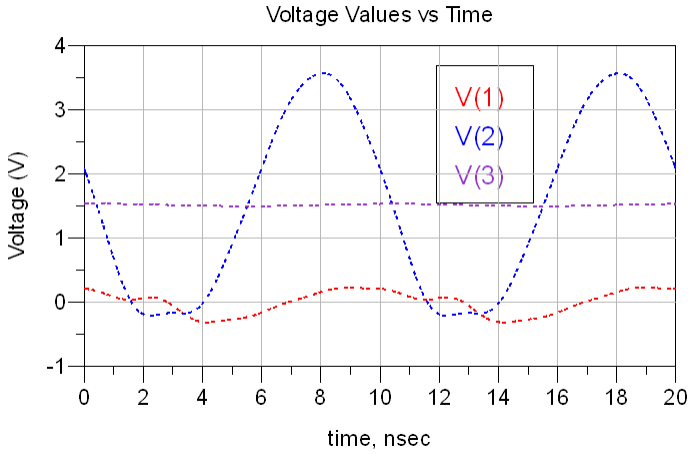

Figure 5.21: Voltage Values for 3-Port Network Simulation

As of the dependency of the DC output voltage as well as of the harmonics on the input power, figure 5.22 is presented. Again the results are similar to the observed previously.

In this case for the simulation the SDD block had to be replaced with an ideal diode, since the obtained results were not satisfactory, probably due to some problem on the formula results for variable input power.

Here it is seen that both the curve of the DC value and second harmonic for variable input power are in agreement with the previous results, since similar behaviour is observed when comparing with figures 5.1 and 5.2.

It can be then concluded than the 3-port analysis made is perfectly valid, since it matches the results obtained through the use of other methods.

5.4 Simple Rectifier Implementation

Having made an extensive study of the series and parallel simple rectifier circuits, based on simulation results, sufficient knowledge was obtained about it's operation and characteristics

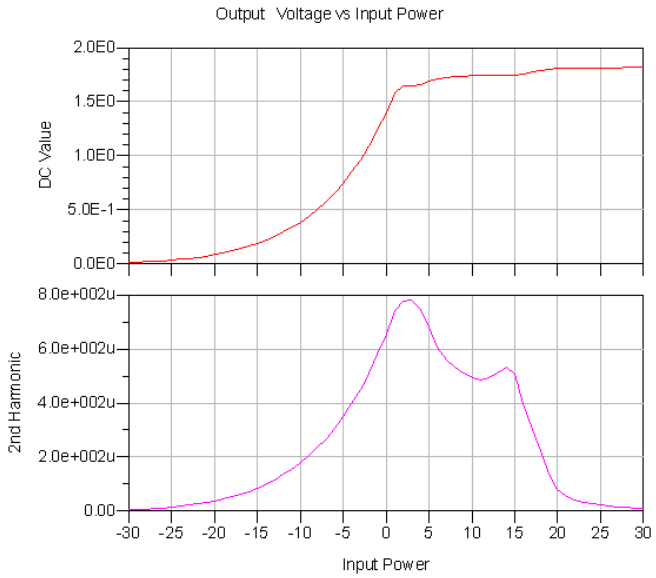

Figure 5.22: Output Voltage Values vs Input Power for 3-Port Network Simulation

so as to implement these high-efficient circuits.

The built circuits results were not however, as good as expected in the first trials, and various modifications had to be made during the process of implementation. These are explained in more detail for the case of the series diode but that doesn't mean that the actions taken for this circuit were not taken for the others, they were just not referred since this would only bring redundancy.

The important to retain here is that careful analysis and optimization of the built circuits was made to obtain the best outputs possible, maintaining a set of key characteristics such as the circuit dimensions, the overall low cost of the system and the frequency.

5.4.1 Diode in Series

The results for this rectifier are organized in a sequence of steps, or trials, where a rather careful explanation of the optimization process is made, in order to provide an insight over the implications of dimensioning such a sensitive circuit.

1st Trial

In this first experimental trial, the circuit consisted in a basic rectifying cell containing a non-linear element in series with the input signal. It was built on top of a generic FR-4 substrate, and used regular off-the-shelf components, with unknown quality and tolerance values. The rectifying element chosen was the one considered in the simulations, that is, a HSMS-2850 diode.

The circuit components were chosen so as to maximize the efficiency for the range of $P_{in} = [0, 10]dBm$, by testing different values for R_L, C_3 and L_1, as in figure 4.6, together with the source-pull mechanism developed. This technique ensured that the best results could be achieved, by minimizing the reflections on the circuit. The matching network consisting on C_1

and L_1, was selected accordingly to the best source impedance retrieved from the source-pull mechanism.

As of the first results obtained, these were rather unsatisfactory, since the obtained efficiency was less than 5% while the expected result, obtained from simulation was above 65%. The main reasons for this drop in efficiency were:

- Use of an invalid diode model, with an unsuitable diode IV curve, and disregard for the package parasitic components;
- Consideration of infinite quality factor inductors with no series resistance;
- No simulation of the layout transmission lines ;
- Use of roughly approximated components, instead of exact valued one's.

Some of these problems were solved, simply by replacing the components with others with more specific values, and greater quality factors, and by including in the simulation all the elements of the built circuit.

The diode model however, that proved to be inaccurate, was obtained manually trough the use of a simple test circuit consisting in the diode in series with an $1K\Omega$ resistance.

The measurements were then applied to two methods of regression, a quadratic and an exponential, and resulted in the curves of figure 5.23.

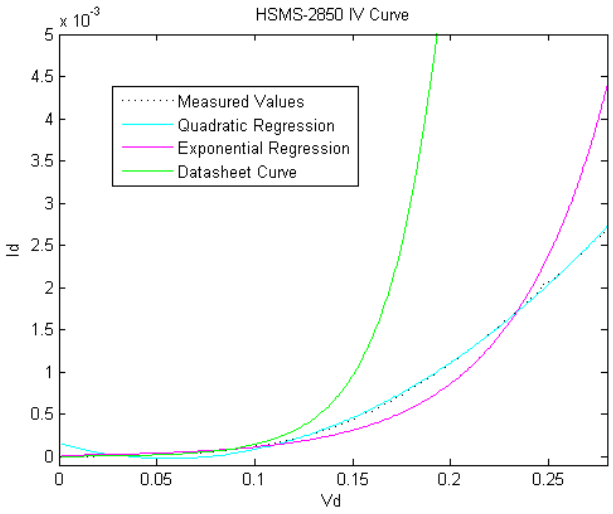

Figure 5.23: HSMS-2850 IV Curve

It can be seen for this figure that the datasheet exponential curve greatly differs from the measured values, and that although the exponential regression represents an improved curve that better suits the results than it's counterpart, the best regression is evidently the quadratic that very much overlaps with the measurements.

On the other hand the use of an exponential model in the ADS HB simulation, which is iterative, results that no convergence is achieved, and so no simulation can be carried out with this particular model, which is rather unfortunate. Therefore, the model chosen to represent this device in the simulation and to serve as reference for the components selection was the exponential.

2nd Trial

Having made the necessary changes, better results were obtained, being these depicted in figure 5.24, where the efficiency values for an input power variation from $[-20, 10]dBm$ are presented.

These results are however still not the expected, something that can be explained with the:

- Poorly characterized subtract (FR-4), since the simulated characteristics might differ greatly from the real model;
- Non-ideal inductor, L_1, with series resistance different than zero, even if lower than other general use component's;
- The regression curve that better suits the measures is not applicable to simulation;
- Components tolerance is excessive (5%), meaning the components considered in simulation may vary slightly from the real ones.

Taking into account that the first three problems were not easily solvable, not much could be done, however as of the last point, the tolerance of the components was at this point taken into account. In order to assess the exact relevance of this factor in the results the ADS mechanism of *Monte Carlo Optimization* was used to obtain the best and worst case scenarios for the efficiency values, assuming a 5% uncertainty, resulting in a series of plots that were also extended to the voltage values and to the following circuits.

The plot that represents the best and worst possible efficiencies for the series rectifier with 5% tolerance components are presented in figure 5.24, together with the experimental results, as well as the same set of results for the output voltage values.

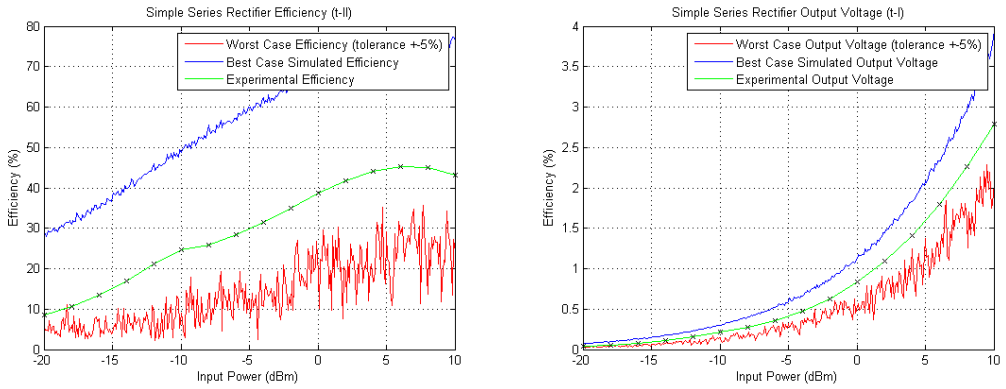

Figure 5.24: Efficiency and Output Voltage with 5% Tolerance Components (Series Circuit)

This graphic helps explaining one of the reasons why the obtained results were so inferior to the expected. In fact in light of the used components the efficiency was still above the worst case scenario, which is very positive since it indicates that the results could probably be improved by acting on the components tolerance.

Another conclusion that can be drawn is that there is a very large dependency of the circuit matching and respective results on the component's values, so these have to be very

accurate so as to correctly match the circuit. This was found specially true for the value of L_1 whose manual modifications revealed that a 5% tolerance was too much, and had significant effect over the results.

In order to solve this problem and obtain higher efficiencies, an obvious solution was followed, which consisted in using components with less tolerance, meaning that most of the 5% components were replaced with equivalent 2%.

3nd Trial

Having made the desired modifications it was verified that the simulations results effectively improved, reducing the margin of uncertainty for both the output voltage and efficiency, however the experimental results didn't followed the same trend, as seen in figure 5.25.

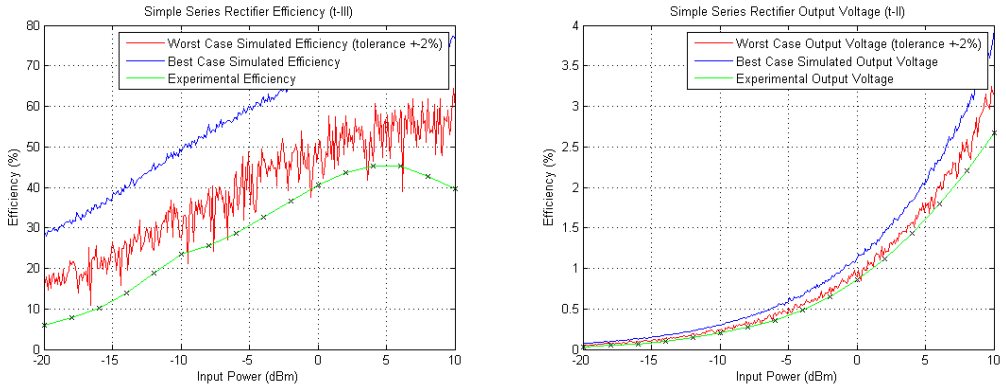

Figure 5.25: Efficiency and Output Voltage with 2% Tolerance Components (Series Circuit)

In fact a slight deterioration on the results happened, with the efficiency and output voltage levels reducing a bit, thus showing that the tolerance of the components was not the most important factor. Although unexpected since all the variables were apparently inserted into simulation, with the exception of the exact IV curve and subtract characteristics, another possible cause was regarded. This additional factor consisted in the transmission lines length uncertainty, and eventual solder effects on the lines characteristics. For instance, the placement of the components over the transmission lines in a specific position could change it's effective length, and since very short lines were used in the circuits, the percentage variation could be reasonable. A possible solution for this problem was attempted by implementing a circuit with much longer transmission lines than the previously implemented circuits, thus leading us to the 4th trial.

Prior to this however, the frequency response for this circuit, pictured on figure 5.26, where it is verified that the circuit was correctly tuned for the desired frequency, having reasonable results for a bandwidth of $20MHz$ around the central frequency. This graphics, being in concordance with the previous on the variation over input power, also show that the experimental results are lower than expected.

4th Trial

Having made the considered changes on the circuit, so as to have longer transmission lines, the results from figure 5.27 were achieved.

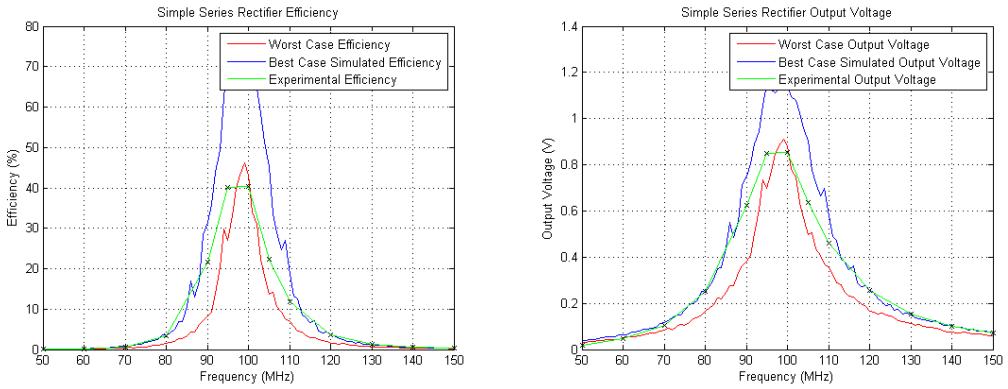

Figure 5.26: Frequency Response with 2% Tolerance Components (Series Circuit)

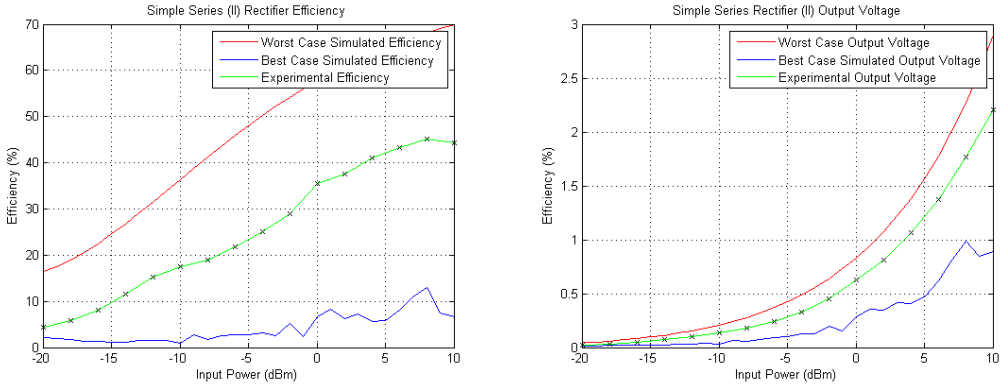

Figure 5.27: Efficiency and Output Voltage with Longer Transmission Lines (Series Circuit)

For this trial the results achieved were closer to the best simulation results, thus showing that the significant effect of the transmission lines was reduced with success. At this point it can be pointed out that the use of non-specific components was now the major cause of mismatch between the expected and obtained results.

The simulation values themselves were not very high, since there was an unavailability of the specific components that would result in higher values, as is the case of the inductor's parasitic resistance, which reduced the overall efficiencies in more than 10%.

Finally the frequency response for this same circuit, can be found on figure 5.28 and shows that altough the simulated circuit is tuned to a frequency slightly above, the experimental results show it's maximum for the $100MHz$ frequency.

5.4.2 Diode in Parallel

Having made a more complete study over the series circuit, for which different phases were surpassed, the know-how obtained from it's trials was applied in the development and implementation of the parallel circuit, thus simplifying it's designing process. This circuit also used 2% tolerance components, similarly to the best simulated case of the series counterpart.

However, the problems related with the transmission lines uncertainty couldn't be avoided, since the circuit from the 4th trial was made posteriorly, and so a similar mismatch between

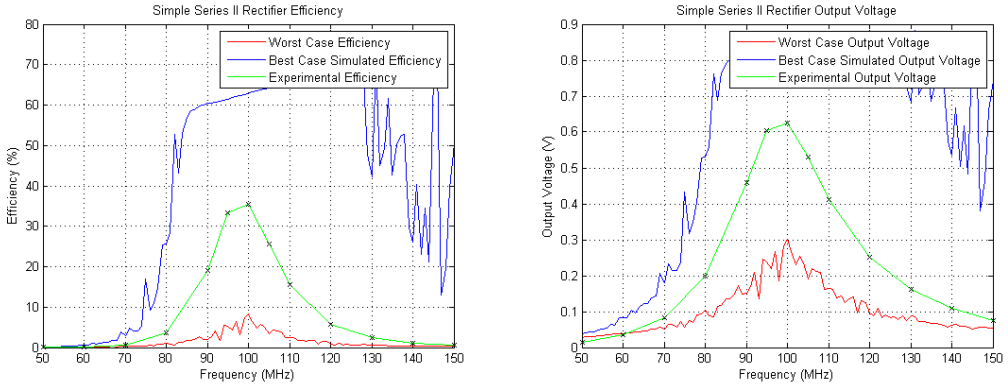

Figure 5.28: Frequency Response with Longer Transmission Lines (Series Circuit)

the simulations and measurements similar to the 3rd trial of the series rectifier was observed, as seen in figure 5.29.

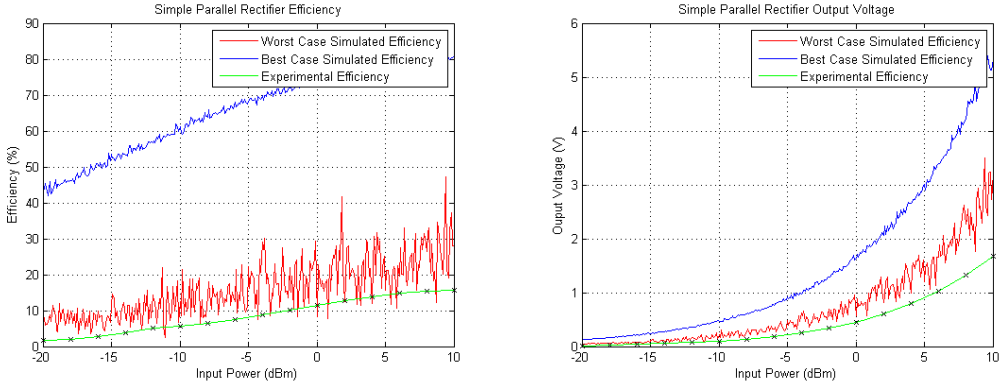

Figure 5.29: Efficiency and Output Voltage (Parallel Circuit)

Additionally, a comparison with the results from the 3rd trial shows that this circuit had worse results both in the efficiency, which is always lesser 10% and in the output voltage.

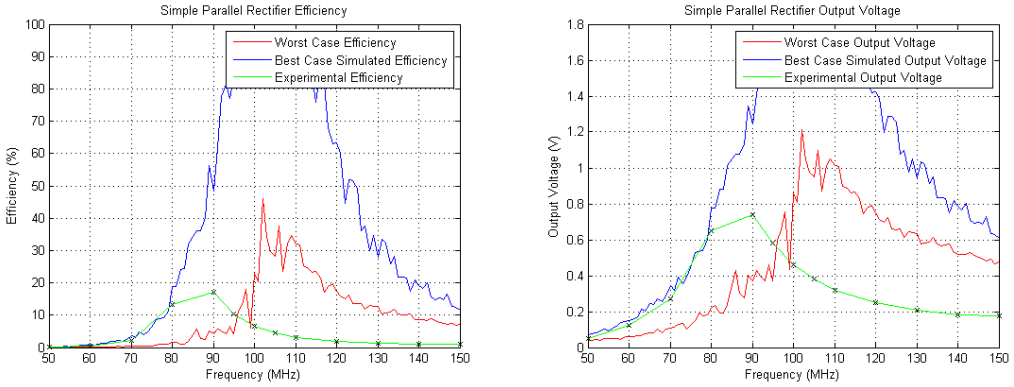

Figure 5.30: Frequency Response (Parallel Circuit)

As of the frequency response, pictured in figure 5.30 an interesting effect is verified, the experimental circuit is optimized for a different frequency than expected, that is, for $90MHz$ instead of $100MHz$. For this frequency the results are then closer with the obtained from the series rectifier, still being the measurements relatively bellow the expected.

5.5 Voltage Multipliers Implementation

As seen before the illumination system powering needs are distinct from the basic rectifiers output, since those only output a maximum of $2V$ for input power values of $10dBm$, which is not even enough to power up one LED.

Because of this the voltage multipliers introduced in the previous chapter were implemented, both in the Dickson and the Villard configurations. A similar study made for the simple rectifiers was made here, plotting both the best and worse case efficiencies and output voltages for the components tolerance, however in this case the circuit's design was made with more consideration on the output voltage levels and less importance on the efficiency obtained.

5.5.1 Villard Voltage Multiplier

This first circuit, whose equivalent circuit can be found on figure 4.12 presented, for the variable input power study, the results found on figure 5.31.

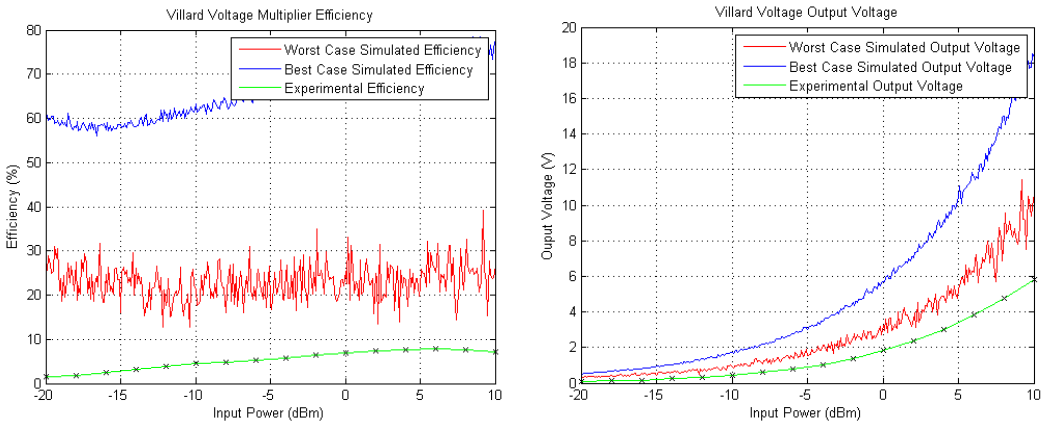

Figure 5.31: Efficiency and Output Voltage (Villard Multiplier)

Here a couple of conclusions can be drawn, in comparison with the previous cases:

- Experimental results remain well below the expected (efficiency and output voltage);
- Efficiency in overall less than the previous;
- Larger independence of the efficiency with variable P_{in};
- Output voltage is a much higher than before;
- The system may feed 2 LEDs with an input $P_{in} = 10dBm$;

As of the frequency response, found on figure 5.32, basically corroborates the previous conclusions, only adding the information that reasonable results can be obtained for a bandwidth of $20MHz$ around the central frequency.

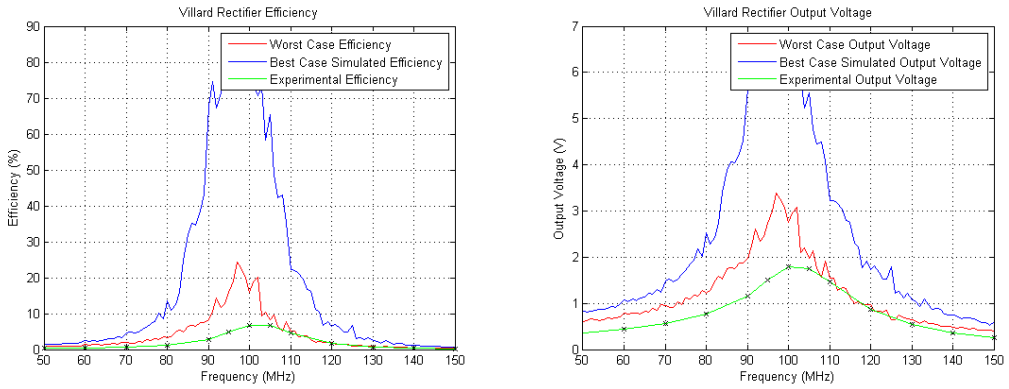

Figure 5.32: Frequency Response (Villard Multiplier)

5.5.2 Dickson Voltage Multiplier

As of the Dickson voltage multiplier, the implemented circuit can be found on figure 4.12.

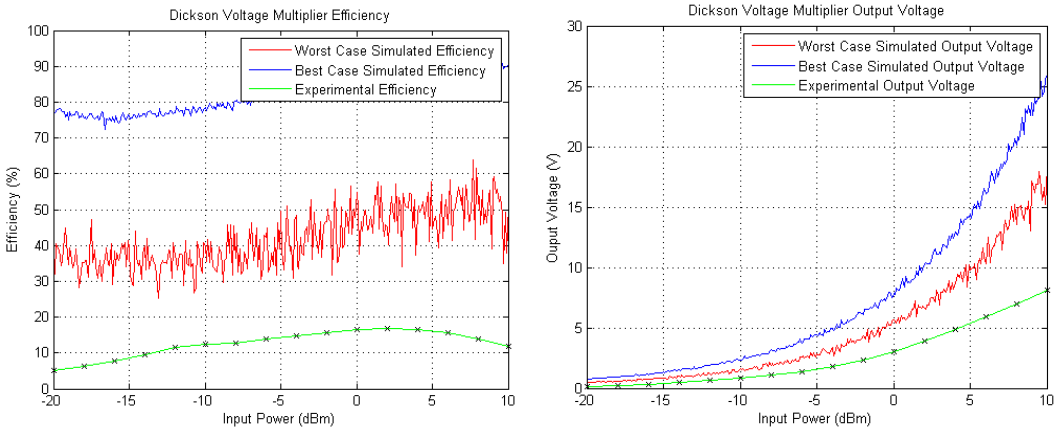

Figure 5.33: Efficiency and Output Voltage (Dickson Multiplier)

For this case, comparing with the Villard configuration, the results obtained were reasonably better, obtaining an efficiency of almost 20% for an input of $0dBm$, which generated an output voltage above $8V$. This last value, being higher than the obtained from the other voltage multiplier circuit was sufficient for powering up an entire 3 LED cell for an input power of $10dBm$, and thus allowed the development of the lighting system presented in the next section.

The frequency response follows the same trend of the previous circuits, confirming the previous conclusions on the circuit. A note still for the fact that an extremely careful design of the system would result in efficiencies around 90% and output voltages above $25V$ for an input power of $10dBm$, as seen from both figures best cases.

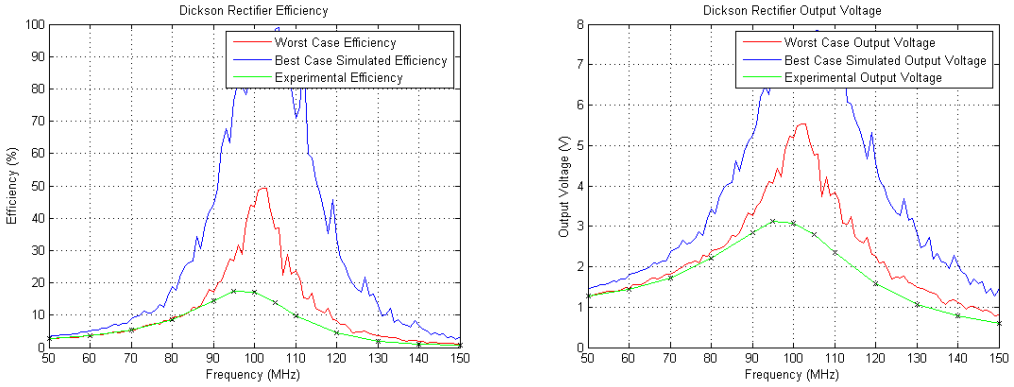

Figure 5.34: Frequency Response (Dickson Multiplier)

5.6 Lighting System

Having obtained sufficient voltage for the 3-LEDs cell characterized previously, the system presented in the end of the previous chapter, consisting in a 2-stage Dickson multiplier with the respective modifications seen in figure 4.14, was implemented.

As of the results obtained by connecting the implemented system, pictured in figure 5.35, to a frequency synthesiser, this worked correctly for an input power above $9dBm$ at $100MHz$, and showed a bandwidth of $24MHz$ for an input of $10dBm$, from $83MHz$ to $107MHz$.

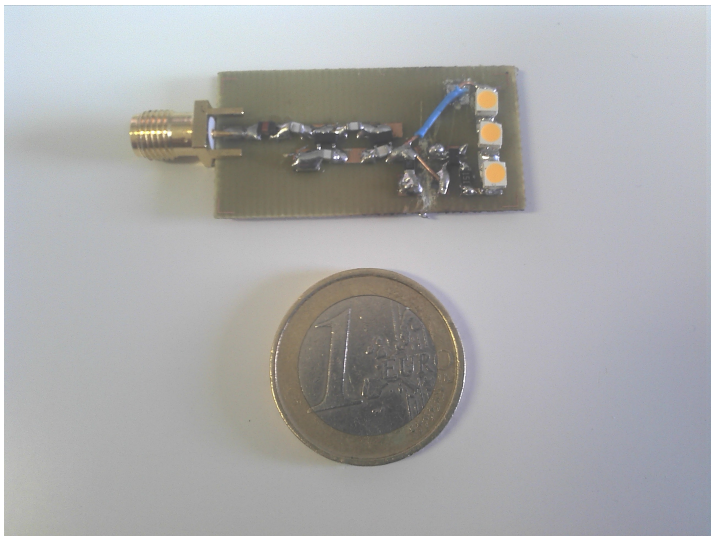

Figure 5.35: Dickson Multiplier with 3-LEDs Cell (shorter lines)

However a margin for improvement was still available, so, following the line of the previous study on the simple series rectifier, where the transmission lines length was increased for better results, this same study was made here, having been developed a similar but slightly larger board, pictured in figure 5.36.

Effectively the results were better for this case, since an input power of $7dBm$ was the minimum required for lighting up the LEDs at $93MHz$, being this value $8.5dBm$ at $100MHz$.

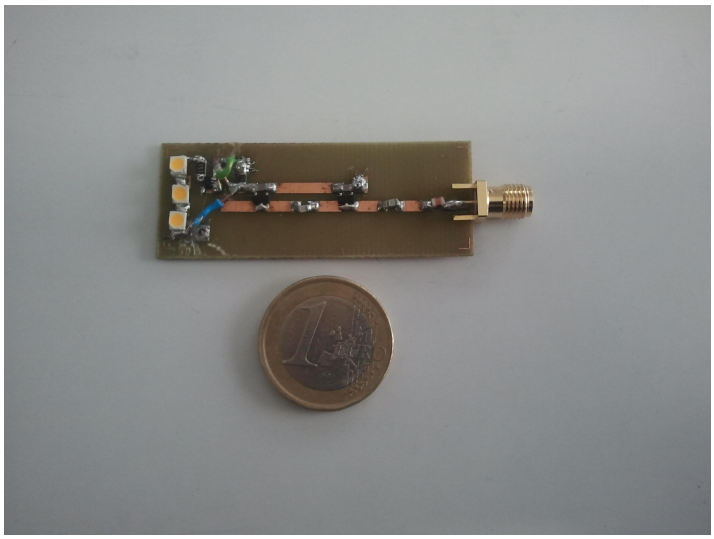

Figure 5.36: Dickson Multiplier with 3-LEDs Cell (longer lines)

As of the bandwidth, this system worked efficiently with $10dBm$ from $80MHz$ to $102MHz$, thus resulting in a bandwidth of $22MHz$.

Having made the study of the circuits characteristics recurring to a frequency synthesiser, good results were obtained, since the illumination systems worked for input power values slightly bellow $10dBm$, however these were obtained under laboratory conditions.

In order to assess the operation of both systems on a real situation, that is, harvesting from a radio emitter, an antenna had to be developed. Since it's purpose was only to proof the concept, the development of the antenna was seen as secondary, and so a simple Yagi antenna was built, being the final prototype pictured in figure 5.37. Due to the large dimensions, inherent of the frequency only one director and one reflector were used, together with the active element in order to keep a reasonable size. As of the length, spacing and position of these elements, it was calculated first with a Yagi modeller software, and then carefully tuned by measuring the input impedance of the antenna with a network analyser.

Due to the large dimensions of this antenna, but specifically the low frequency, it was not possible to obtain neither the radiation diagram, the gain or the front back ratio, since the anechoic chamber available only permitted measurements above $1.0GHz$. The cause for this is the absorber on the chamber walls, which has miserable attenuation for low frequencies. Out of curiosity, for obtaining an attenuation of just $25dBm$ at $100MHz$ instead of the typical $50dBm$ obtained above $1GHz$, the absorbing pyramids would have to be more than $2m$ tall, which is obviously not the case for the available anechoic chamber absorber.

Some reference values for these parameters can however be taken from the simulation software, being the gain $\approx 8.5dBi$, the front-back ratio $\approx 21dB$ and the radiation diagram consisting in three lobes, a very large in the front and two small in the back.

As of the antenna impedance, or equivalently S_{11} parameter, the measurements revealed $S_{11} = -8.2dB$ for the central frequency of $100MHz$, and a minimum of $S_{11} = -12dB$ for the frequency of $97MHz$, which is not critical, since both the systems generate the maximum light slight above the $100MHz$.

Finally, a simple monopole antenna was built to attest the correct operation of the Yagi

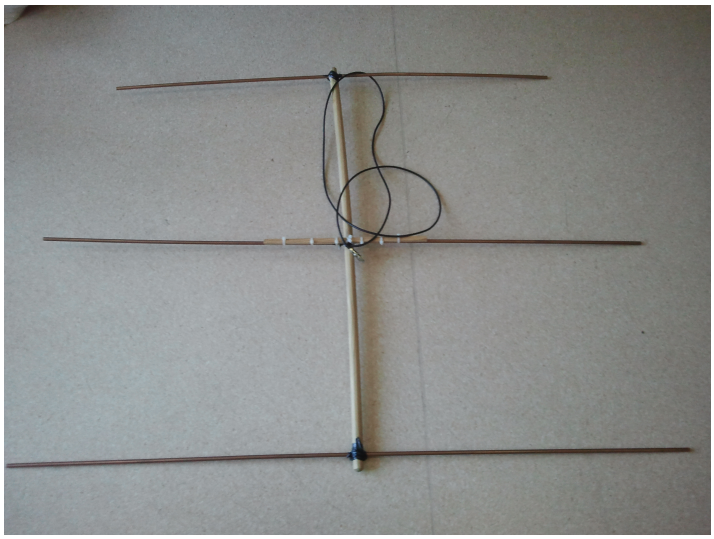

Figure 5.37: Yagi Antenna for $100MHz$

antenna with the system developed, being that the testing configuration consisted in the frequency synthesiser with an output of $18dBm$ at $97MHz$ connected to the monopole that was placed near the Yagi. This receiver was connected first to a spectrum analyser to verify the gathered power and posteriorly to the developed system (the Dickson rectifier with longer transmission lines and illumination cell), so as to measure the voltage output.

For the first measurement around $0dBm$ were received by the Yagi antenna, while the second revealed that the DC generated was around $5V$. The loss of around $18dBm$ from the emitter to the receiver is justified with the poor behaviour of the monopole essentially and with the signal attenuation in the air. These measurements proved however the validity of the concept showing that with an increased radiated power, the system would work correctly. An additional factor that may have conditioned the results was the interference generated on the signal by the laboratory devices, and the influence of the metal around the antennas on their behaviour.

5.6.1 Outdoor Measurements

With the correct operation of the system under laboratory conditions proven, both with the frequency synthesiser connected directly to the circuit and with a monopole emitting to a Yagi antenna, the developed system was taken to the field to assess it's operation on a real situation.

To serve as emitters, two commercial FM radio emitters were located, in the region of Aveiro, $510m$ apart from each other. These antennas, array's of simple dipoles, are characterised in table 5.1.

For the necessary trials both the first Dickson rectifier, and the posterior developed circuits with the lighting system integrated were used, these last with a slight modification. In order to attest the concept of no-cost illumination at higher distances from the emitter the 3-LED cells were replaced with 1 and 2 LEDs in the shorter and longer boards, respectively, so the electrical needs could be reduced.

With this in mind, two sets of experiments were made, the first to verify the On/Off

Characteristics	Antenna X	Antenna Y
Frequency (MHz)	96.5 MHz	94.4 MHz
Radio Station	Comercial	Moliceiro
Power (W)	2000	2000
Power (dBm)	63	63
Number of dipoles	5	9
Polarization	circular	circular

Table 5.1: FM Antennas Characteristics

response of the lighting system at different distances from the emitters, with the two latter circuits, and the second, using the simpler voltage multiplier, consisted in observing and registering the voltage output in different points around the antenna, by connecting it to a multimeter.

Both these results are registered in figures 5.38 and 5.39, where the map of the location around the antennas is shown with the measurements made and respective locations.

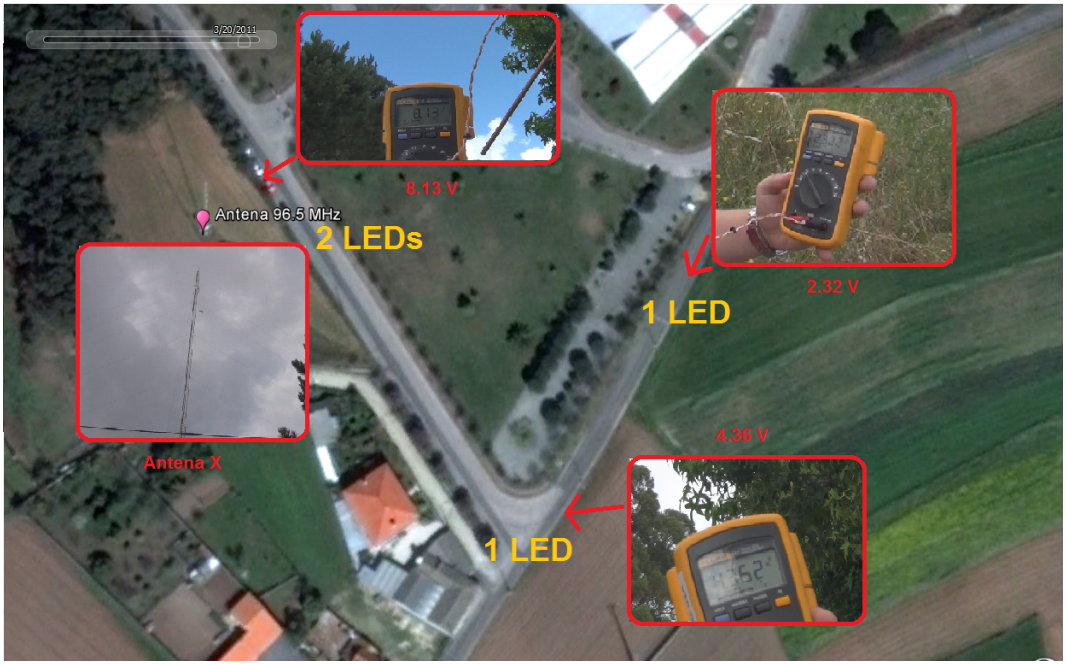

Figure 5.38: Map Location with Antenna X

From the analysis of these two maps and the experience on the field, one could conclude that:

- A voltage of $5.34V$ was generated harvesting from an antenna $400m$ away;
- The system with the 2 LEDs worked correctly at this same distance;
- The results for the antenna Y showed good results harvesting from farther distances;
- The near field behaviour was more unpredictable, unlike the far-field, as proven bellow;

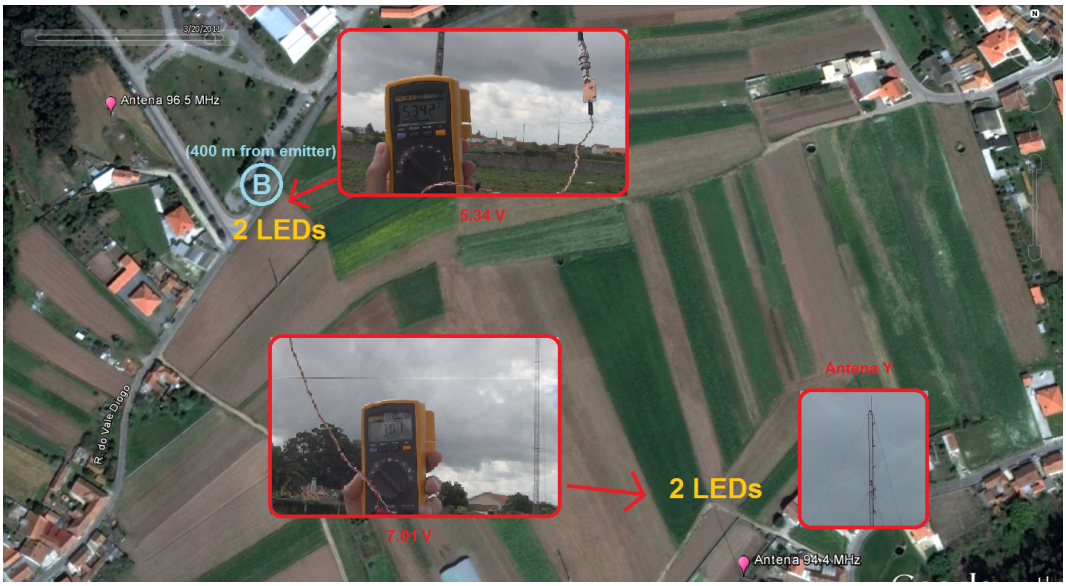

Figure 5.39: Map Location with both Antennas

- Although the polarisation of the emitter antennas was circular, the results were very dependant on the orientation of the antenna (vertical and horizontal disposition generated distinct values, being the latter the best option);
- This sensibility to polarisation, undermined possible better results;
- The concept of no-cost illumination was then successfully proven to a reasonably large area around the antennas;

Taking these results into account, so as to provide some theoretical background, a couple of calculations were made on top of this information, considering the simplified Friis equation bellow, and the reference point B (in light blue), in figure 5.39.

$$P_{r(dBm)} = P_{t(dBm)} + G_t + G_r + 20log_{10}\left(\frac{\lambda}{4\pi R}\right) \tag{5.2}$$

Considering that the emitter dipoles have a gain of $2.15dBi$ and emitting power of $63dBm$, the receiver had an expected gain of $8.5dBi$ as said before, and the distance between emitter and receiver was $400m$, we have:

$$P_{r(dBm)} = 63dBm + 2.15dBi + 8.5dBi + (-64.4)dBm = 9.17dBm \tag{5.3}$$

Observing the map on figure 5.39, an output voltage of $5.34V$ was measured, instead of the $7V$ expected for an input power on the rectifier of $9.17dBm$ (as seen on figure 5.34), being this explained with:

- The effect of the Fresne ellipsoid, since the antenna was very close to ground (less than $2m$);
- The mismatch between the antenna impedance and the rectifier's;

- The actual gain of the emitter, which ought be smaller than the considered;
- The gain of the receiver, which was estimated with the simulator and not measured, thus probably being lower than expected;

Nevertheless the expected value was still close to the obtained, and so the theoretical approach valid.

5.7 Conclusion

In this chapter the previous chapter considerations were complemented with the results obtained for the purposed systems. Starting with the polarized systems, very interesting qualitative results were obtained exposing the variation of the diode response with the input power and polarization values, with optimal points appearing for these variations. On the other hand the efficiencies obtained, being extremely low, together with the direct dependence of the DC output with the polarization, showed no practical interest in implementing such a circuit.

The posterior study, made over the source-pull system developed, resulted in very high simulated efficiencies, in some cases over 70%, for both the circuits developed, however it revealed itself very sensitive to components variation, specially for lower input values, as could be seen from the results presented.

As of the 3-port network study results, these proved to be in accordance with the outcome of the other studies over the parallel circuit, and so the mathematical background proved valid.

The simple rectifier implemented circuits, resulted in lower efficiencies than expected from the source-pull simulations, being that a series circuit with longer transmission lines was the circuit with more similarity between simulations and measurements, showing that the simulation model had to be very carefully selected, in order to predict the real behaviour of the circuits.

The voltage multiplier circuits, following the same trend of the previous, still resulted in very interesting results, since voltages as high as $8V$ were obtained for input power values of $10dBm$ on the Dickson rectifier.

Lastly, using the voltage multiplier with the best output voltage results, two systems containing an illumination source were properly implemented, being able to light up 3 low consumption LEDs with less than $10dBm$, as well as a simple Yagi antenna to harvest the energy from a radio emitter. This experiment was made both under laboratory conditions and harvesting from an actual FM emitter, for each very reasonable results were obtained.

Chapter 6

Conclusions and Future Work

6.1 Conclusions

An overview over the accomplished work over the initial objectives and problems, reveals that the results obtained were very satisfactory, verifying an evolution of the work from theoretical ideas to implementable solutions.

The first objective, which consisted in polarizing the non-linear element, generated very interesting simulation results, having proved that the efficiency and voltage values were dependent on the bias point of the element, as initially predicted, however these were not reliable for implementation, and carried qualitative and not quantitative outputs.

A main problem here was the correct set up of the simulations, particularly with the parameter sweep and harmonic balance instead of a simpler transient analysis (which would carry prohibitive simulation times, due to the high non-linearities), because the experience with the simulator was very brief, something that changed during development of the work, since this tool was intensively used. Besides, the parasitic resistance of the diode made it harder to find the correct region of operation to be studied, since for larger current magnitudes, only the influence of this resistance would be noticeable, resulting in constant slope IV curves.

Since the work focus changed dynamically with the challenges, these results led to a more power behaviour-aware study on the circuits, so considerations over the reflections became priority, and so the matching of the circuit. This matching was not done with tradition adaptation of the input impedance, for it was dependent on the input power level, so a graphical tool was developed, using the source-pull mechanism.

This tool, which consisted in plotting constant circles of output voltage and efficiency and was done over the data window of ADS, required some work on the many equations responsible for the plotting of these circles, however it revealed immensely useful in the design of posterior circuits.

As of the implemented circuits, starting with the simple rectifiers, many obstacles had to be overcome so as to implement circuits with similar results with the simulations. Problems such as the invalid diode model, disregard for the quality factor of the components or the use of low tolerance devices in a first phase, and the simulation of invalid effective transmission lines later, showed that a very thrill characterization of the real circuit on the simulation was essential for obtaining results in accordance with the simulations, what denoted a very sensibility of the matching.

However consideration of all these factors led to experimental results close to simulations,

as can be stated from the 4th trial made on the series rectifier circuit, were increasing the transmission lines length reduced the percentage variation due to the placement of the components over the lines, and resulted in efficiencies around $\approx 45\%$ for $5dBm$. This study of increasing transmission lines, was not however made on the parallel circuit nor the voltage multipliers at the time of this report, thus remaining as further work to be done.

The voltage multipliers, Dickson and Villard, faced the same problems as the previous, however good voltage values were still obtained, specially for the Dickson circuit were $\approx 8V$ were achieved, and so a specific circuit containing the illumination part of the system was implemented, being capable of generating light for an input power above $9dBm$.

The practical implementation of the system, and respective measurements both in laboratory and outdoor conditions presented very interesting results. For input power values lower than $8dBm$ in lab conditions the system with the 3-LEDs unit worked correctly, while with outdoor conditions, harvesting from an FM emitter as far as 400 m, 2 LEDs were powered enough to generate light. Both these results can be seen as good examples of the system correct operation and the concept validity, showing that the main objectives purposed in this work were achieved.

Also important is to note that beside these results were good, they can still be significantly improved, both acting in the efficiency of the rectifiers which was rather low for these voltage multipliers, $\approx 20\%$, or improving the receiving antenna. Part of these improvements are inclusively suggested as further work, in the next section.

Finally, it should be kept in mind that these improvements in the efficiencies and output voltages are always limited to relatively small values, and so these must be accompanied with the reducement of the systems power consumptions, in order to create systems with complete energy autonomy.

6.2 Further Work

As of the work to be done on this research, as well as future directions, a couple of points can be named:

- Extend the concept of longer transmission lines to all the developed circuits to achieve better results;
- Test other non-linear elements as rectifying elements (GaAs, SiC or GaN MOSFETs and diodes)
- Develop circuits for higher frequencies (use of transmission lines instead of discrete components to achieve experimental results closer to simulations);
- Develop and implement a reasonable small antenna for $100MHz$;

The future work must thus be based on developing a complete system with both the rectifier and the antenna, built together to maximize the results, presenting itself as a final prototype of possible practical application.

Bibliography

[1] K. Fujimori, K. Tada, Y. Ueda, M. Sanagi, and S. Nogi, "Development of high efficiency rectification circuit for mw-class rectenna," in *Microwave Conference, 2005 European*, vol. 2, oct. 2005, p. 4 pp.

[2] T. Takagaki, T. Yamamoto, K. Fujimori, M. Sanagi, and S. Nogi, "Efficient design approach of mw-class rf-dc conversion rectenna circuits by fdtd analysis," in *Microwave Conference, 2006. APMC 2006. Asia-Pacific*, dec. 2006, pp. 1945 –1948.

[3] D. Graham-Rowe, "Wireless power harvesting for cell phones - technology," Jun. 2009. [Online]. Available: http://www.technologyreview.com/communications/22764/

[4] P. Evans, "Intel researchers demo rf energy harvester," Jan. 2009. [Online]. Available: http://www.gizmag.com/intel-researchers-demo-rf-energy-harvester/10837/

[5] W. Brown, "The history of power transmission by radio waves," *Microwave Theory and Techniques, IEEE Transactions on*, vol. 32, no. 9, pp. 1230 – 1242, sep 1984.

[6] J. Landt, "The history of rfid," *Potentials, IEEE*, vol. 24, no. 4, pp. 8–11, 2005.

[7] M. I. of Technology, "Goodbye wires... mit experimentally demonstrates wireless power transfer," Jun. 2007. [Online]. Available: http://phys.org/news100445957.html

[8] A. Chansanchai, "In the future, will our tvs be wireless?" 2006. [Online]. Available: http://www.msnbc.msn.com/id/16042887/ns/technology_and_science-innovation/t/future-will-our-tvs-be-wireless/#.T749MNym_Id

[9] H. S. Works, "How wireless power works," 2007. [Online]. Available: http://electronics.howstuffworks.com/everyday-tech/wireless-power2.htm

[10] J. Fildes, "Wireless energy promise powers up," Jun. 2007. [Online]. Available: http://news.bbc.co.uk/2/hi/technology/6725955.stm

[11] Z. Popovic, D. Beckett, S. Anderson, D. Mann, S. Walker, and S. Fried, "Lunar wireless power transfer feasibility study," *Power*, vol. 60, p. 45, 2008.

[12] K. Walters and B. Werner, "Introduction to schottky rectifiers," *MicroNotes*, no. 401.

[13] R. Cory, "Schottky diodes," feb 2009.

[14] A. T. Inc, "Surface mount zero bias schottky detector diodes, hsms-285x series," 2004. [Online]. Available: www.agilent.com/semiconductors

[15] H. Yan, J. Montero, A. Akhnoukh, L. de Vreede, and J. Burghartz, "An integration scheme for rf power harvesting," in *Proc. STW Annual Workshop on Semiconductor Advances for Future Electronics and Sensors*, 2005, pp. 64–66.

[16] F. Pan and T. Samaddar, *History of the high-voltage charge pump*. McGraw-Hill, 2006.

[17] K. Fujimori, S. Tamaru, K. Tsuruta, and S. Nogi, "The influences of diode parameters on conversion efficiency of rf-dc conversion circuit for wireless power transmission system," in *Microwave Conference (EuMC), 2011 41st European*, oct. 2011, pp. 57 –60.

[18] T. Yamamoto, K. Fujimori, M. Sanagi, and S. Nogi, "The design of mw-class rf-dc conversion circuit using the full-wave rectification," in *Microwave Conference, 2007. European*, oct. 2007, pp. 905 –908.

[19] ——, "The fundamental design approach of the rf-dc conversion circuit for optimizing its characteristics," in *Microwave Integrated Circuit Conference, 2008. EuMIC 2008. European*, oct. 2008, pp. 370 –373.

[20] ——, "The mw-class high efficient rf-dc conversion circuit using the resonance structure," *Proceedings of ISAP 2007*, 2007.

[21] F. Mustafa, N. Parimon, S. Rahman, A. Hashim, and M. Osman, "Rf-dc power conversion of schottky diode fabricated on algaas/gaas heterostructure for on-chip rectenna device application in nanosystem," in *Electron Devices and Solid-State Circuits, 2009. EDSSC 2009. IEEE International Conference of*, dec. 2009, pp. 150 –153.

[22] K. Buisman, L. Nanver, T. Scholtes, H. Schellevis, and L. de Vreede, "High-performance varactor diodes integrated in a silicon-on-glass technology," in *Solid-State Device Research Conference, 2005. ESSDERC 2005. Proceedings of 35th European*, sept. 2005, pp. 117 – 120.

[23] J. Lim, H. Cho, K. Cho, and T. Park, "High sensitive rf-dc rectifier and ultra low power dc sensing circuit for waking up wireless system," in *Microwave Conference, 2009. APMC 2009. Asia Pacific*, dec. 2009, pp. 237 –240.

[24] X.-C. Z. Y. L. X.-M. H. Dong-Sheng Liu, Feng-Bo Li and X.-F. Tao, "New analysis and design of a rf rectifier for rfid and implantable devices," in *Sensors 2011, 11*, april 2011, pp. 6494–6508.

[25] H. Jabbar, Y. Song, and T. Jeong, "Rf energy harvesting system and circuits for charging of mobile devices," *Consumer Electronics, IEEE Transactions on*, vol. 56, no. 1, pp. 247 –253, february 2010.

[26] S.-M. Wu, C.-Y. Lin, and L.-C. Pai, "Analysis and design of an efficient rf/dc rectifier for uhf power harvester," in *Wireless Information Technology and Systems (ICWITS), 2010 IEEE International Conference on*, 28 2010-sept. 3 2010, pp. 1 –4.

[27] T. Tanzawa and T. Tanaka, "A dynamic analysis of the dickson charge pump circuit," *Solid-State Circuits, IEEE Journal of*, vol. 32, no. 8, pp. 1231–1240, 1997.

[28] G. DiCataldo and G. Palumbo, "Design of an nth order dickson voltage multiplier," *Circuits and Systems I: Fundamental Theory and Applications, IEEE Transactions on*, vol. 43, no. 5, p. 414, 1996.

[29] M. Muramatsu and H. Koizumi, "An experimental result using rf energy harvesting circuit with dickson charge pump," in *Sustainable Energy Technologies (ICSET), 2010 IEEE International Conference on*, dec. 2010, pp. 1 –4.

[30] H. Yan, M. Popadic, J. Macías-Montero, and L. de Vreede, "Design of an rf power harvester in a silicon-on-glass technology."

[31] T. Sogorb, J. Llario, J. Pelegri, R. Lajara, and J. Alberola, "Studying the feasibility of energy harvesting from broadcast rf station for wsn," in *Instrumentation and Measurement Technology Conference Proceedings, 2008. IMTC 2008. IEEE*, may 2008, pp. 1360 –1363.

[32] A. Buonanno, M. D'Urso, and D. Pavone, "An ultra wide-band system for rf energy harvesting," in *Antennas and Propagation (EUCAP), Proceedings of the 5th European Conference on*, april 2011, pp. 388 –389.

[33] T. Umeda, H. Yoshida, S. Sekine, Y. Fujita, T. Suzuki, and S. Otaka, "A 950-mhz rectifier circuit for sensor network tags with 10-m distance," *Solid-State Circuits, IEEE Journal of*, vol. 41, no. 1, pp. 35 – 41, jan. 2006.

[34] D. Bouchouicha, F. Dupont, M. Latrach, and L. Ventura, "Ambient rf energy harvesting," in *International Conference on Renewable Energies and Power quality, Granada, Spain*, 2010.

[35] M. Ebrahimian, K. El-Sankary, and E. El-Masry, "Enhanced rf to dc cmos rectifier with capacitor-bootstrapped transistor," in *Circuits and Systems (ISCAS), Proceedings of 2010 IEEE International Symposium on*. IEEE, 2010, pp. 1655–1658.

[36] H. Takhedmit, B. Merabet, L. Cirio, B. Allard, F. Costa, C. Vollaire, and O. Picon, "A 2.45-ghz dual-diode rf-to-dc rectifier for rectenna applications," in *Microwave Conference (EuMC), 2010 European*. IEEE, 2010, pp. 37–40.

[37] T. Ungan, X. Le Polozec, W. Walker, and L. Reindl, "Rf energy harvesting design using high q resonators," in *Wireless Sensing, Local Positioning, and RFID, 2009. IMWS 2009. IEEE MTT-S International Microwave Workshop on*. IEEE, 2009, pp. 1–4.

[38] S. Borgaonkar and S. Rao, "Broadband matching of high-q resonant loads using coupled lines," *Microwaves, Optics and Acoustics, IEE Journal on*, vol. 2, no. 5, pp. 153–155, 1978.

[39] K. Hatano, N. Shinohara, T. Mitani, K. Nishikawa, T. Seki, and K. Hiraga, "Development of class-f load rectennas," in *Microwave Workshop Series on Innovative Wireless Power Transmission: Technologies, Systems, and Applications (IMWS), 2011 IEEE MTT-S International*. IEEE, 2011, pp. 251–254.

[40] H. Tong, *Nonlinear time series analysis*. Wiley Online Library, 2005.

[41] M. Priestley, "Non-linear and non-stationary time series analysis," 1988.

[42] R. Graff, *Elements of non-linear functional analysis.* Amer Mathematical Society, 1978, no. 206.

[43] M. FossÃľprez, *Non-Linear Circuits - qualitative analysis of non-linear, non-reciprocal circuits.* John Wiley, 2003.

[44] T. Schubert and E. Kim, *Active and non-linear electronics.* John Wiley, 1996.

[45] J. Pedro and N. Carvalho, *Intermodulation distortion in microwave and wireless circuits.* Artech House Publishers, 2003.

[46] W. Vander Velde, *Multiple-input describing functions and nonlinear system design.* New York: McGraw-Hill, 1968.

[47] S. El-Rabaie, V. Fusco, and C. Stewart, "Harmonic balance evaluation of nonlinear microwave circuits-a tutorial approach," *Education, IEEE Transactions on*, vol. 31, no. 3, pp. 181 –192, aug 1988.

[48] M. Nakhla and J. Vlach, "A piecewise harmonic balance technique for determination of periodic response of nonlinear systems," *Circuits and Systems, IEEE Transactions on*, vol. 23, no. 2, pp. 85 – 91, feb 1976.

[49] M. M. Corporation, "Theory of load and source pull measurement," jul 1999.

[50] H. P. co., "Linear models for diode surface mount packages - application note 1124," 1997. [Online]. Available: http://palgong.kyungpook.ac.kr/~ysyoon/Pdf/an1124.pdf

[51] D. Misra, *Radio-frequency and microwave communication circuits.* John Wiley, 2001.